Revista Mexicana de Ciencias Geológicas, volumen 13, número 1, 1996, p. 10-51
Universidad Nacional Autónoma de México, Instituto de Geología, México, D.F.

VOLCANIC STRATIGRAPHY OF THE AMEALCO CALDERA AND VICINITY, CENTRAL MEXICAN VOLCANIC BELT

Gerardo J. Aguirre-Díaz [1,2]

ABSTRACT

The Amealco caldera is one of five major caldera complexes within the Mexican Volcanic Belt. Stratigraphy indicates five major volcanic units related with the volcanic history of the Amealco caldera: (1) the Amealco Tuff, a widespread pyroclastic sequence that was erupted from the Amealco caldera at about 4.7 Ma and which represents 77 km^3 of magma; (2) Brick pumice, a more localized post-Amealco Tuff pyroclastic sequence representing 2.4 km^3 of magma; (3) Amealco Andesite and Campana Dacite, lava domes that were emplaced along a ring fracture at 4.3 Ma and actually form the topographic expression of the caldera, the former representing 3.5 km^3 of trachyandesitic magma, and the later 0.8 km^3 of trachydacite magma; (4) La Cruz Rhyolite, which consists of five lava domes within the caldera that were emplaced at 3.9 Ma, with a total magma volume of 2.4 km^3; and (5) Santa Rosa Andesite, which includes five trachyandesitic domes that were emplaced at 3.7 Ma, representing a magma volume of 4.3 km^3.

Peripheral activity occurred at several vents: the trachydacitic Palomas volcano at 4.0 Ma (Palomas Dacite); the basaltic-andesitic Hormigas volcano and rhyolitic lava domes (Coronita Rhyolite), both at 3.7 Ma; a 2.5 Ma hornblende andesite dome (Garabato Andesite); and finally, a 2.2 Ma andesitic scoria cone (El Comal Andesite). In addition to the peripheral volcanism, Amealco Tuff is overlain by the 2.9 Ma El Rincón Rhyolite, a lava dome complex 12 km to the north of the caldera, and by a widespread 3.5-Ma felsic ignimbrite, here named the Huichapan Tuff, which is exposed 20 km to the east of the caldera and previously had been misidentified as Amealco Tuff. Amealco Tuff overlies 5.7 Ma basalts and 4.7 Ma felsic ignimbrites.

Key words: Stratigraphy, volcanic rocks, Amealco caldera, Mexico.

RESUMEN

La caldera de Amealco es uno de los cinco principales complejos de caldera dentro de la Faja Volcánica Mexicana. La estratigrafía indica la existencia de cinco unidades volcánicas principales relacionadas con la historia volcánica de la caldera de Amealco: (1) la Toba Amealco, una secuencia piroclástica ampliamente extendida cuya extrusión tuvo lugar hace aproximadamente 4.7 Ma a partir de la caldera de Amealco y cuyo volumen es de 77 km^3 de magma; (2) la pómez Ladrillo, una secuencia piroclástica posterior a la Toba Amealco, de menor extensión que ella, cuyo volumen es de 2.4 km^3 de magma; (3) la Andesita Amealco y la Dacita Campana, domos de lava que fueron emplazados a lo largo de una fractura anular hace 4.3 Ma y que producen la expresión topográfica de la caldera; la primera consiste en 3.5 km^3 de magma traquiandesítico, y la segunda en 0.8 km^3 de magma traquidacítico; (4) la Riolita La Cruz, que consiste en cinco domos dentro de la caldera que fueron emplazados hace 3.9 Ma, con un volumen total de magma de 2.4 km^2; y (5) la Andesita Santa Rosa, que incluye cinco domos traquiandesíticos, que fueron emplazados hace 3.7 Ma, con un volumen total de magma de 4.3 km^3.

Una actividad periférica tuvo lugar en varias fuentes: el volcán traquidacítico Palomas, hace 4.0 Ma (Dacita Palomas); los domos riolíticos (Riolita Coronita) y el volcán basáltico-andesítico Hormigas, ambos hace 3.7 Ma; un domo de andesita de hornblenda (Andesita Garabato), hace 2.5 Ma; y finalmente un cono de escoria andesítica (Andesita El Comal), hace 2.2 Ma. Además del volcanismo periférico, la Toba Amealco está cubierta por la Riolita El Rincón, de 2.9 Ma, un complejo de domos a 12 km al norte de la caldera, y por una ignimbrita félsica de 3.5 Ma, aquí nombrada Toba Huichapan, la cual está expuesta a 20 km al este de la caldera y que había sido reconocida erróneamente como Toba Amealco. La Toba Amealco cubre basaltos de 5.7 Ma e ignimbritas félsicas de 4.7 Ma.

Palabras clave: Estratigrafía, rocas volcánicas, caldera de Amealco, México.

INTRODUCTION

The Amealco caldera is a volcanic center, approximately 11 km in diameter, located in the central part of the Mexican Volcanic Belt (MVB)(Figure 1). It is one of five major caldera complexes occurring along this volcanic province. The others are La Primavera, Huichapan, Mazahua, and Los Humeros. Another large volcanic complex which might be a caldera is Los Azufres (Figure 1), but its origin is still debatable (Dobson and Mahood, 1985; Carrasco-Núñez, 1989; Cathelineau *et al.*, 1987; Ferrari *et al.*, 1991, 1993; Pradal and Robin, 1994).

The best studied calderas in the MVB are La Primavera and Los Humeros. They both lie in complex tectonic settings. La Primavera is near what has been interpreted as a triple continental rift junction (Mahood, 1980; Luhr *et al.*, 1985; Allan *et al.*, 1991) in the western portion of the belt (Figure 1). Los Humeros is in the eastern portion of the MVB and overlies lavas of calc-alkalic and alkalic composition (Robin and Nicolas, 1978; Negendank *et al.*, 1985). Within the central portion of the MVB, Huichapan caldera has received some attention (Yáñez-García, 1984; Silva-Mora, 1991; Milán *et al.*, 1993), and Mazahua caldera was just recently reported (Anguita *et*

[1]*Estación Regional del Centro, Instituto de Geología, Universidad Nacional Autónoma de México, Apartado Postal 376, 36000 Guanajuato, Gto., México (current address).*
[2]*Department of Geological Sciences, University of Texas at Austin, U.S.A.*

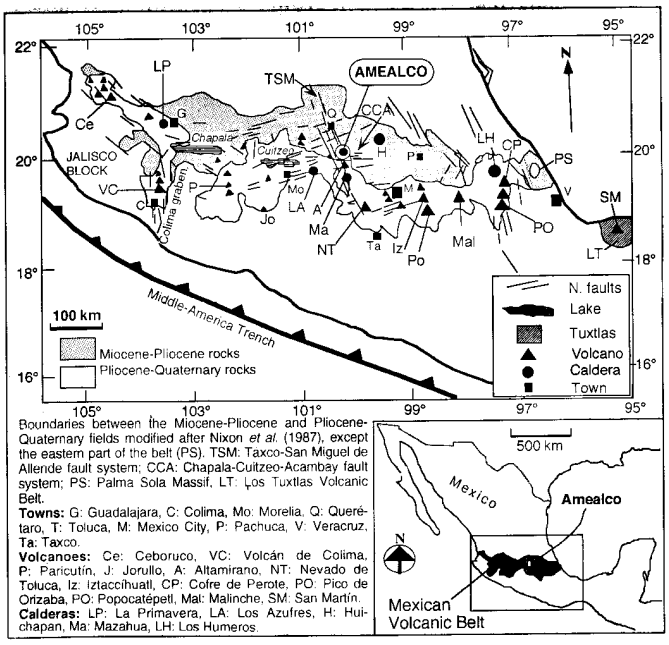

Boundaries between the Miocene-Pliocene and Pliocene-Quaternary fields modified after Nixon *et al.* (1987), except the eastern part of the belt (PS). TSM: Taxco-San Miguel de Allende fault system; CCA: Chapala-Cuitzeo-Acambay fault system; PS: Palma Sola Massif, LT: Los Tuxtlas Volcanic Belt.
Towns: G: Guadalajara, C: Colima, Mo: Morelia, Q: Querétaro, T: Toluca, M: Mexico City, P: Pachuca, V: Veracruz, Ta: Taxco.
Volcanoes: Ce: Ceboruco, VC: Volcán de Colima, P: Paricutín, J: Jorullo, A: Altamirano, NT: Nevado de Toluca, Iz: Iztaccíhuatl, CP: Cofre de Perote, PO: Pico de Orizaba, PO: Popocatépetl, Mal: Malinche, SM: San Martín.
Calderas: LP: La Primavera, LA: Los Azufres, H: Huichapan, Ma: Mazahua, LH: Los Humeros.

Figure 1. Index map of the Mexican Volcanic Belt and of several volcanic centers in it. Amealco caldera is in the central portion of the belt, where two major fault systems intersect: the NNW Taxco-San Miguel de Allende (TSM) and the E-W Chapala-Cuitzeo-Acambay (CCA). Modified after Nixon and coworkers (1987). Inset shows regional location of figure.

al.,1991). Therefore, there is the need of more studies in tne volcanic centers of the central MVB. These needed studies have to document the geology, geochronology, petrology, and the physical volcanic processes that formed these complexes in order to get a more complete understanding of their evolution.

In this work, it is described the geology and petrography of the products erupted by the Amealco caldera, and provided the K-Ar ages that support the stratigraphy. The description is based on the systematic mapping in the Amealco area, during which 26 stratigraphic sections were measured. Because there were no previous works on the volcanic stratigraphy in this area based on measured sections, the sections and detailed descriptions of the units are provided in Appendix A. Twenty-five K-Ar ages were performed; the data are shown in Table 1, and the details of the K-Ar analytical procedure are described in Appendix B. A brief petrographic description of each unit is provided in the main text, and a more detailed petrographic description, only of the Amealco caldera products, is provided separately in Appendix C. Since previous studies of the Amealco caldera have reported a large variety of values for the volume of the Amealco caldera products, the procedure for estimating the volume of the Amealco caldera units is also briefly explained in Appendix D. The chemical classification for the units is based on Le Bas and coworkers (1986); major element chemistry is shown in Table 2.

A total of 4,200 km^2 were mapped on 1:50,000 CETENAL (now called INEGI) topographic quadrangles (CETENAL, 1972, 1974a, 1974b, 1976, 1979, 1988, 1989). Three geologic maps of the studied area are provided, and will be referred to as Plate 1, Plate 2, and Plate 3. K-Ar age samples location and that of the measured stratigraphic sections are indicated in Plates 1, 2 and 3 (Appendix A includes and index map of the measured sections, too). Figure 2 shows the distribution of the caldera-related pyroclastic sequence, which the author names the Amealco Tuff. A simplified geologic map of the immediate surroundings of the Amealco caldera is shown in Figure 3, and a composite stratigraphic section of the Amealco area, that includes a summary of the K-Ar ages, in Figure 4. All distances mentioned in the text are from the center of the caldera.

PREVIOUS WORK

The first formal reference to the Amealco caldera was made by Sánchez-Rubio (1978), in which a short description of the caldera and a few major element analyses are reported. A larger compilation is found in Sánchez-Rubio's thesis work (Sánchez-Rubio, 1984), which includes a reconnaissance geologic map of the caldera and its surroundings, and a description of the units associated with it. The map was later published by Sánchez-Rubio (1986) in a field-trip guide. Carrasco-Núñez (1988) also studied the Amealco caldera as part of his master's thesis. His contribution was a larger set of chemical data on Amealco's products. These data were published together with numerous isotopic (Sr and Nd) analyses by Verma and coworkers (1991). In a previously published abstract, Verma and coworkers (1989) reported Pb isotope data but that were not included in Verma and coworkers (1991). Fries and coworkers (1965) described the physical and chemical characteristics of a pyroclastic sequence near Tlalpujahua, Estado de México; their work is a detailed study of the Amealco Tuff ignimbrites, but Fries and coworkers (1965) did not recognize that these deposits were derived from the Amealco caldera.

STRATIGRAPHY

PRE-CALDERA UNITS

Tlalpujahua plutonic and metamorphic complex

The oldest units in the mapped area are meta-sedimentary Mesozoic rocks exposed about 30 km south of the Amealco caldera, near Tlalpujahua, Estado de México (Figure 2; Plate 3). The metamorphic rocks include low-grade pelitic schist, that can be black, yellow-brown and white-gray. The schist is locally overlain by slightly metamorphosed black limestone. The Tlalpujahua metamorphic complex was described in detail by Flores (1920), and more briefly by Fries and coworkers (1965). No fossils have been reported in it, but various ages have been proposed, based on correlation with other localities in central Mexico, including Triassic (Flores, 1920), Triassic-Cretaceous (Fries *et al.*, 1965), Jurassic-Creta-

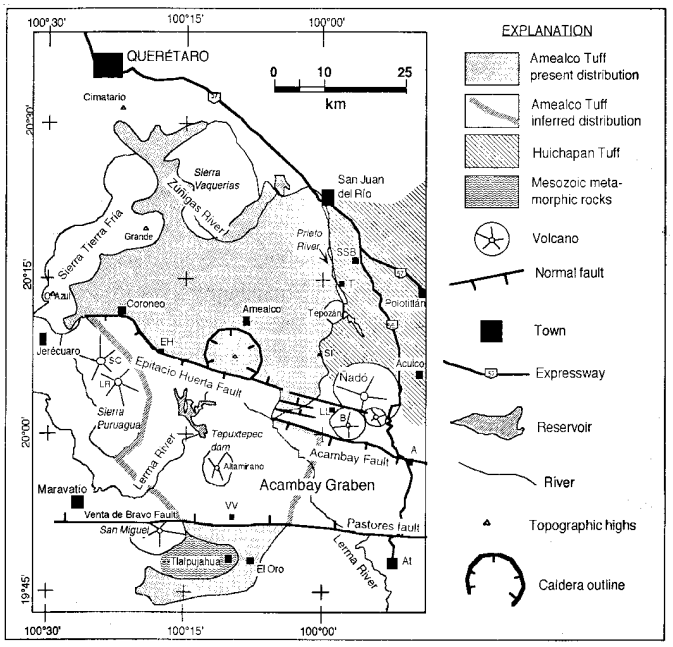

Figure 2. Distribution of the Amealco Tuff, the main product erupted by the Amealco caldera, and index map of the major volcanoes, volcanic complexes, and other geologic features within the mapped area. EH: Epitacio Huerta, LL: Santa María La Loma, A: Acambay, At: Atlacomulco, SSB: San Sebastián Barrancas; SI: San Ildefonso, T: Taxhie, VV: Venta de Bravo, B: Boti volcano, LR: Los Rosillos volcano, SC: Siete Cruces volcano (after Aguirre-Díaz, 1995).

ceous (Campa *et al.*, 1974), or Late Jurassic (Suter *et al.*, 1995). Unmetamorphosed (?) basaltic, andesitic and rhyolitic dikes and sills intruded the metasedimentary rocks (Flores, 1920), but they have not been dated. Amealco Tuff overlies in angular unconformity white schist at the El Carmen (Tlalpujahua) river. The metamorphic sequence is locally also covered by lava flows issued from the Cerro San Miguel (3,000 m a.s.l.), a large composite volcano older than Amealco Tuff (Figure 2), and by other volcanic rocks (Silva-Mora, 1979, 1995). Important gold and silver mineralization hosted in veins and stockworks occurs in the Tlalpujahua-El Oro mining districts (Flores, 1920). It has been hypothesized that the mineralization was related to intrusion of the mafic and rhyolitic dikes into the meta-sedimentary rocks (Flores, 1920), perhaps during the Miocene, as Salas (1988) indicates, but he does not explain his basis for this age assignment. The dikes have a general NW trend. The Pliocene-Quaternary volcanic rocks of the MVB are post-mineralization and were not intruded by the dikes.

Pre-Amealco caldera volcanic rocks

Intermediate volcanism. There are several composite volcanoes with satellite scoria and lava cones that shed intermediate-composition lava flows. The largest volcanic complexes are: (1) Ñadó (3,320 m a.s.l.), which is located 20 km to the east-southeast of the caldera (Figure 2; Plate 2), and includes volcanoes Boti (3,300 m a.s.l.) and El Gallo (3,080 m a.s.l.); (2) volcanoes Las Siete Cruces (3,050 m a.s.l.) and Los Rosillos (3,180 m a.s.l.), that make the core at the northern portion of the NW trending (25 km long) Sierra Puruagua, which is located 20 km west of Amealco caldera (Figure 2; Plate 2); and (3) the Sierra Vaquerías, a volcano and lava dome complex, located 22 km to the north of the caldera (Figure 2). A K-Ar age of 5.7 Ma was obtained from an olivine-bearing basaltic andesite (sample Am-67, Table 1) from the southern, lower flank of the Sierra Vaquerías complex.

La Loma Andesite is the name assigned by Sánchez-Rubio (1984) to intermediate lava cropping out approximately 15 km to the east of the Amealco caldera (Figure 3); the name was taken from the village of Santa María La Loma, which lies on lava issued from a satellite vent on the southwest flank of Ñadó volcano (Figure 2). The unit La Loma Andesite is defined in this study as the undifferentiated intermediate material (lava and pyroclastic deposits) that was erupted from volcanoes Ñadó, Boti and El Gallo, and the peripheral cones to them that are older than the Amealco Tuff. However, most of the volume of La Loma Andesite may have been erupted from Ñadó volcano.

Several other smaller volcanoes and lava domes that are older than the Amealco caldera are partly covered by the widespread Amealco Tuff. These volcanic structures include the El Tepozán (La Muralla), and El Añil, both to the east of the caldera (Figure 3; Plate 2), which are composed only of lava, and could be deeply eroded volcanoes or lava domes. Also to the east is the 5 Ma andesite reported by Sánchez-Rubio (1984) (Plate 2).

Silicic volcanism. Among the silicic volcanoes prior to the Amealco caldera, the Sierra Tierra Fría lava dome complex is outstanding in terms of its size. It is nearly 20 km long and 12 km wide (Figure 2). Its highest peak is Cerro Azul (2,980 m a.s.l.), which is 30 km to the west-northwest of the Amealco caldera (Plate 1). Several widespread quartz and K-feldspar-bearing, felsic, welded, pink to light gray ignimbrites were presumably erupted from this volcanic complex. Farther to the west is Sierra Los Agustinos, a volcanic complex that includes also felsic ignimbrites. A K-Ar age of 4.7 Ma was obtained from one of these ignimbrites (sample Am-84, Table 1).

Two isolated and small felsic lava domes occur near the Amealco caldera. One is the Galindillo dome, 14 km to the north of the Amealco caldera (Plate 1), which is a low mound almost totally buried under the Amealco Tuff. The other is the El Espía lava dome (Figure 3), a plug-like hill, 9 km to the east of the caldera. Galindillo dome was briefly described by Sánchez-Rubio (1984). The rock of Galindillo is a perlitized, pale gray glass, with distinct flow banding, which swirls around the inferred vent. It is phenocryst-poor (<5 vol. %), with sanidine, quartz, biotite and scarce iron-titanium oxides. Its chemical composition corresponds to a slightly peraluminous, high-silica rhyolite (Aguirre-Díaz, 1993a).

The rock of El Espía dome is a deeply weathered, yellow-white rock, with a white clayey matrix. It may originally have been a glassy, flow-banded rock. *In situ* boulders still preserve a crude circular arrangement, suggesting a charac-

Table 1. K-Ar ages of units of the Amealco caldera region.

Unit	Sample	Location		Material	K [%]	Weight [g]	Ar x10^{-6} scc/g	^{40*}Ar [%]	Age [Ma]	±1σ† [Ma]	Assigned age [Ma±1σ]
		Lat. N	Long. W								
Pre-Amealco	Am-67	20°21'8"	100°6'50"	wr	1.27	0.611	0.269	33.2	5.69	0.35	5.69 ± 0.35
					1.26	0.611	0.294	31.8			
	Am-84	20°10'33"	100°27' 54"	fsd	0.97	0.261	0.175	27.4	4.70	0.19	4.70 ± 0.19
					0.99	0.327	0.183	38.5			
Amealco Tuff	Am-1	20°8'3"	100° 18'10"	gl	4.64	0.263	0.854	18.5	4.74	0.15	4.68 ± 0.10
					4.61						
					4.63						
	Am-1			fds	0.53	0.316	0.094	19.9	4.54	0.28	
					0.53						
	Am-12	20°16'35"	100°9'7"	fds	0.46	0.301	0.082	13.1	4.55	0.40	
					0.46						
	Am-22	20°8'1"	100°18'8"	gl	3.62	0.432	0.640	35.9	4.71	0.14	
					3.53	0.277	0.664	31.1			
					3.56						
					3.53						
	Am-208	19°50'45"	100°11'15"	gl	2.90	0.606	0.542	34.4	4.71	0.19	
					2.91	0.278	0.524	38.8			
					2.86						
Amealco And.	Am-62	20°10'16"	100°10'17"	gms	2.00	0.668	0.342	58.0	4.42	0.21	4.31 ± 0.12
					1.97						
	Am-58	20°10'13"	100°9'23"	wr	2.31	0.579	0.385	45.3	4.30	0.24	
					2.29						
	Am-46	20°6'38"	100°7'0"	wr	3.42	0.588	0.519	16.6	4.14	036	
					3.41	0.459	0.584	18.6			
	Am-195	20°7'54"	100°6'55"	wr	2.28	0.666	0.371	22.3	4.30	0.15	
					2.30	0.440	0.395	21.7			
Campana Dac.	Am-79	20°10'0"	100°15'22"	gl	3.79	0.618	0.618	42.6	4.31	0.10	4.31 ± 0.10
					3.76	0.246	0.650	44.4			
Palomas And.	Am-41b	20°9'19"	100°16'8"	gms	0.58	0.546	0.096	16.9	3.96	0.40	3.96 ± 0.40
					0.57	0.461	0.083	14.7			
						0.429	0.089	14.2			
La Cruz Rhy.	Am-63	20°10'4"	100°10'20"	gl	4.16	0.278	0.633	41.4	3.91	0.14	3.90 ± 0.14
					4.16						
	Am-63			fds	1.38	0.284	0.209	19.8	3.89	0.27	
					1.37						
Sta. Rosa And.	Am-61	20°8'49"	100°10'7"	gms	3.36	0.552	0.474	13.6	3.69	0.25	3.74 ± 0.25
					3.31	0.681	0.478	13.0			
					3.30						
					3.32						
	Am-51	20°7'32"	100°9'43"	gms	2.82	0.723	0.374	19.2	3.79	0.26	
					2.72	0.353	0.423	20.2			
					2.69	0.494	0.416	17.3			
Coronita Rhy.	Am-179	20°7'7"	100°19'33"	gl	3.83	0.516	0.524	42.8	3.52	0.10	3.72 ± 0.27
					3.82						
					3.83						
	Am-179			fds	4.20	0.285	0.627	54.0	3.90	0.10	
					4.15	0.493	0.642	61.5			
					4.30						
Hormigas And.	Am-78	20°10'13"	100°12'31"	gms	1.14	0.533	0.174	32.3	3.70	0.39	3.70 ± 0.39
					1.14	0.592	0.144	26.5			
						0.518	0.174	31.9			
Huichapan Tuff	Am-81	20°8'38"	99°56'36"	gl	3.96	0.604	0.553	48.4	3.59	0.09	3.52 ± 0.16
					3.96						
	Am-81			fds	3.58	0.274	0.443	23.3	3.36	0.21	
					3.52	0.414	0.482	58.0			
					3.54						
					3.50						
El Rincón Rhy.	Am-122	20°14'15"	100°14'25"	gl	4.86	0.664	0.555	4.5	2.92	0.44	2.92 ± 0.59
					4.89						
Garabato And.	Am-18	20°6'0"	100°11'50"	wr	2.39	0.558	0.252	19.8	2.54	0.26	2.54 ± 0.26
					2.37	0.588	0.218	29.0			
El Comal And.	Am-19b	20°5'59"	100°9'48"	gms	1.91	0.779	0.161	31.3	2.18	0.07	2.18 ± 0.07
					1.90	0.647	0.163	24.9			

Mat.: Material used for K-Ar analysis—gl: glass, wr: whole rock, gms: groundmass, fds: feldspar.
^{40*}Ar: Radiogenic argon content of sample, in percent of total ^{40}Ar.
scc/g: Standard cubic centimeter per gram.
†: Error of age at one sigma, see text for details.
Assigned age: Weighted mean of the different ages obtained for a particular unit.
^{40}K/K = 1.167 x 10^{-4} moles/mole λ_β = 4.963 x 10^{-10}/ yr $\lambda_{\varepsilon+\epsilon}$ = 0.581 x 10^{-10}/ yr

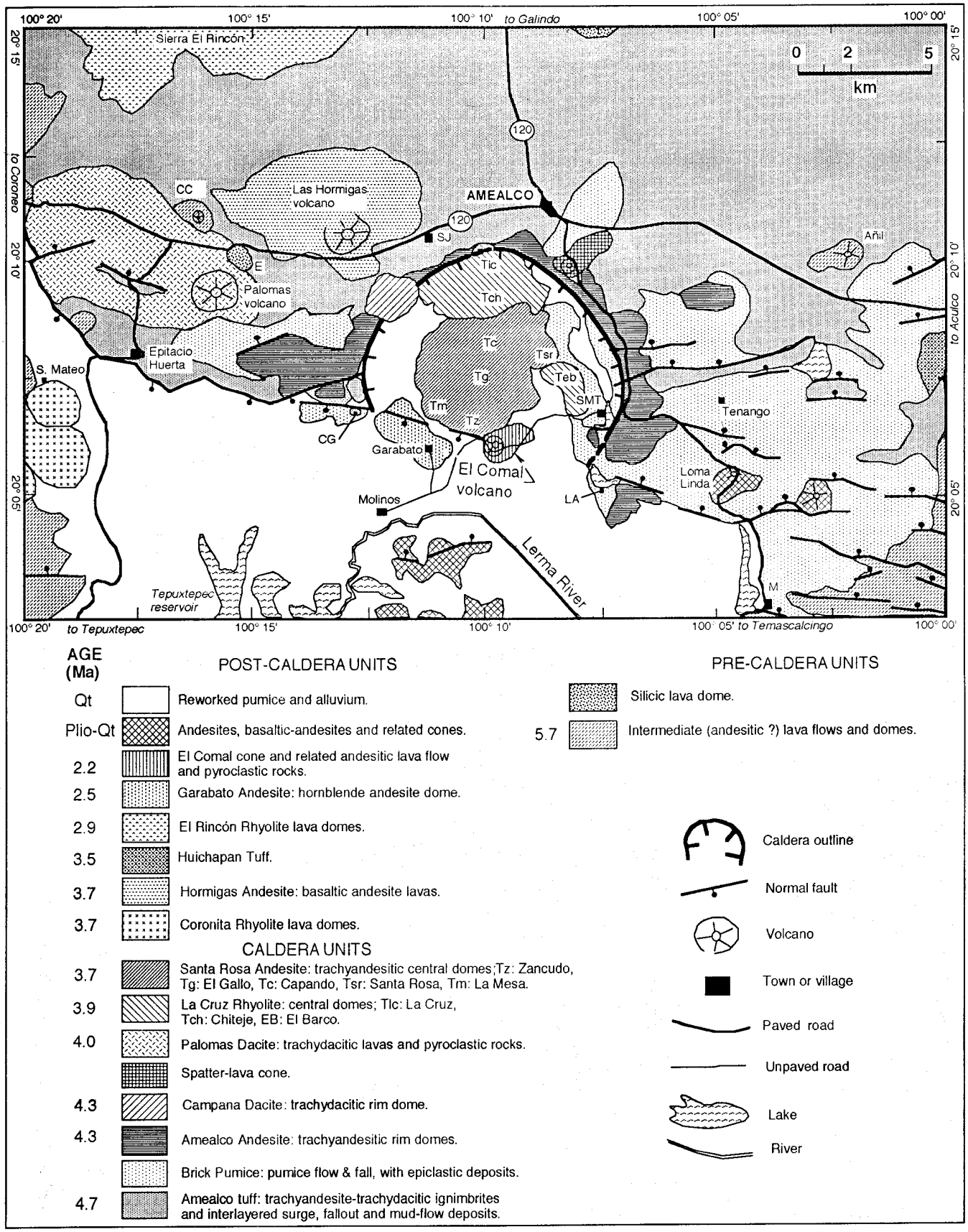

Figure 3. Simplified geologic map of the Amealco caldera and peripheral volcanism. CC: Cerrito Colorado cone, E: El Espía dome, SJ: San Juan Hedó, LA: Los Arcos, SMT: San Miguel Tlascaltepec, M: Mexquititlán, CG: Cañada de García.

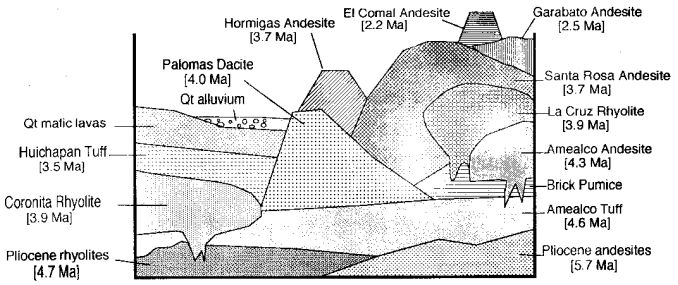

Figure 4. Composite stratigraphic column and K-Ar ages of the volcanic units in the Amealco caldera area (not to scale).

teristic lava dome structure. Verma and others (1991) assigned a post-Amealco Tuff age to the El Espía dome, but as originally stated by Sánchez-Rubio (1984), it may be older than the Amealco ignimbrites. A clear contact between the two units was not found, but the dome is overlain by lava flows of Palomas volcano at the north, west and south, which is younger than the Amealco Tuff (Figure 3). El Espía dome is similar to the rocks of the Sierra Tierra Fría complex, and with a similar degradation state, thus El Espía dome may be of similar age to that of Sierra Tierra Fría.

CALDERA UNITS

Amealco Tuff

Definition. Amealco Tuff is the most important unit both in terms of volume and distribution. Its eruption was the cause of the caldera. The work of Sánchez-Rubio (1984) provides a brief description of the ignimbrites contained within Amealco Tuff, which he named "Amealco Ignimbrite". In a more recent publication about the Amealco caldera, Verma and coworkers (1991) also named Amealco Ignimbrite (or Unit D) the ignimbrites of Amealco Tuff. The name Amealco Tuff is proposed here for the voluminous pyroclastic sequence erupted during the climactic volcanic phases of the Amealco caldera at about 4.7 Ma (weighted mean of five ages, Table 1). Amealco Tuff includes three major ignimbrites, which are interlayered with minor unwelded ignimbrites, pumice fallout, surge, and mud-flow deposits. The three major ignimbrites are named, from first- to last-erupted, Amealco I, Amealco II, and Amealco III (Figure 5). They are coextensive for at least 25 km from the caldera (Figure 6). Farther away, individual flows form isolated lobes; thus the most distal outcrops of Amealco Tuff contain two or only one of the three major ignimbrites extending as far as 45 km to the north and the south from the caldera.

It is proposed to abandon the term "Amealco Ignimbrite" introduced by Sánchez-Rubio (1984) to designate this unit, because the lithostratigraphic unit includes other types of pyroclastic and epiclastic deposits in addition to the ignimbrites (surges, fallouts, and mud-flows), which all together are as voluminous as the major ignimbrites (Appendix D).

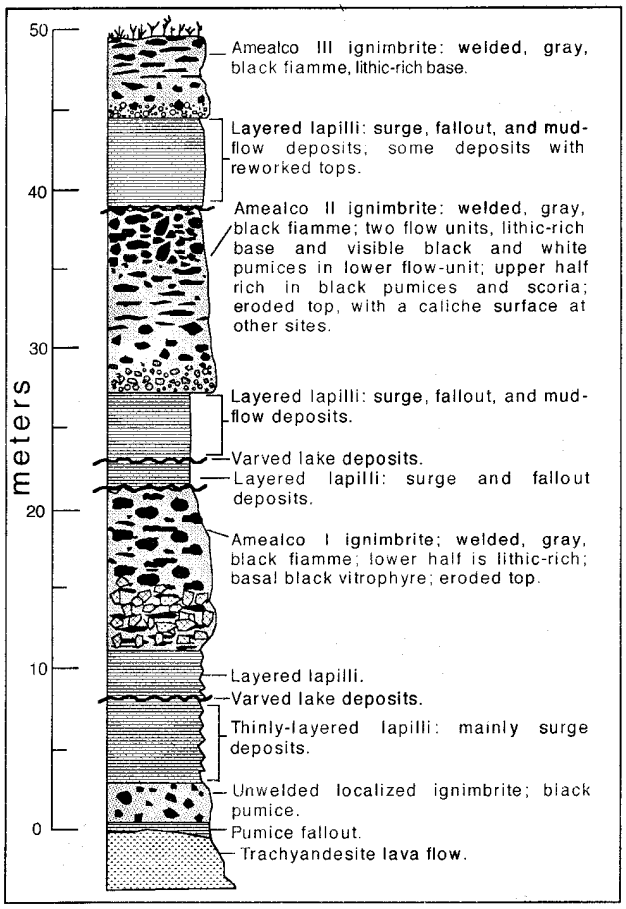

Figure 5. Representative section of the Amealco Tuff at a proximal location (15 km to the west), measured at Epitacio Huerta, Michoacán. This section has been simplified for clarity. Wavy thicker lines indicate unconformities. See section 1, Appendix A for a detailed description.

Distribution and volume. Amealco Tuff filled and leveled the area next to and around the Amealco caldera, except for the highest pre-existing peaks (*e.g.,* Añil, El Espía, Figure 3). Farther away from the source, the ignimbrites ponded against the highest pre-existent mountains around the caldera, such as the Sierra Vaquerías to the north, Sierra Tierra Fría to the west, Ñadó volcano to the east, and the hills near Tlalpujahua to the south (Figure 2; Plates 1, 2 and 3). Today's physiography is that of an intermontane ignimbrite-filled plateau to the west, north and east of the caldera, and of a fault-bounded depression south of the caldera, in which the ignimbrite plateau is covered by younger volcanic and lake deposits. Amealco Tuff is found farther to the south and beyond this tectonic depression, south of Venta de Bravo fault (Suter *et al.*, 1991, 1992) (Figure 2). These southern outcrops were mapped and named as Las Américas Formation by Fries and coworkers (1965), but they did not continue their mapping north of the Venta de Bravo fault, and thus did not recognize Amealco caldera as the source of the deposits. Las Américas Formation is considered here as the southern distal outcrops of Amealco Tuff based on evidence presented elsewhere (Aguirre-Díaz, 1993a, b).

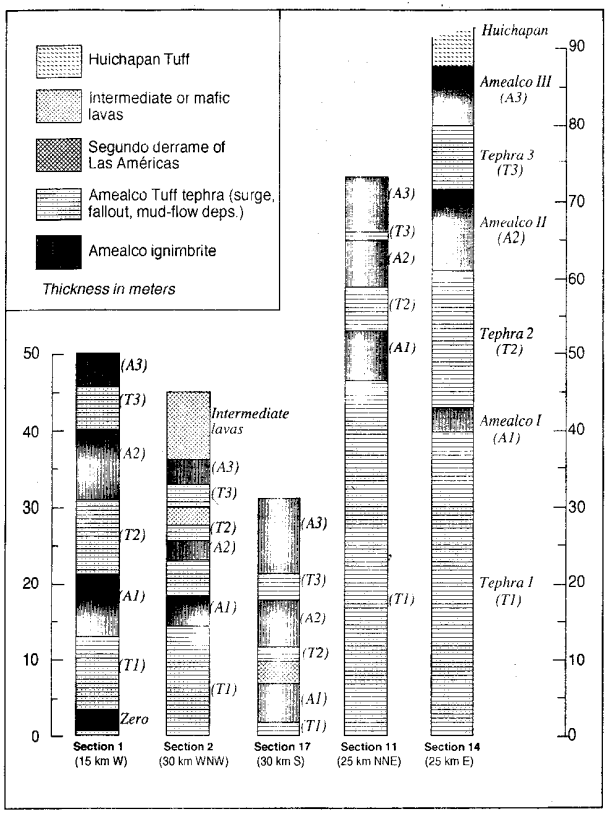

Figure 6. Representative sketch sections of the Amealco Tuff at different localities. Site and distance to the center of the caldera are shown at the bottom of each section. Detailed descriptions of the sections are provided in Appendix A.

The ignimbrites are found as far as 45 km to the north of the caldera, 44 km to the south, and 33 km to the west. To the east, about 20 km from the Amealco caldera, Amealco Tuff is covered by a major felsic ignimbrite (Figure 2), that yielded a K-Ar age of 3.5 Ma (sample Am-81, Table 1). The source of this younger unit is the Huichapan caldera, which is 40 km to the east of its contact with the Amealco Tuff. This felsic ignimbrite is described below as the Huichapan Tuff (see *Post-Amealco Units*). The contact between the Huichapan and Amealco tuffs approximately coincides with the axis of the Río Prieto canyon, which has a general north-south orientation (Figure 2; Plate 2).

Based on its extent and thickness variations, Amealco Tuff has an estimated rock volume of 103 km^3. The dense rock equivalent (DRE) volume is 77 km^3, based on measured bulk rock densities from representative samples gathered at Epitacio section (Figure 5) (Appendix D). These are minimum volume estimates as they do not include: (1) the intracaldera tuff, which is not exposed, (2) the distal air-fall tuffs (those that traveled farther than the ignimbrites), and (3) the co-ignimbrite ash-fall (ash-cloud) deposits, which have been eroded away.

If all the isolated outcrops are connected as a continuous unit (Figure 2), Amealco Tuff presently would cover an area of approximately 2,880 km^2. The boundary of the Amealco Tuff distribution was taken in this study as that marked by the ignimbrites. These limits were mapped in the field and were not inferred, except for the places where the ignimbrites are covered by younger deposits (*e.g.*, as in the Acambay graben, or at the eastern front). No attempt was made to find the limit of the Amealco Tuff's air-fall deposits (both co-ignimbrite and fallout), which surely reached farther than the ignimbrites.

The best exposures of Amealco Tuff occur in deep canyons to the north and to the east of the caldera, for instance at Zúñigas and Río Prieto canyons (measured sections 11 and 14, Appendix A) and along the uplifted block of Epitacio fault, near the village with the same name, about 15 km west of the caldera (Figures 2 and 3; measured section 1, Appendix A). The easternmost outcrops of Amealco Tuff occur about 25 km to the northeast of the caldera, where the tuff is exposed in a canyon that cuts through the Huichapan Tuff plateau, down to the base of the Amealco Tuff (measured section 13, Appendix A).

Because Amealco Tuff is a widespread unit, it is overlain by many different units, either erupted from the Amealco caldera, or from other sources, for instance, Brick pumice, Amealco Andesite, Palomas and Hormigas volcanoes, Sierra Tierra Fría, and Huichapan Tuff, among others. Amealco Tuff serves as a distinct stratigraphic marker in the region, because of its widespread distribution, its distinct lithologic features that make it easy to recognize in the field, and because its well constrained age is documented with several K-Ar determinations.

Field description. Figure 6 shows five schematic sections that are representative of Amealco Tuff. As is expected for volcanic deposits, each section shows particular characteristics, but in general, all contain the three major ignimbrites, Amealco I, Amealco II, and Amealco III, interlayered with a few minor nonwelded ignimbrites, pumice fallout, ash-flow, mud-flow, and surge deposits, that are referred altogether to as Tephra 1, Tephra 2 and Tephra 3 in Figure 6. The stratigraphic section measured at Epitacio Huerta (Figure 5; measured section 1, Appendix A), is regarded as the most representative; it is also one of the best exposed and the one with easiest access, as it is a road cut, on kilometers 6 to 8 (from north to south), along the highway that connects Tepuxtepec with the Highway 120 junction (Figure 3; Plate 2). Because of these characteristics, it is proposed as the type section for the Amealco Tuff. However, a type locality for the Amealco Tuff is difficult to assign because the pyroclastic deposits vary on a local scale, so that some sections contain units that in other sections are missing. Therefore, auxiliary sections are recommended (Figure 6): Epitacio Huerta, is representative of the proximal facies (west), Zúñigas canyon (measured section 11, Appendix A), is representative of the distal facies (north), and the Río Prieto canyon (measured section 14, Appendix A), representative of the intermediate facies (east). The Río Prieto section includes also the voluminous Huichapan Tuff (described below).

Another complete section of Amealco Tuff was measured at the distal western facies (measured section 2, Appendix A). In this site, the Amealco sequence is interlayered with basaltic andesite lava flows; one flow is at the base, another in the middle, and a third one caps the Amealco Tuff (Figure 6).

The ignimbrites Amealco I, II, and III are low-aspect ratio (aspect ratio = average thickness/distance from the source 2 to $3x10^{-4}$), sheet-shaped deposits. Thicknesses of individual ignimbrites are generally within the 3-10 m range. The ignimbrites are generally partly to densely welded and form resistant cliffs traversed by wide (generally 2-4 m) joint columns with 3 to 6 sides. In several sites (*e.g.*, Río Prieto and Epitacio sections), layers 2a and 2b of the ignimbrites (*sensu* Sparks *et al.*, 1973) are clearly exposed (Figure 7). Layer 2a is sometimes bracketed by narrow (1-3 cm thick) shear zones, that may have been formed by differential movement between this layer and the ground at its base, and layer 2b at its top, during the pyroclastic flow emplacement.

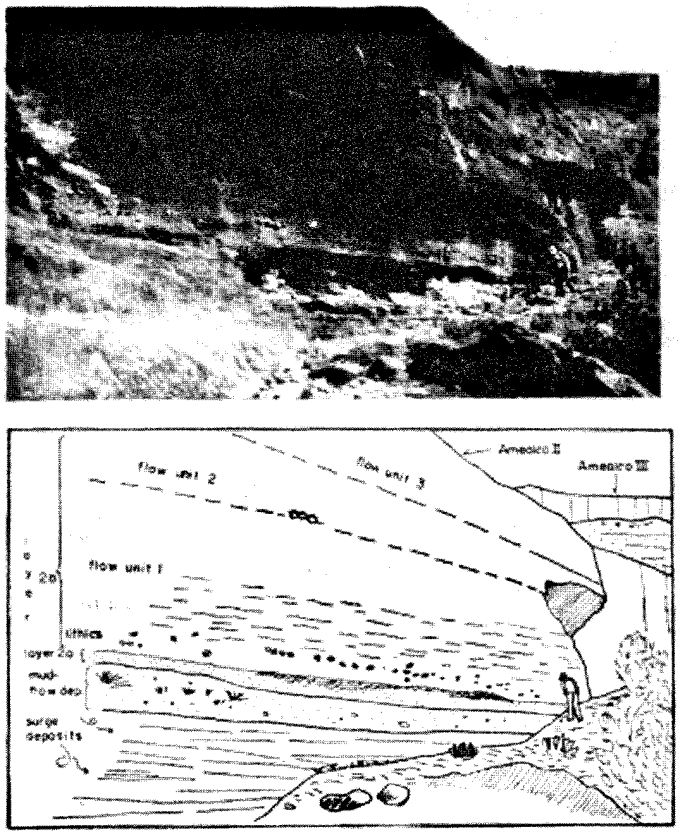

Figure 7. Amealco II ignimbrite in the southern wall of the Río Prieto canyon. Sketch helps to visualize the layers 1 (surge deposits), 2a and 2b (*sensu* Sparks *et al.*, 1973), and three different flow units of the ignimbrite. Note the dark color and dense welding of the ignimbrite, which are typical of the Amealco ignimbrites. Person for scale in the lower right.

The ignimbrites are generally gray to dark gray, with reddish tops where oxidized by vapor phase alteration (*e.g.*, the outcrops of Amealco III at the northern flank of Amealco caldera). The ignimbrites contain abundant black pumice fragments, as large as 40 cm in the distal facies (25 km from the source), but generally the black pumices are 3-10 cm, either in the near-vent, proximal, intermediate, or distal facies (Figure 8, a). Black fiamme are commonly found in the densely welded zones of the ignimbrites. They are exceptionally up to 30 cm long, but their average size is in the 2-7 cm range. Black pumices and fiamme make 5 to 40% of the volume of individual flow units, with pumice size and abundance increasing upward from the base of each flow unit. Black pumice and fiamme show a wide range in crystal content, from nearly aphyric (*e.g.*, those in Amealco I ignimbrites in Epitacio section), to crystal-rich, with crystal contents on the order of 35 vol. % (*e.g.*, Amealco II ignimbrite at Epitacio section, Figure 5). White or light-colored pumice fragments also occur in the ignimbrites, but they are less abundant and generally smaller (Figure 8, a). White pumices could be as abundant as 20% of the volume of the ignimbrite in a few sites (*e.g.*, north of Coroneo, Figure 3), and with sizes up to 10 cm, but generally they make less than 5% of the volume and are often smaller than 3 cm. Banded pumices of black and white glass (Figure 8, b) are not common, but they do occur in several localities in all directions and distances around the caldera (*e.g.*, at Epitacio Huerta, Tlalpujahua, Zúñigas and Río Prieto canyons, Figure 2).

Surge deposits are commonly found beneath the major ignimbrites. At some sites these deposits are cross-bedded (Figure 8, c), but at other places they are planar-bedded or with a very low angle cross-bedding. The surge deposits generally occur forming stacks that can be several meters thick. Pyroclastic surges reached to distances over 25 km of the caldera.

Lithic fragments are concentrated at the base of each pyroclastic flow unit. They comprise generally less than 10% of the volume, but two particular ignimbrites, Amealco I and Amealco III, contain zones in the proximal and vent facies that are lithics-rich; 30-35 vol. % and 50-55 vol. %, respectively. Amealco I is lithics-rich in its lower half. The lithics are practically of one type: gray aphanitic trachyandesite. The lithics have angular shapes, and several have ropy lava surfaces. They are probably the remnants of a hypothetical lava dome or cone, that could have been obstructing the vent through which Amealco I was erupted, and that was destroyed during eruption of this pyroclastic flow. The fact that lithics are not deformed next to contorted fiamme favors their interpretation as accidental fragments.

A co-ignimbrite lithic lag breccia deposit related to Amealco III was found in a narrow (~1 km wide) area along the northwestern caldera rim (Figure 8, d). The lag-breccia gradually changes from a blocky deposit to a more pumiceous ignimbrite, within one kilometer of the caldera rim. Along what presumably was the vent, the lag-breccia is well exposed in road-cuts on a dirt road that goes along the northwestern rim of the caldera, from San Juan Hedo to Epitacio Huerta. The breccia is a matrix-supported, polylithologic deposit, with

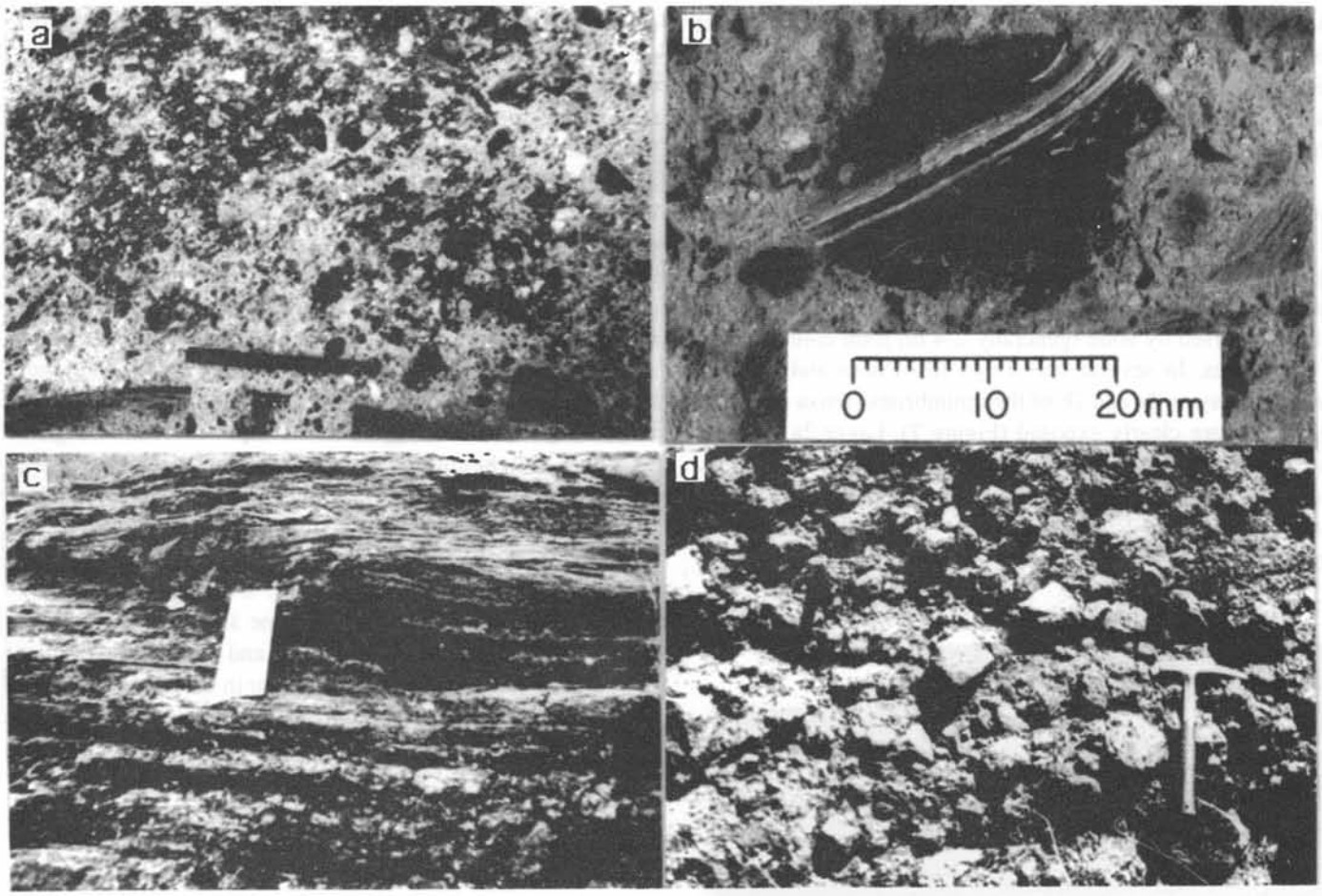

Figure 8. Amealco Tuff ignimbrites showing typical megascopic features. (*a*) Distinct pumice populations, black and white, totally unsorted, in Amealco III ignimbrite (distal west facies); this feature is common in all three Amealco ignimbrites (pen is 13 cm long). (*b*) Banded pumice in Amealco III ignimbrite (distal southern facies). The black glass is trachyandesite and the white is rhyolite (Aguirre-Díaz, 1993a). Note also discrete pumices with different gray shades, indicating the presence of different glass populations. (*c*) Cross-bedded pyroclastic surge deposits of the Amealco Tuff. This particular deposit lies between Amealco I and Amealco II ignimbrites in Epitacio Huerta site (white card is about 16 cm long). (*d*) Co-ignimbrite lithic lag breccia of Amealco III ignimbrite at the vent facies. The breccia is polylithologic, with mafic, intermediate, and felsic volcanic clasts in a pumiceous, weathered matrix. Blocks can be up to 1.5 m in diameter (not shown in picture).

blocks up to 1.5 m. The matrix is pumiceous, weathered, brown to yellow. The matrix becomes more abundant as the distance to the caldera increases. The breccia includes a large variety of volcanic rock fragments, including felsic lava and welded ignimbrites, black scoria, dark-gray intermediate lava, and light-gray porphyritic rocks, which are the most abundant. A single clast of granulite was also found in this breccia (Aguirre-Díaz, 1993c).

Amealco Zero is the name given to an unwelded ignimbrite that is exposed at the base of Epitacio Section (Figure 5). This ignimbrite was only found in this section. Thus, it is believed to have a localized distribution. Pumice fragments are black and 8 cm long in average, and up to 45 cm. The matrix is scoriaceous. The ignimbrite was oxidized to a red, scoria-looking, flow. Black pumice of Amealco Zero yielded the most mafic composition of the Amealco Tuff, and is one of the most mafic products erupted from Amealco caldera (SiO_2=61.6%, in wt. %, normalized volatile-free; sample Am-39, Table 2).

Petrography. Fresh glass is abundant in these rocks as uncollapsed pumice, fiamme, or as shards in the ignimbrite's matrix. A peculiarity of the Amealco ignimbrites, and in some cases the interlayered tephra deposits, is the occurrence of different glass populations (Figures 8, a, b and 9, a). Mingled glasses are found at both the macroscopic and microscopic scales. The matrix of the ignimbrites is composed of glass shards of assorted colors and compositions, and there are also pumice fragments with different colors in the deposit. Amealco's ignimbrites are totally unzoned with respect to the glass compositions; instead, the different pumices and shards are randomly mingled, mostly as discrete fragments. Even though banded pumices are rare, they are ubiquitous and distinctive in the Amealco Tuff.

The ignimbrites contain abundant plagioclase, hypersthene, augite, ilmenite, titanomagnetite, accessory apatite and scarce olivine. Crystal contents vary both laterally and vertically within a single flow unit, but more markedly between flow units. Crystal contents (bulk ignimbrite) range

Table 2. Representative whole rock analyses.

Product	Pre-Amealco Tuff		Amealco Tuff						Rim Lava Domes	
Sample	Am-40	Am-280	Am-39	Am-35	Am-22	Am-21	Am-255	Am-256	Am-133b	Am-195
Unit	Epitacio	Galindillo	Zero	Ame-I	Ame-II	Ame-II	Ame-III	Ame-III	Ame. And.	Ame. And.
Latitude	20°8'1"	20°16'20"	20°8'1"	20°8'1"	20°8'0"	20°8'5"	20°8'5"	20°21'2"	20°9'30"	20°7'54"
Longitude	100°18'8"	100°6'55"	100°18'8"	100°18'8"	100°17'50"	100°17'55"	100°17'54"	100°6'6"	100°8'5"	100°6'55"
Quadrangle	F14C86	F14C86	F14C86	F14C86	F14C86	F14C86	F14C86	F14C86	F14C86	F14C86
SiO_2	60.54	73.27	58.84	59.51	64.38	60.83	63.85	61.14	63.14	59.53
TiO_2	1.25	0.09	1.20	1.21	0.81	1.05	0.71	0.82	1.11	1.42
Al_2O_3	15.52	12.15	15.95	15.97	15.46	15.72	15.25	14.42	15.64	16.09
Fe_2O_3	4.14	0.34	3.53	3.21	1.79	2.40	2.58	2.08	1.95	2.98
FeO	2.85	0.81	3.27	3.92	3.15	4.53	2.15	3.39	4.93	3.84
MnO	0.08	0.03	0.13	0.12	0.09	0.12	0.09	0.12	0.13	0.12
MgO	1.31	0.18	1.79	1.50	1.08	1.49	0.91	1.50	1.59	2.26
CaO	3.72	0.54	4.57	4.02	2.78	4.24	2.73	3.94	3.87	4.87
Na_2O	5.01	3.02	3.85	4.34	4.67	5.24	3.36	3.94	4.90	4.39
K_2O	2.67	5.65	1.96	2.28	3.35	2.83	5.57	3.03	2.88	2.59
P2O5	0.45	0.01	0.47	0.50	0.20	0.37	0.20	0.29	0.39	0.47
$H2O^+$	1.78	3.21	2.29	1.57	1.11	1.55	1.81	2.48	0.22	0.85
$H2O^-$			0.59	0.44	0.15	0.15	0.53	0.52	0.02	0.34
CO_2			0.00	0.00	0.17	0.00	0.00	0.36	0.0.2	0.00
Total	99.12	99.30	98.43	98.58	99.19	100.51	99.74	98.03	100.78	99.75
Normalized, volatiles-free										
SiO_2	62.19	76.25	61.58	61.62	65.86	61.57	65.55	64.58	62.81	60.40
TiO_2	1.28	0.10	1.26	1.26	0.83	1.06	0.73	0.87	1.11	1.44
Al_2O_3	15.94	12.64	16.69	16.54	15.81	15.91	15.66	15.23	15.56	16.33
Fe_2O_3	4.25	0.35	3.69	3.32	1.83	2.42	2.65	2.20	1.94	3.02
FeO	2.72	0.84	3.42	4.06	3.22	4.58	2.21	3.58	4.90	3.90
MnO	0.08	0.03	0.13	0.12	0.09	0.12	0.09	0.12	0.13	0.12
MgO	1.35	0.19	1.87	1.56	1.10	1.51	0.94	1.58	1.58	2.29
CaO	3.82	0.56	4.79	4.17	2.84	4.29	2.81	4.16	3.85	4.94
Na_2O	5.15	3.14	4.03	4.49	4.78	5.30	3.45	4.17	4.87	4.46
K_2O	2.75	5.88	2.05	2.36	3.43	2.86	5.71	3.20	2.86	2.63
P_2O_5	0.46	0.01	0.49	0.52	0.20	0.37	0.20	0.31	0.39	0.48
CIPW Norm (wt%, volatiles-free)										
q	13.59	33.14	17.99	15.37	16.57	8.83	16.88	17.20	12.34	11.59
c		0.13	0.37	0.26						
or	16.19	34.75	12.12	13.95	20.27	16.90	33.74	18.91	16.90	15.54
ab	43.58	26.57	34.10	37.99	40.45	44.85	29.19	35.29	41.21	37.74
an	12.26	2.71	20.56	17.29	11.55	11.18	10.38	13.39	12.15	16.77
wo										
di	2.87				1.02	6.42	1.81	4.31	3.69	3.71
hy	2.03	2.49	6.05	6.74	5.43	5.44	2.30	5.35	7.89	6.42
mt	2.96	0.01	5.35	4.81	2.65	3.51	3.84	3.19	2.81	4.38
il	2.43	0.19	2.39	2.39	1.58	2.01	1.39	1.65	2.11	2.73
ap	1.07	0.02	1.14	1.20	1.58	0.86	0.46	0.72	0.90	1.11
Total	99.99	100.01	100.01	100.00	101.10	100.00	99.99	100.01	100.00	99.99
TT index	75.15	94.56	64.20	67.32	77.29	70.58	79.82	71.39	70.45	64.88
A	48.46	86.90	40.37	43.38	57.17	48.95	61.23	50.03	47.86	43.50
F	43.24	11.27	47.21	46.74	35.17	41.99	32.49	39.24	42.35	42.45
M	8.29	1.83	12.42	9.88	7.66	9.06	6.28	10.73	9.78	14.05
Mg	46.9	28.2	49.4	40.6	37.9	37.0	43.1	44.0	36.5	51.2

Table 2 (continued). Representative whole rock chemical analyses.

Unit	Central dome					Peripheral post-central dome						
Sample	Am-178	Am-53	Am-61	Am-63	Am-64	Am-41	Am-78	Am-179	am-122	Am-18	Am-19b	Am-181
Locality	Campana	Sta. Rosa	Sta. Rosa	La Cruz	La Cruz	Palomas	Hormigas	Mateo	Rincón	Garabato	Comal	Comal
Latitude	20°9'35"	20°7'50"	20°8'49"	20°10'4"	20°9'58"	20°9'28"	20°10'13"	20°7'7"	20°14'15"	20°6'0"	20°5'59"	20°5'57"
Longitude	100°12'8"	100°8'48"	100°10'7"	100°10'20"	100°10'20"	100°16'13"	100°12'31"	100°19'33"	100°14'25"	100°11'50"	100°9'48"	100°9'47"
Quadrangle	F14-C86	F14-C86	F14-C86	F14-C86	F14-C86	F14-C86	F14-C86	F14-C86	F14-C86	F14-C86	F14-C86	F14-C86
SiO_2	65.69	55.55	62.14	68.45	67.37	64.06	56.24	73.55	70.00	61.52	59.19	56.81
TiO_2	0.60	1.44	0.77	0.31	0.32	0.80	1.44	0.04	0.13	0.74	1.06	1.18
Al_2O_3	15.43	17.24	15.87	14.36	14.37	15.71	17.19	12.52	12.50	16.61	15.70	16.59
Fe_2O_3	1.75	3.30	2.10	1.28	0.99	2.19	3.13	0.66	0.89	2.07	1.13	2.56
FeO	2.73	3.48	2.92	1.30	1.62	2.76	4.83	0.46	0.91	2.24	4.53	4.70
MnO	0.08	0.11	0.09	0.04	0.05	0.09	0.13	0.03	0.04	0.09	0.10	0.12
MgO	0.97	3.29	1.65	0.55	0.56	1.64	4.39	0.04	0.19	2.62	4.13	5.35
CaO	2.85	6.75	4.24	1.76	1.79	3.65	7.87	0.50	0.47	5.64	6.09	7.74
Na_2O	4.29	3.98	4.04	3.96	4.31	4.08	3.99	4.14	1.90	3.65	3.69	3.79
K_2O	3.79	1.65	3.29	4.57	4.05	3.23	1.36	4.95	5.93	2.83	2.22	1.78
P_2O_5	0.18	0.39	0.21	0.66	0.08	0.21	0.30	0.01	0.01	0.30	0.31	0.34
H_2O^+	2.44	0.80	1.15	2.89	2.11	1.08	0.62	1.92	4.88	1.07	1.03	0.51
H_2O^-	0.30	1.02	0.31	0.32	0.40	0.51	0.32	0.34	0.90	0.36	0.09	0.22
CO_2	0.00	0.01	0.05	0.00	0.00	0.07	0.00	0.00	0.00	0.18	0.21	0.00
Total	101.09	99.01	98.83	100.45	98.01	100.07	101.80	99.15	98.74	99.93	99.48	101.68
Normalized, volatile-free												
SiO_2	66.79	57.16	63.85	70.40	70.54	65.09	55.76	75.91	75.30	62.57	60.31	56.28
TiO_2	0.61	1.78	0.79	0.32	0.33	0.81	1.43	0.04	0.13	0.76	1.08	1.17
$Al2O_3$	15.69	17.74	16.31	14.76	15.05	15.96	17.04	12.92	13.45	16.89	16.00	16.43
Fe_2O_3	1.78	3.40	2.16	1.32	1.04	2.23	3.10	0.68	0.96	2.11	1.15	2.54
FeO	2.78	3.58	3.00	1.34	1.70	2.80	4.79	0.47	0.98	2.29	4.62	4.66
MnO	0.08	0.12	0.09	0.05	0.05	0.09	0.13	0.03	0.04	0.09	0.10	0.12
MgO	0.99	3.39	1.69	0.56	0.58	1.66	4.35	0.04	0.20	2.66	4.21	5.30
CaO	2.89	6.95	4.35	1.81	1.87	3.71	7.80	0.51	0.50	5.74	6.21	7.66
Na_2O	4.36	4.10	4.15	4.07	4.51	4.15	3.95	4.27	2.04	3.71	3.76	3.76
K_2O	3.85	1.70	3.38	4.70	4.24	3.28	1.34	5.10	6.38	2.88	2.26	1.76
P_2O_5	0.19	0.40	0.22	0.68	0.09	0.22	0.30	0.01	0.01	0.31	0.32	0.34
CIPW Norm (wt%, volatile-free)												
q	18.56	8.77	15.29	25.52	22.72	18.00	6.00	30.61	30.61	15.14	10.27	4.97
c				1.31								
or	22.75	10.05	19.98	27.78	25.06	19.38	7.92	30.14	30.14	17.02	13.36	10.40
ab	36.89	34.69	35.12	34.44	38.16	35.12	33.43	36.13	36.13	31.39	31.82	31.82
an	11.87	24.98	15.89	4.54	8.30	15.23	24.81	1.02	1.02	20.93	20.11	22.76
wo								0.23	0.23			
di	1.02	5.45	3.46		0.32	1.41	9.59	0.76	0.76	4.38	7.00	10.46
hy	4.73	7.41	5.11	2.33	3.09	5.58	10.34			5.92	13.02	12.93
mt	2.58	4.93	3.13	1.91	1.51	3.23	4.49	0.99	0.99	3.06	1.67	3.68
il	1.16	2.81	1.50	0.61	0.63	1.54	2.72	0.08	0.08	1.44	2.05	2.22
ap	0.44	0.93	0.51	1.58	0.21	0.51	0.70	0.02	0.02	0.72	0.74	0.79
Total	100.00	100.02	99.99	100.02	100.00	100.00	100.00	99.98	99.98	100.00	100.04	100.03
TT index	78.21	53.51	70.39	87.73	85.94	73.53	47.35	97.29	97.29	63.56	55.44	47.19
A	59.67	35.87	52.36	73.14	72.49	52.62	30.18	88.73	88.73	48.28	37.63	30.63
F	33.14	43.17	35.88	22.19	22.70	35.62	45.01	10.89	10.89	32.23	36.06	39.96
M	7.19	20.96	11.75	4.67	4.81	11.76	24.81	0.38	0.38	19.49	26.31	29.41
Mg#	38.8	62.8	50.2	42.9	38.0	51.4	61.8	12.9	26.9	67.5	61.9	67.0

Mg#, molecular using volatile-free normalized values. Mg# = MgO / (MgO + FeO)·100.
TT index is the Thornton and Tuttle index of differentiation (Thornton and Tuttle, 1960).
A, F, M are AFM triangle coordinates (Tilley, 1960). A = Na_2O + K_2O, F = FeO + Fe_2O_3, M = MgO, in wt. % normalized volatile free.
All samples were analyzed by Gerardo Aguirre-Díaz in the University of Texas at Austin, using Inductively Coupled Plasma-Atomic Emission Spectroscopy (ICP-AES), the Penfield method for total water determination, and the acid-evolution-gravimetric method for CO_2 (modified after Johnson and Maxwell, 1981).
Ferrous iron was determined titrimetrically using Wilson's method (Johnson and Maxwell, 1981).
Optimus data quality in estimated error in % for the ICP-AES is: SiO_2 (1.5-2.5), TiO_2 (1.5-2.5), Al_2O_3 (0.5-1.5), FeO total (1.5-2.5), MnO (1.5-2.5), MgO (1.0-2.5), CaO (1.5-3.0), Na_2O (1.5-3.0), K_2O (1.5-3.0), P_2O_5 (1.5-2.5).

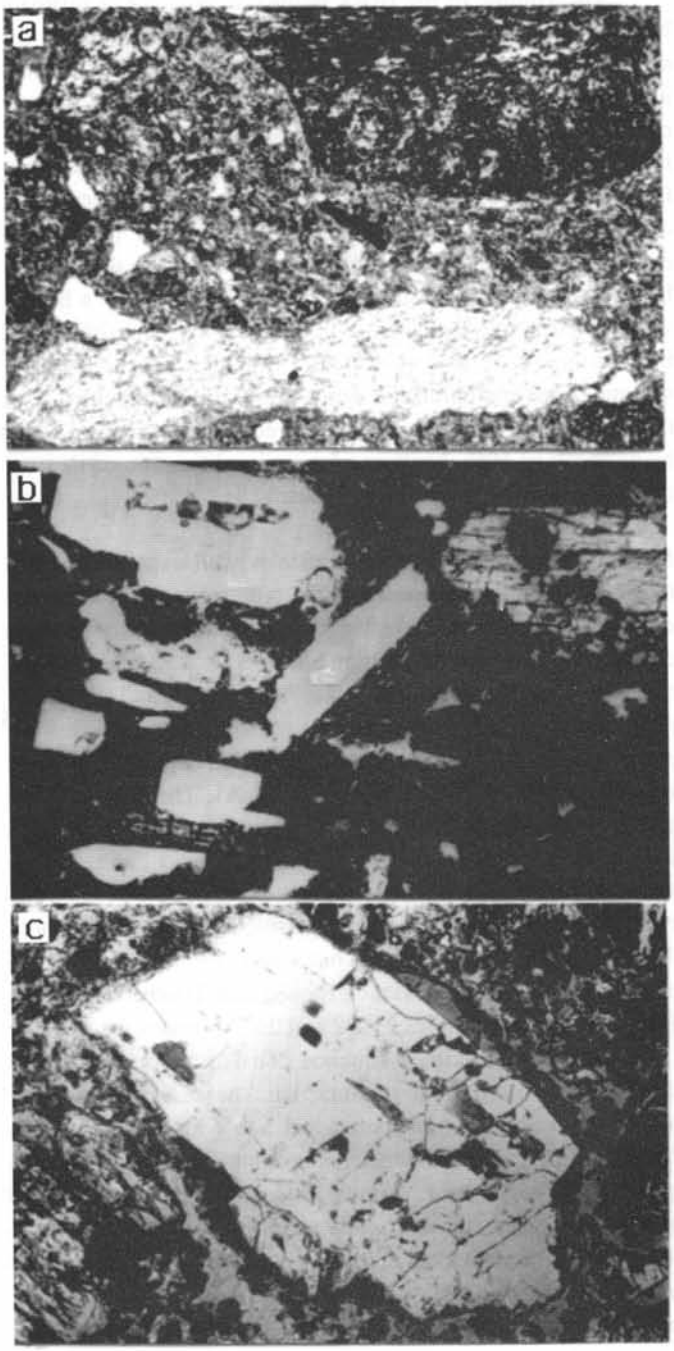

Figure 9. Microscopic features of the Amealco Tuff ignimbrites. All photomicrographs taken with transmitted light (Pl: plagioclase, Opx: orthopyroxene, Cpx: clinopyroxene). (*a*) Different glass populations in the form of black and white pumices. Both pumices deformed equally during welding and compaction of the ignimbrite (longest dimension is 11 mm). (*b*) common mineral phases in the Amealco Tuff ignimbrites: plagioclase, clinopyroxene, orthopyroxene and Fe-Ti oxides; plagioclase (upper-left) exhibits large glass and fluid (bubble) inclusions (longest dimension is 3.5 mm). (*c*) another example of large glass inclusions in plagioclase of the Amealco ignimbrites (longest dimension is 1.7 mm).

from <5 to 37 vol. %. The most common crystal content is around 20 vol. %. Large brown and pale yellow glass inclusions commonly occur within plagioclase phenocrysts (Figure 9, b, c). Occasionally, inclusions of Fe-Ti oxides occur in plagioclase too. The large glass inclusions may have formed by resorption due to fast decompression (Nelson and Montana, 1992), or by trapping of glass during fast growth of the plagioclase (Halsor, 1989), rather than by resorption of the plagioclase by mixing of magmas (Tsuchiyama, 1985). Large glass inclusions in plagioclase are also reported in products of magma mingling (J. Pallister *et al.*, in press).

Brick pumice

Definition. Volcanoclastic deposits that include pumice-flows, epiclastic deposits, coarse-grained pumice fallouts, and fine-grained surge deposits, overlie the Amealco Tuff near the caldera. These deposits were informally named "Brick pumice" by Sánchez-Rubio (1984), as the indurated pumice deposits are quarried in the form of bricks which are locally used for construction (Figure 10, a, b). This name is retained in this study. The pyroclastic and epiclastic deposits of the Brick pumice either underlie, overlie, or are interbedded with the lava of the rim lava domes (Amealco Andesite; described below). No attempt was made to map them as separate (pre-, co-, or post-rim lava domes) volcanoclastic units. This is because in localities where units from the rim lava domes are absent, for instance, farther than 7 km from the caldera rim (Plate 2), they are megascopically indistinguishable from each other. Therefore, Brick pumice is the unit that includes the pyroclastic and interbedded epiclastic deposits that were erupted before, during, and after the rim lava domes. Brick pumice represents the last relatively large explosive episodes of the Amealco caldera after the Amealco Tuff. No chemical analyses were performed in this unit because no fresh samples were found; most of the pumice is weathered.

Distribution and volume. The pumice deposits have a more localized distribution than the Amealco Tuff. They crop out up to 20 km from the caldera, and occur mainly east of it (Figure 3; Plate 2). Brick pumice is practically absent in the north-northwestern directions. The exposed area occupied by the Brick pumice is nearly 134 km^2, of which 111 km^2 occur in the eastern and southeastern outcrops, 5.5 km^2 in the northeastern outcrops, and 17 km^2 in the western and southwestern outcrops.

Some Brick pumice episodes occurred contemporaneously with the emplacement of the rim lava domes. At the western caldera rim, the Brick pumice occurs either interbedded with, or overlying the rim lava domes (measured sections 19 and 20, Appendix A). On the northeastern flank of the caldera, and along the Amealco-Temascalcingo highway, these deposits are covering the rim lava domes (measured sections 21, 22, and 23, Appendix A). Near Los Arcos, at the southeastern caldera rim (Figure 3), and also at a site 8 km to the southeast of the caldera, Brick pumice deposits occur beneath lava from the rim lava domes. Farther (>7 km) from the caldera rim, Brick pumice generally overlies only the

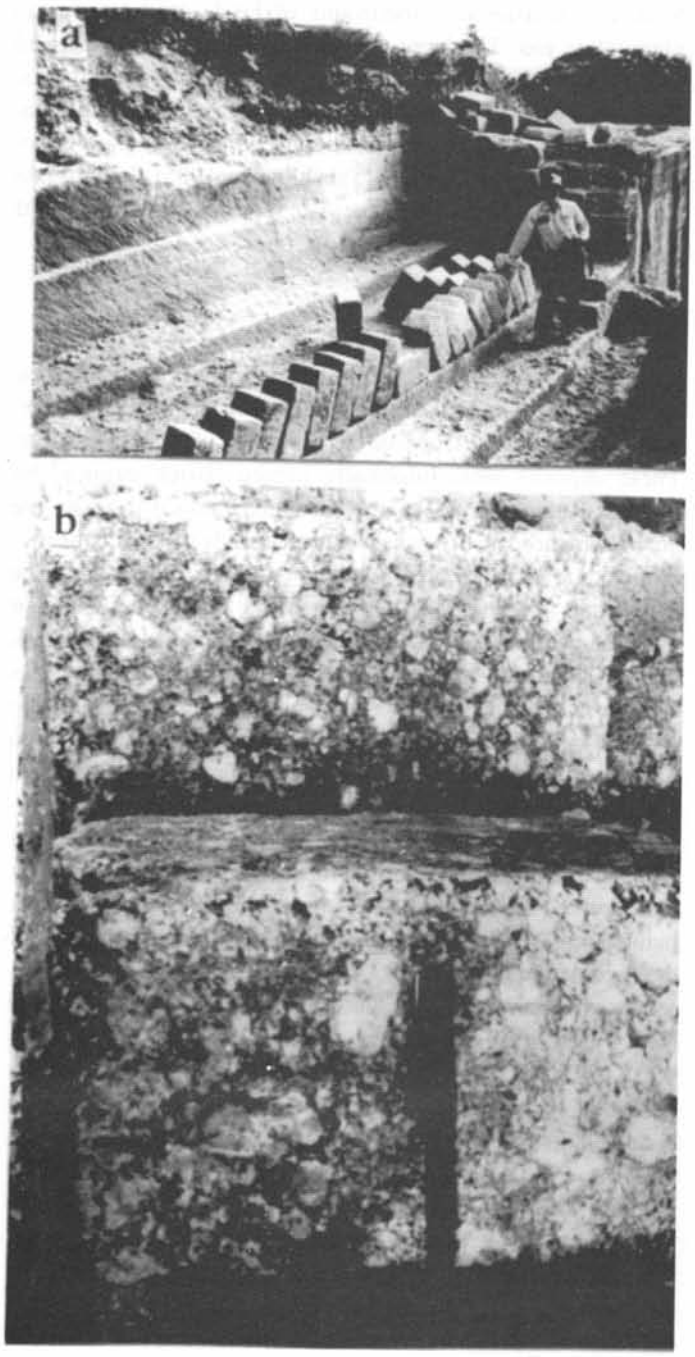

Figure 10. Brick pumice in a quarry on the eastern caldera rim. (*a*) Post-Amealco Andesite indurated pumice flow that is quarried for bricks, which is the reason of the name of this unit; the deposit is soft, easy to quarry, and light, but still well indurated by sintering in such a way that it does not disaggregate and makes the rock an ideal building material. (*b*) Detail of deposit shown in (*a*); note the unsorted nature of the pumice clasts (pen is 13 cm long).

Amealco Tuff, but it also covers La Loma Andesite 15-17 km to the east of the caldera (Plate 2). To the west, Brick pumice is covered by lava erupted from Palomas volcano (Plate 2). In the most distal outcrops, about 20 km east of the caldera, it is overlain by the Huichapan Tuff (Plate 2); a 1 m thick paleosoil separates the Huichapan Tuff from the Brick pumice at this locality (section 15, Appendix A).

The volume of the Brick pumice is difficult to estimate because the sequence is generally incomplete. In addition, the deposits have a very irregular distribution with local thickness and lithologic variations. For instance, some sections include epiclastic deposits, others do not, and others are massive (>15 m thick pumice flows; *e.g.*, Los Arcos pumice), whereas others include several meters of thinly layered surges. Nevertheless, a minimum volume of 3.9 km^3 of rock, and 2.3 km^3 (DRE) was estimated for this unit, assuming that half of the deposit are lithic-rich surges and mud-flows, and the other half a highly vesiculated aphyric pumice, which is a rough simplification, but reasonable in most sites. This value includes the physical volume of several epiclastic deposits that are interbedded with the pumice deposits. The error involved in the estimation could be as much as 50%, because of oversimplification of the real distribution and nature of the deposits.

Field description. The Brick pumice is well exposed in three localities, which are proposed as the type sections for members erupted before, during, and after the emplacement of the rim lava domes. The pre-rim dome section is at a sequence 8 km to the SW of the caldera (measured section 24, Appendix A) and at a quarry near Los Arcos village, along the faulted southeastern flank of the caldera (Figure 3), where 15 m of a pumice deposit is exposed incompletely (section not in Appendix A). The co-rim dome deposit is located at the southwestern caldera rim, near Cañada de García, along a normal fault of the Epitacio Fault system, where a complete pyroclastic section is exposed bracketed between lava of the rim lava domes (measured section 19, Appendix A; Plate 2). The post-rim dome outcrops occur adjacently to the eastern caldera margin, and are exposed near Tenango (Figure 3; Plate 2; measured sections 21, 22 and 23, Appendix A).

The pre-rim dome sequence consists of pumice flows interbedded with pumice fallouts. Thicknesses of fall or flow units are variable, ranging between 1.5 to 4 m. Pumice in both flow and fall deposits is white, coarse lapilli (1-3 cm), subangular, and crystal-poor. Pumice flow deposits are indurated and pumice fragments are totally unsorted. Pumice fall deposits are not indurated, lack matrix, and show sorting, either normal or inverse. The quarry near Los Arcos is a 15 m thick massive pumice flow deposit. This section was not measured. In contrast to other pre-dome sequences, the deposit at Los Arcos is unlayered. This may be because the pumice at Los Arcos is the near-vent facies of a pumice flow (or flows?) and represents a single eruption from a ring fracture vent of the Amealco caldera, whereas sites farther from the vent include fall and flow units. In general, the pumice clasts at Los Arcos quarry are coarse-grained, angular to subangular, unsorted, and up to 5 cm in diameter, but generally 2-3 cm in size. The pumice is white to pale yellow. It is crystal-poor, with less than 5 vol. % of phenocrysts. Vesicles in pumice are generally spherical, but occasionally pipe vesicles are also observed. The pumice deposit is overlain by an intermediate lava flow associated with the rim lava domes.

The co-rim dome sequence is exposed complete near Cañada de García (Figure 3; measured section 19, Appendix A). The Brick pumice rests atop intermediate lava flows and breccias associated with the emplacement of a rim lava dome, and it is covered by an approximately 10 m thick platy-jointed trachyandesitic lava flow that was erupted from El Bellotal rim lava dome (Figure 3). The sequence consists of a lower stack of massive, unlayered, white, pumice flows, which are overlain by a stack of thin-bedded blue-gray pyroclastic surge deposits that contain abundant dark-green scoria fragments rich in mineral clots of clinopyroxene+orthopyroxene+glass. The surge beds are composed of lithics and crystals, with a pumiceous+lithics matrix. A couple of pumice fallouts with wavy layering is intercalated with these deposits at about the middle of the sequence. The wavy layering was due to mantling of pre-existing uneven topography by the air-fall deposits. This and other nearby co-rim dome deposits apparently overlie a densely welded ignimbrite issued from Amealco, but the contact among them is covered.

The post-rim dome sequence (measured sections 20, 21 and 22, Appendix A) is composed of indurated pumice flow, epiclastic, and surge deposits. The sequence is layered, with each deposit generally less than 1 m thick. Pumice in the pumice flow deposits is generally white, or yellow when weathered, but the upper deposits in the sequence contain gray or black pumice and scoria. The pumice is not deformed by compaction. Induration of the deposits was caused to primary sintering of the pumice fragments by a fine (generally <1 mm) pumiceous matrix. The epiclastic deposits are not indurated and consist of reworked pumice mixed with fluvially transported, rounded lithics, up to 30 cm in diameter. Some of them could be classified as mud-flow deposits, others as fluvial torrent flows (Cas and Wright, 1987, p. 297); mud-flows are richer in matrix than the fluvial torrent flows, which in turn are more clast-rich. At the site where section 22 was measured peculiar pumice veins cut part of the pumice sequence. Veins are up to 3 cm wide, and do not show a preferred orientation. Dip orientation is N40–80°W and its inclination is 56–70°. The pumice veins were probably formed by loading of later erupted pumice over earlier erupted pumice, which was still hot and was squeezed through joints into the younger deposits. These veins are more resistant to erosion than the poorly consolidated pumice deposits that host them, and now they crop out as a thin-walled network of indurated pumice standing several centimeters above the surrounding croded pumice. Surge deposits generally occur at the top of the post-rim dome sequence. They are commonly blue-gray and thinly layered (layers 5-10 cm thick), rich in angular and small (<1 mm) lithics and crystals, in a pumiceous and lithics matrix.

An equivalent, but distal, post-rim dome sequence occurs near Santiago Mezquititlán (measured section 16, Appendix A). It includes pumice flow deposits interlayered with epiclastic deposits. The main differences between the proximal and distal deposits are that (1) the distal facies lack surge deposits; (2) the lithics in the proximal facies are mainly of welded Amealco ignimbrites, whereas in the distal facies the deposits are richer in lithics of andesite from underlying La Loma andesite, and (3) the size of the pumice lapilli, which is smaller in the distal facies. A little farther to the east, at the bridge of the Amealco-Aculco highway over the Piedras Grandes stream (measured section 15, Appendix A), layered pumice deposits similar to those of the Brick pumice at Tenango and Mezquititlán are covered by pumice deposits of the Huichapan Tuff. It is not clear, however, if these deposits correspond to the Brick pumice unit or to uppermost pyroclastic deposits of the Amealco Tuff, that were preserved in this site due to protection by Huichapan Tuff. A brown paleosoil, up to 1 m thick, separates Amealco's pumice deposits (either Brick pumice or Amealco Tuff) from those of the Huichapan Tuff at measured section 15 (Appendix A).

Petrography. Three main types of pyroclastic deposits are found in the Brick pumice unit: pumice-flows, surges, and pumice fallouts. All three contain the same mineralogy as the Amealco Tuff deposits: plagioclase, orthopyroxene, clinopyroxene, and Fe-Ti oxides. Total crystal content ranges from 10 to 25 vol. %. Pumice flows contain a thin glassy matrix, whereas pumice fall deposits lack this matrix. Both are mainly composed of coarse pumice lapilli, which is sorted and with a crude normal gradation in the fall deposits and unsorted and ungraded in the flow deposits.

Amealco Andesite (rim lava domes)

Definition. Several lava domes, intermediate in composition, were emplaced along a ring-fracture at about 4.3 Ma (Table 1), forming an arcuate belt with an almost perfect circular shape, 11 km in diameter (Figure 3; Plate 2). This unit was named Amealco Andesite by Sánchez-Rubio (1984, p. 117). Although the rock is not really andesite but trachyandesite (samples Am-133b and Am-195, Table 2), the name is retained in this study because it does not create stratigraphic discrepancies, and because the rock does look like a mafic, porphyritic andesite, both in hand specimen and in thin section. Only with the aid of chemical analysis it is possible to distinguish it as trachyandesite.

Distribution and volume. Amealco Andesite is mostly confined to the rim of the caldera, forming a <1.5 km wide arcuate belt, but a few lava flows and breccia that extend beyond and outward from this belt were derived from ring-fracture vents along the caldera rim, and are also part of the Amealco Andesite. These flows reach up to 4.5 km from the rim. The outward distribution of Amealco Andesite and the appearance of being cut by caldera-related faults (Plate 2; the arcuate thick, ticked line in Figure 3 represents the caldera outline and not a caldera fault), suggest that collapse may have continued after emplacement of the Amealco Andesite. Although this could have occurred, no evidence of faulting was observed along the caldera rim, neither were found caldera-mar-

gin collapses of megablocks or megabreccias, generally related to caldera collapse. Thus, it is still uncertain if Amealco Andesite (and coeval Brick pumice) were emplaced when collapse was still occurring, or are post-collapse.

The DRE volume estimated for this unit is 3.5 km^3 and covers an area of 7.7 km^2, which includes the lava flows associated with the domes. The domes have elevations up to 2,750 m a.s.l. (400 m of relief with respect the adjacent Tepuxtepec reservoir), but generally are hills with elevations around 2,650-2,700 m a.s.l. The lowest part of the inner caldera valley is 2,400 m a.s.l., therefore the height of the rim lava domes with respect to the elevation of the inner caldera valley is 250 to 300 m.

Amealco Andesite is generally well exposed, particularly at road-cuts along the Amealco-Temascalcingo highway on the eastern caldera rim, and through dirt roads along the northern and northwestern rim (Plate 2). Access is more difficult in the western rim, but Amealco Andesite is also well exposed along the inner caldera rim (measured section 20 at El Bellotal, Appendix A).

Field description. Amealco Andesite is generally platy-jointed, dark gray to black when fresh (Figure 11, a). It shows a wide range in textures, from porphyritic and relatively crystal-rich to phenocryst-free, glassy rocks. The most common occurrence is porphyritic. A wide spectrum of lithofacies is also observed; the rock can be massive, platy-jointed, blocky and brecciated, or vesiculated. The textures and rock type variations are due to the different lithofacies that a single dome can exhibit from its internal to external zones. For instance, a 152 m section measured at the western rim (measured section 20, Appendix A) is an exposure on the inner side of the caldera rim at El Bellotal lava dome (the highest of all; Plate 2). The lithology gradually changes from a volcanic breccia at the bottom of the sequence, to platy-jointed lava flows interbedded with pumice plus lithics lapilli layers in the middle of the sequence, to glassy and crystal-poor lava at the top, over which more tephra was deposited. The interbedded and overlain pyroclastic deposits correspond to the Brick pumice. They indicate that explosive activity, although minor, was still occurring during, and after, the emplacement of the Bellotal dome. The glassy top may be the chilled margin of the lava dome, and the basal brecciated zone may represent the initial emissions or the external brecciated zone of this dome.

Another example occurs on the eastern caldera rim, along the road to San Miguel Tlascaltepec (Figure 3). At this site there is also a good exposure of one of the rim lava domes that shows the different zones that are commonly associated with lava domes. Within a few tens of meters, the rock in the lava dome changes from massive in its internal zone to platy-jointed (Figure 11, a) outwards, to a narrow zone of vesicular blocky rock that quickly changes to a very blocky, almost brecciated, external zone. The rock also changes from crystal-rich at its inner zone to more glass-rich at the outer zone. Although a glass crust at the outermost "layer" of the dome was not found, black, phenocryst-free, glassy crusts were found at several sites along the rim. All these characteristics (high domes protruding from, or with, external crumble breccia surrounding them, associated with pyroclastic and lava flow events during their growth) suggest that they grew as something intermediate between peléean type and coulée type domes (as defined in Blake, 1990), and are thus exogenous domes (Fink, 1987; Blake, 1990).

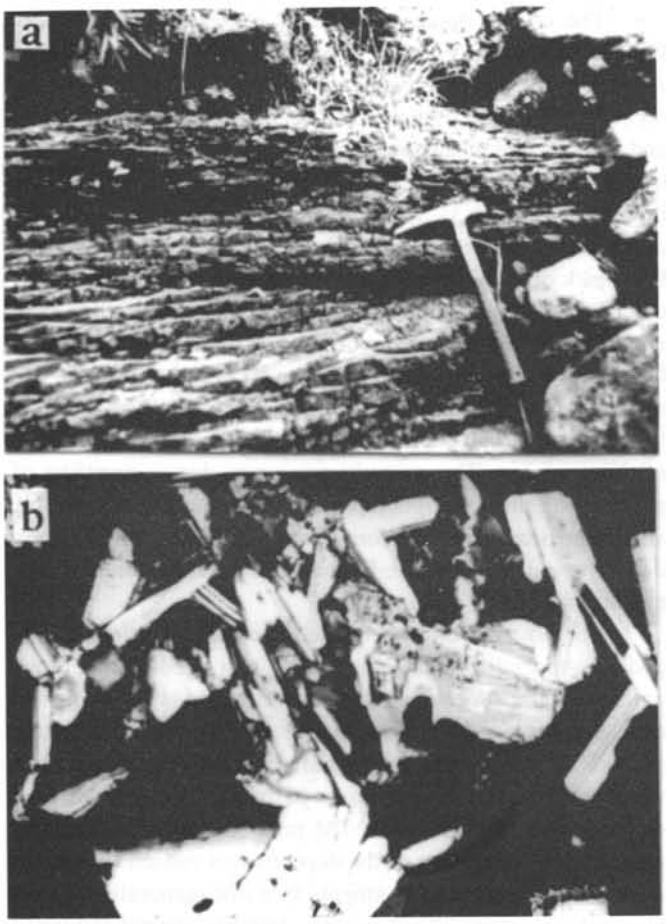

Figure 11. Amealco Andesite: (*a*) Outcrop on the northern caldera rim, near San Juan de Hedo, showing the well-developed platy-jointing of the rock. (*b*) Photomicrograph of the rock shown in (*a*); glomerocryst of plagioclase+pyroxenes+Fe-Ti oxides in a fine-grained, glass-rich, matrix (polarized light, longest dimension is 1.7 mm).

Leached and oxidized zones, up to 300 m wide, are observed at several sites along the caldera rim, particularly at road-cuts in the Amealco-Temascalcingo highway. These altered zones contain fossil fumaroles and vertical breccias that cut through the lava domes. Botryoidal chalcedony coats these breccias and fills vesicles and cavities in the host brecciated rocks. Opal is also found sparsely in these altered zones. The altered rock and fumarolic zones probably indicate the proximity of the vents that fed the domes.

Petrography. Amealco Andesite contains plagioclase, orthopyroxene, clinopyroxene, Fe-Ti oxides, apatite, and rare olivine.

Glomerocrysts containing these phases (except olivine) are quite common (Figure 11, b), and make about 15 vol. % of the crystal content. Glomerocrysts are rather large, up to 6 mm in size. Glass in the glomerocrysts is either intergranular or, more commonly, also attached externally to the phenocrysts.

Campana Dacite

Definition. Campana dome was the name given by Sánchez-Rubio (1984, p. 115) to a lava dome that lies on the northwestern caldera wall (Plate 2). He described it as rhyolite, but it really is trachydacite (SiO_2=66.8%, normalized volatile-free; sample Am-178, Table 2). Verma and others (1991) included this dome in their "silicic domes" group. Campana dome is closer in time and location to the rim lava domes (Amealco Andesite); its age of 4.3 Ma falls within the range of Amealco Andesite (sample Am-79, Table 1), and the dome is right on the caldera rim. However, in spite of lying close in time and in space to Amealco Andesite, Campana dome is a more evolved rock. In addition, it has a different geomorphology; it is a cone-shaped structure with steep flanks that stands above the caldera rim. Because of these differences with respect to Amealco Andesite, the author decided to describe it as a separate unit. The name of Campana is retained, but redefined as "Dacite" (in fact a trachydacite), and as an independent unit, which is not part of the central lava domes (La Cruz Rhyolite) or the rim domes. The lava dome overlies Amealco Andesite and its lower flank inside the caldera is overlain by La Cruz Rhyolite (Plate 2; Figure 3).

Distribution and volume. Campana dome has a very localized distribution, confined practically to the proximity of the vent (its single source), right on the northwestern rim of the caldera (Figure 3). It covers an area of 2.62 km^2, and comprises a volume of 0.8 km^3. The dome overlies the co-ignimbrite lithic lag breccia of Amealco III ignimbrite. Its southern and southeastern flanks cover Amealco Andesite down to the bottom of the inner caldera valley, where the Campana dome is in turn covered by reworked pumice deposits. To the west it covers the crest of Amealco Andesite's rim domes. It is overlain by La Cruz Rhyolite at its southeastern flank.

Field description. Campana Dacite is a dark-gray, glassy rock, with a flow-banded structure, and very hard to break with the hammer. The lava may have been quite viscous since the dome preserves 30° steep flanks. A vent with crater shape is still observed at its top giving the dome the appearance of a cinder cone in aerial photographs. The dome is heavily covered with vegetation, so it is well exposed in few sites. Particularly good outcrops are found aside the dirt road between San Juan Hedo and Epitacio Huerta. No brecciated or layered lava was found. Apparently the dome is wholly composed of a massive but flow-banded lava body, with no evidence of breaks. Crystals are parallel, but no jointing is observed.

Petrography. The rock is porphyritic, with a perlitized, colorless, glassy matrix (vitrophyric texture). Phenocryst content (25 vol. %) includes plagioclase (15%), clinopyroxene (3%), orthopyroxene (3%), Fe-Ti oxides (3%) and biotite (1%). Glomerocrysts are uncommon, with sizes up to 4 mm, and are formed of plagioclase, two pyroxenes, and Fe-Ti oxides. Single plagioclase crystals contain abundant, colorless glass inclusions with irregular amoeboid shapes. Some plagioclase shows skeletal growth in the core, mantled by an inclusion-free zone, but with a jagged, resorbed margin. All these characteristics suggest that plagioclase grew relatively fast, re-equilibrated with the surrounding liquid, and then was resorbed. Orthopyroxene and clinopyroxene are much smaller than plagioclase, with sizes up to 1 mm. Crystal clots invariably contain both pyroxenes in addition to plagioclase and Fe-Ti oxides. Both pyroxenes commonly contain large Fe-Ti oxide inclusions, up to 0.2 mm. Biotite is rare, but when present it is up to 2 mm in size. It is mottled and shows a reaction corona of Fe-Ti oxides and clinopyroxene.

Palomas Dacite

Definition. This unit was named the Palomas Rhyolite by Sánchez-Rubio (1984). However, Palomas is not rhyolite but trachydacite (according to the classification of Le Bas *et al.*, 1986, Table 2). Verma and coworkers (1991) misinterpreted this volcano as a dome, but they do not provide a field description of this unit, so their reasoning for interpreting it as a lava dome is unclear. Furthermore, Verma and coworkers (1991) and Sánchez-Rubio (1984) assigned a pre-caldera age to this volcano, but the lava of the Palomas volcano overlies the Amealco Tuff (see below). Aguirre-Díaz (1993a) named it Palomas Andesite, as in hand specimen and petrographically looks like an andesite, but since it has not an andesite composition that name is also misleading. Thus, the name "Palomas" is retained in this study, but with the modification of "Dacite" instead of "Dome" or "Rhyolite" or "Andesite" as defined before in other reports.

Distribution and volume. The Palomas volcano has an almost perfect conical shape, with slopes of about 15°, and a height of 200 m with respect to the adjacent plateau, which is covered by lava erupted by this volcano. The volcano and associated lava flows cover an area of approximately 40 km^2. A DRE volume of 0.6 km^3 is estimated for this unit. The cone itself has an area of only 2.2 km^2, but the lava flows erupted from it reach as far as 8 km to the northwest of the volcano, where they are cut by the Epitacio fault (Figure 3). The flows flooded the area west of the vent, probably due to the relatively flat pre-existing terrain left by the Amealco Tuff ignimbrites. The lava of Palomas flowed easily down to the west on this smooth surface. The peak of El Espía dome, just to the north of Palomas volcano, is almost totally surrounded by the Palomas lava flows. Cerrito Colorado, a small scoria cone to the west of the Palomas vent is also partly buried by the Palomas flows (Figure 3), however, Cerrito Colorado had previously been almost totally covered by the Amealco Tuff, and

probably was not a difficult obstacle to surmount by the Palomas flows. The westernmost outcrops of the Palomas lava flows are cut by the NW-oriented Epitacio fault at the west and by another E-W fault at the northwest (Figure 3); thus, the westward flows of the Palomas volcano surely reached farther from the vent than the presently exposed distribution. The Palomas lava overlies pre-Amealco Tuff andesite near the site where they are cut by Epitacio fault (Figure 3). The eastern flows are rather short, reaching only 2 km from the vent. Palomas Dacite is not overlain by younger volcanic rocks.

Field description. The cone is composite, made up of several lava and scoria flows with a horizon of tephra intercalated. The Palomas unit is well exposed along the western flank of the cone and at outcrops along Federal Highway 120 (Figure 3). The lava flows show distinct textures from the first-erupted to the last-erupted. The lowermost observed flows, which directly overlie the El Espía dome and the Amealco Tuff to the north of the cone, are crystal-rich, porphyritic, gray rocks, but their main feature is the relatively large hornblende content (10 vol. %). These hornblende-rich flows make a smooth hill northwest of the vent and surround the El Espía dome on its western side. They are overlain by a sequence of more lava flows, scoria-flows and tephra. The phenocryst content, particularly hornblende, decreases up section, so that the last erupted lava either lacks hornblende or contains little. The scoria flows have a localized distribution, only seen within and next to the cone. They are reddish-brown or purple-gray vesicular rocks. The last-erupted lava flows occur to the west of the volcano. They are black aa lava, yellow in weathered surfaces. Immediately to the west of the volcano, an E-W normal fault cuts these blocky flows (Figure 3). Along the fault scarp, it is possible to observe their base overlying Amealco III ignimbrite.

Petrography. The volcanic sequence erupted from Palomas volcano shows marked textural differences from the first to the last erupted products (see Appendix C for details). Phenocryst content and crystal size decrease with time; phenocryst content varies from about 30 to 15 vol. %, and crystal sizes from 3.2-1 mm to 2-0.3 mm. It includes plagioclase, hornblende, orthopyroxene, clinopyroxene, and Fe-Ti oxides. Hornblende is abundant in the early-erupted products (10 vol. %) and is practically absent in the middle and late products (scoria flows and aa lava). This change is parallel with an increase in the orthopyroxene content with time. The last erupted products (aa lava) are practically similar in texture to some lithofacies of the Amealco Andesite. The textural variation observed through the volcanic evolution of Palomas is not rare in volcanoes about the size of Palomas; for instance, Parícutin and Jorullo volcanoes exhibit textural and compositional differences from early to last erupted products (Wilcox, 1954; Luhr and Carmichael, 1985).

La Cruz Rhyolite

Definition. Five rhyolitic lava domes were erupted within the Amealco caldera at 3.9 Ma, named here La Cruz Rhyolite. Sánchez-Rubio (1984) named San Miguel Rhyolite the domes occurring west of San Miguel Tlascaltepec, in the center of the caldera, and Amealco Dacite the domes clustered in the northern part of the caldera (Figure 3; Plate 2). The name Amealco Dacite should be abandoned, because the rock so defined is not dacite, but rhyolite, in many cases a perlitized flow-banded glass. Another reason is because this name separates the felsic lava domes from the north of the caldera (Amealco Dacite) from those in the center of the caldera (San Miguel Rhyolite). Both Amealco Dacite and San Miguel Rhyolite are rhyolite and should be given the same name, proposed here as La Cruz Rhyolite, because the lava domes that make the hills with this name represent this felsic unit well. Therefore, La Cruz Rhyolite includes La Cruz de Chiteje and La Cruz de San Juan (former Amealco Dacite), and the three small domes of El Barco (former San Miguel Rhyolite).

Distribution and volume. The lava domes that form La Cruz Rhyolite occur in two clusters, one in the northern portion of the caldera, and the other in the central-eastern part (Figure 3). The northern domes, La Cruz de Chiteje and La Cruz de San Juan, are the largest of the rhyolite domes. They ponded against the northern caldera wall (Figure 3). One of them, La Cruz de San Juan, partly covers the caldera rim. The El Barco domes form the cluster in the center. They are three smooth low hills (Figure 12) with a north-south alignment (Figure 3). La Cruz Rhyolite covers the Amealco Andesite along the northern rim of the caldera (Figure 3). It is partially covered by lava from the Santa Rosa Andesite in the center of the caldera (Figure 3).

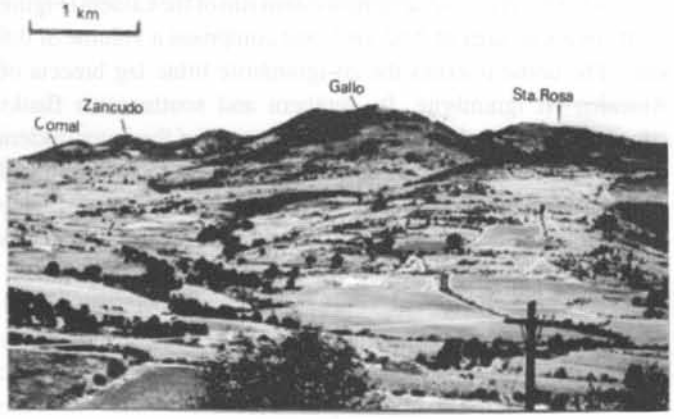

Figure 12. View to the west from the eastern caldera rim of the central lava domes; the highest hill is the trachyandesitic El Gallo dome, with an elevation of 3,000 m a.s.l. South and north of it are the Zancudo and Santa Rosa domes, respectively (also trachyandesite). All these trachyandesite lava domes are named Santa Rosa Andesite. The rhyolite domes (La Cruz Rhyolite) are the smooth low hills at the foreground (El Barco domes); others lie farther to the north from Santa Rosa dome (not shown). El Comal cone is the small, last hill to the left (south) and lies on the fault that displaced the southern portion of the caldera (see also Figure 3).

The total volume of La Cruz Rhyolite is 2.4 km^3, of which the northern domes make 1.9 km^3, and the El Barco

domes 0.5 km^3. The volume of La Cruz Rhyolite represents only 5% of the total magma emitted by Amealco caldera; the remaining 95% is practically of intermediate magma (this estimate does not include the rhyolitic—white—pumice mingled with the dark pumice of the Amealco Tuff, which commonly is 5-10 vol. % of a flow unit, and rarely 20 vol. %). Thus, the bulk of the caldera products are intermediate in composition.

Field description. La Cruz Rhyolite is a glassy, perlitized, flow-banded and light-gray lava. Fresh rock is harder to find than in the intermediate domes, which are more resistant to weathering. More commonly the felsic domes have weathered crust, several cm thick, of a white, clayey material or are covered by soils in heavily forested areas. Several outcrops are found along, and/or near the dirt road that enters the caldera from the northern rim (San Juan Hedo) mentioned above. A particularly different kind of rock crops out on the western lower flank of La Cruz de Chiteje dome, before entering into the canyon of Las Canoas stream. The rock at this site consists of *in situ* boulders with a concentric circular arrangement. In contrast to the pale-gray, glassy and flow-banded rhyolite of other sites, the rock is dark-gray and porphyritic when fresh and without flow-banding. A thin (a few mm), yellow weathered crust covers the fresh rock. In spite of these textural differences, the rock has a low-silica rhyolite composition (SiO_2=70 wt. % normalized volatile-free, Table 2). Another uncommon occurrence is a crumble breccia; that is, a matrix-free, clast-supported breccia, exposed at a quarry on the eastern flank of La Cruz de Chiteje dome. The breccia consists of subangular equant-sided pebbles and blocks ranging in size from a few cm to 30 cm. The deposit shows a crude layering, with layers 0.5 to 2 m thick. The layers are dipping steeply (30°) outward from the dome. The blocks are a flow-banded, porphyritic, glassy rock, pink to light gray. A channeled block-and-ash flow, 3 m wide and 2 m thick is also observed in this quarry. The flow contains blocks similar to those in the crumble breccia. It may have been formed as a Merapi-type eruption from the flank or the summit of La Cruz de Chiteje lava dome. This flow has a very local distribution and was exposed thanks to the digging in a quarry. Perhaps similar flows are more common, but they remain unexposed.

The domes of El Barco are flow-banded, gray, glassy rhyolite. A peculiar characteristic of these domes is that they contain round, green enclaves as big as 3 cm. The enclaves are crystal clots with two pyroxenes (see *Petrography*, below). The freshest lava of El Barco domes is found at the lowermost outcrops along the road to San Miguel Tlascaltepec, near the San Miguel dam. The rock at these outcrops is quite fresh, dark gray, glassy, and porphyritic.

Petrography. La Cruz Rhyolite has distinct features with respect to the Amealco caldera units so far described. Mineralogy is practically the same, but textural differences are evident. The rhyolite has a perlitic vitreous texture. It is porphyritic, with a crystal content varying between 10 and 15 vol. %. The matrix is a perlitized, colorless to pale pink glass. It contains plagioclase (8-10 vol. %), orthopyroxene (2-3 vol. %), Fe-Ti oxides (1-2 vol. %), and sparse biotite (<1 vol. %). Some domes, such as El Barco, also exhibit clinopyroxene (1-2 vol. %) and rare olivine phenocrysts that form part of crystal clots (see below). Apatite is accessory. Although the rock has a rhyolite composition, modal quartz and alkali feldspar are absent. Large (up to 3 cm in diameter) enclaves, green in hand specimen, are common features in these rocks. The enclaves are crystal clots with an interlocking texture, of plagioclase + pyroxene + Fe-Ti oxides and rare olivine (Figure 13); the space among crystals is occupied by yellow-brown glass. These enclaves may be fragments from the solidification zone of the magma chamber (Langmuir, 1989).

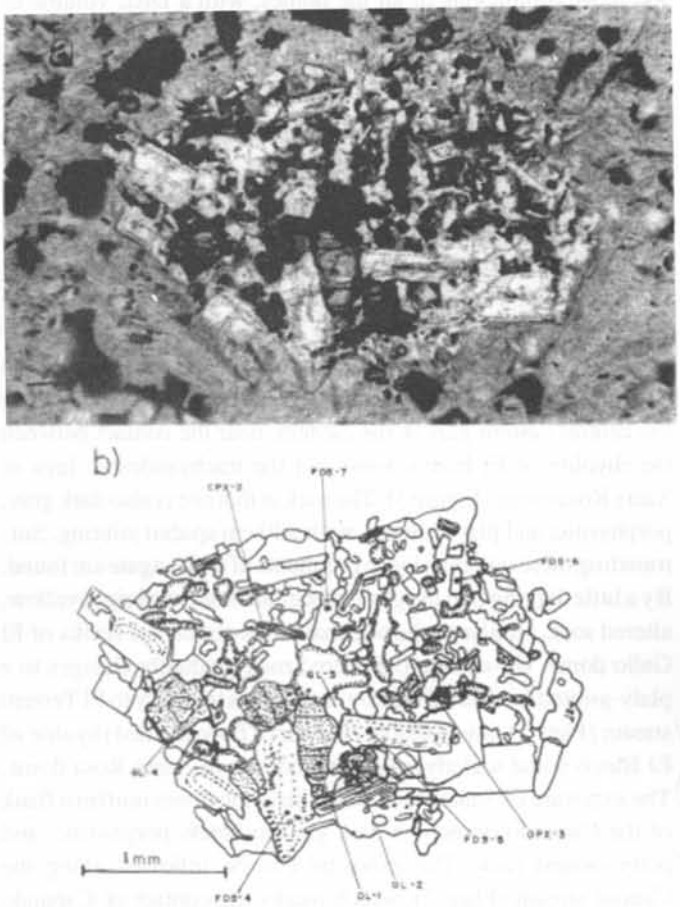

Figure 13. La Cruz Rhyolite lava dome. Enclave of interlocking minerals in La Cruz Rhyolite lava dome. The enclave contains plagioclase, clinopyroxene, orthopyroxene and olivine. Note also the vesicular glass between the interlocking mineral assemblage. (*a*) Photomicrograph (parallel light); (*b*) sketch of (*a*), indicating also scale.

Santa Rosa Andesite

Definition. Five trachyandesite-trachydacite lava domes were emplaced in the center of the caldera at *ca.* 3.7 Ma. Sánchez-Ru-

bio (1984, p. 113) named these domes Santa Rosa Andesite, from the outcrops at Cerro Santa Rosa (a lava dome; Tsr in Figure 3), and the name is retained here because at the Santa Rosa lava dome there are good exposures of these rocks, and because in the original definition by Sánchez-Rubio the unit includes the El Gallo and Zancudo lava domes, which are domes also intermediate in composition (Figures 3 and 12; Plate 2). Two additional intermediate lava domes must be included in this group and were omitted in Sánchez-Rubio's definition. These are the Capando dome, which lies between the El Gallo and Santa Rosa domes, and the La Mesa lava dome, immediately to the southwest of El Gallo (Figure 3; Plate 2).

Distribution and volume. The domes of the Santa Rosa Andesite are clustered in the center of the caldera. They cover an area of about 20 km^2 and comprise a total DRE volume of 4.3 km^3. The El Gallo lava dome, right at the center of the caldera, is the highest and most voluminous of all the domes, with a DRE volume of about 1.8 km^3. It forms the highest peak in the caldera complex, Cerro El Gallo, with an elevation of 3,000 m a.s.l.

Field description. Santa Rosa Andesite is quite similar to the lava of Amealco Andesite (rim domes). It is generally a dark gray, porphyritic, platy-jointed rock. In a few places, the lava is brecciated and/or vesiculated. The best outcrops occur in three sites. One is on the eastern flank of El Gallo dome. At the lowermost flank crops out a bright yellow clay that resulted from the intense alteration or weathering of the rock. Fresh, dark gray, porphyritic and platy-jointed lava is found uphill. The parallel joints are generally about 15 to 30 cm apart. Other exposures are found in the central-eastern part of the caldera, near the contact between the rhyolite of El Barco dome and the trachyandesitic lava of Santa Rosa dome (Figure 3). The rock at this site is also dark gray, porphyritic, and platy-jointed, with >20 cm spaced jointing. Surrounding these outcrops loose fragments of white agate are found. By a little digging into the ground one can observe a bright yellow, altered rock, similar to the one that crops out on the flanks of El Gallo dome. Up-stream, the altered rock gradually changes to a platy-jointed fresh lava. Nearby and along a tributary to El Terrero stream (Plate 2), it is possible to observe flow-banded rhyolite of El Barco dome underlying trachyandesite of Santa Rosa dome. The exposure of Santa Rosa Andesite at the lower northern flank of the Capando dome is a dark gray to black, porphyritic, and platy-jointed rock. The exposure can be followed along the Canoas stream (Plate 2), which marks the contact of Capando dome with the La Cruz Rhyolite (Figure 3). Here again La Cruz Rhyolite underlies trachyandesite of Capando dome. At this site the rock is more glassy and less crystal-rich than the other outcrops described above, probably because this rock lies closer to the external zone of the Capando lava dome and the other ones closer to the internal portions of the domes.

Petrography. Santa Rosa Andesite is generally porphyritic with a microlitic groundmass. It contains the same mineralogy of the Amealco Tuff and Amealco Andesite. Textures are similar to those in the Amealco Andesite but with a more crystal-rich groundmass. Large glass inclusions with regular shapes, sometimes parallel to the concentric zoning, occur irregularly in Santa Rosa plagioclase (Figure 14). Less commonly, glass inclusions are concentrated in the cores of the plagioclase, occasionally with an inclusion-free, concentrically zoned plagioclase mantle. Occasionally, oval clots, up to 6.5 mm, of interlocking crystals are also observed. These clots are mostly composed of laths of plagioclase + pyroxenes + Fe-Ti oxides, all <0.3 mm. The space between the interlocking crystals is filled with optically continuous, anhedral plagioclase, which probably formed later than the plagioclase lath network. Since the mineralogy is the same as that of the host rock, these clots may be juvenile. In contrast to the clots observed in Amealco Andesite, there is no intergranular glass in the Santa Rosa Andesite clots, suggesting that these magma bodies were cooled more slowly than the rim lava domes. Both dome types contain plagioclase with large glass inclusions, but maybe with different origins: glass inclusions in the plagioclase of the rim lava domes are probably liquid trapped due to a relatively fast growth of the plagioclase, whereas those in the plagioclase of Santa Rosa Andesite are due to resorption.

Figure 14. Photomicrograph of Santa Rosa Andesite showing plagioclase phenocrysts with abundant large glass inclusions mantled by inclusion-free plagioclase (polarized light, longest dimension is 5 mm).

POST-AMEALCO VOLCANISM

After the emplacement of the central lava domes, volcanism persisted for more than a million years in the periphery and within the caldera rim. This activity includes Hormigas Andesite, Coronita Rhyolite, El Rincón Rhyolite, Garabato Andesite, El Comal Andesite, and although not from a nearby vent, the Huichapan Tuff. These units are briefly described in chronologic order below.

Coronita Rhyolite

The Coronita Rhyolite is the name that Sánchez-Rubio

(1984) gave to two overlapping rhyolitic domes located 15 km southwest of the Amealco caldera, within the Acambay graben (Figure 3). San Mateo village was built next to the northern flank of the northern dome. Besides these two domes, similar structures occur scattered throughout the Sierra Puruagua, a volcanic complex 17 km to the west of Amealco caldera. Aguirre-Díaz (1983) briefly described the Sierra Puruagua rhyolitic domes and referred to them generally as "glassy rhyolitic domes". The name Coronita Rhyolite is adopted here for all these domes. The hill with that name near San Mateo is the type locality of this unit. Each of the two domes at San Mateo forms a smooth hill with an almost perfect dome shape and heights above the adjacent valley of 180 to 200 meters. Paired K-Ar ages of glass and feldspar yielded an average of 3.7 Ma (sample Am-179, Table 1), and thus, emplacement of these lava domes were at about the same time than Hormigas Andesite formation, and just after the central lava domes of the Amealco caldera were placed. The dome pair is covered at its eastern lower flanks by reworked pumice and lake deposits that filled the graben next to the caldera.

The rock at Cerro Coronita is pale gray, porphyritic, perlitized, and with flow-banded structure. Concentric flow foliation is evident. The domes are not obscured by vegetation or soils, so the circular foliation can be followed all around each of the domes. Occasionally, spherulites as large as 1 cm also occur.

Petrographically, the rock is crystal-poor, mainly composed of glass. It has a vitrophyric texture, with phenocrysts of sanidine (10 vol. %) and quartz (5 vol. %). Glass is perlitized, colorless, and makes up about 85 vol. % of the rock. The composition of these domes is a metaluminous, high-silica rhyolite (SiO_2=76 %, in wt. %, normalized volatile-free; sample Am-179, Table 2).

Hormigas Andesite

The Hormigas volcano was briefly described by Sánchez-Rubio (1984), and by Verma and others (1991). In both works the authors assigned a post-"Amealco Ignimbrite" age to Hormigas volcano, which agrees with this work, but they grouped within a single unit products of Palomas, Cerrito Colorado and Hormigas volcanoes. The Hormigas lava flows overlie the Amealco Tuff, and do not overlap lava of the Palomas volcano or reach to Cerrito Colorado (Figure 3) as has been indicated in earlier maps of the area. Hormigas lava flows are the only olivine-bearing lavas of the three volcanoes. Cerrito Colorado is mostly scoria-fall deposits typical of strombolian type eruptions and is older than the Amealco Tuff. Hormigas, Cerrito Colorado and Palomas volcanoes erupted at different times, and are physically, texturally and chemically different. Therefore they can not be correlated. The three different volcanoes and their respective products are thus separated here as different units. The name of the hill that forms the Hormigas volcano is Hormigas, and as Sánchez-Rubio (1984) did, the author uses the name here for this volcano and its products—basaltic andesite (SiO_2= 55.8%; normalized, volatile-free; sample Am-78, Table 2).

The Hormigas volcano was easily weathered. In contrast to Palomas volcano, the cone shape was almost lost, and it is now an irregular-shaped hill, most of it covered by a residual red-orange soil, in parts several meters thick. Beneath this soil, fresh rock occurs. Exposures are found beside Highway 120, about 7 km west of Amealco, and also along the stream that runs around the lava of the volcano to the north. This stream follows the contact between the Hormigas lava and Amealco Tuff. The Hormigas lava overlies the Amealco Tuff, and is not overlain by any other unit. The Hormigas lava yielded a 3.7 Ma K-Ar age (sample Am-78, Table 1).

As with Palomas Dacite, Hormigas Andesite has an asymmetric distribution. The lava flowed on the plateau made by Amealco Tuff and thus they flowed more easily away and downhill from the caldera; that is, northward of the Hormigas volcano. The northern flows reached as far as 5.5 km to the northwest and 3 km to the north and northeast, whereas they only reached up to 1 km away to the south, toward the rim of Amealco caldera. The Hormigas cone and lava cover an area of 26 km^2 and make a dense rock equivalent volume of 0.8 km^3.

Hormigas Andesite is black, phenocryst-poor lava. It weathers easily to a red soil, probably laterite. The rock has an aphanitic texture, with a groundmass of plagioclase laths up to 0.3 mm, microlites of plagioclase and Fe-Ti oxides, pyroxene (clinopyroxene?), and a dark glass. Phenocrysts make only 5% of the volume. They include plagioclase (3 vol. %) and olivine (2 vol. %). Plagioclase phenocrysts could be regarded as large groundmass crystals, since they are just larger laths aligned parallel to the groundmass laths and microlites, and having similar characteristics, such as subhedral-euhedral, tabular shapes; they are unzoned, unresorbed, and have well developed polysynthetic twinning. Olivine is up to 1 mm, and exhibits a narrow iddingsitized rim.

Huichapan Tuff

Huichapan is the name given here to a felsic tuff that apparently was erupted from the Huichapan caldera, which is about 66 km to the east-northeast of the Amealco caldera and about 40 km from its western front in contact with the Amealco Tuff, near San Ildefonso (Figure 2; Plate 2). Sánchez-Rubio (1984, 1986) misinterpreted this tuff as Amealco Ignimbrite. Silva-Mora (1991) also misinterpreted it as Amealco III ignimbrite (see his stop number 3 of the field trip guidebook), and Cas and Wright (1987) also wrongly called it Amealco Ignimbrite (the cover photo in their book Volcanic Successions). However, although it overlaps Amealco Tuff for an unknown but widespread area, and it is exposed close (*ca.* 20 km) to the Amealco caldera, it was not erupted from the Amealco caldera, but from a source that lies east of the study area, probably the

Huichapan caldera. This suggestion is based on the Huichapan Tuff distribution; it is continuously exposed eastward from the contact with Amealco Tuff, until crossing to the eastern side of the Mexico-Querétaro Expressway (Figure 2; Plate 2). A few kilometers to the east of this highway, Huichapan tuff is covered by crop fields. The tuff is exposed again farther to the east, at the Madero water reservoir, about 45 km to the east-northeast of the Amealco caldera and about 20 km from the center of the Huichapan caldera. From there, the exposures are mostly covered by mafic lava flows of Nopala volcano until the Huichapan caldera.

Huichapan ignimbrite, the main part of Huichapan Tuff, gets thicker to the east, from the contact with Amealco Tuff. At its westernmost outcrops, at San Ildefonso, it is <2 m thick; at Zarco stream, about 25 km to the east-northeast of the Amealco caldera, and near Taxhie, it is about 35 m thick (this is the site where the photo on the book cover of Cas and Wright, 1987, was taken), and at the Madero reservoir, east of the crop fields, it is about 50 m thick. Huichapan Tuff ponded against the eastern flank of Ñadó and Tepozán volcanoes (Figure 2; Plate 2).

From the Tepozán volcano and to the north, the contact between Amealco and Huichapan tuffs more or less coincides with or is near to the Río Prieto (Figure 2). A paired glass and sanidine K-Ar age of the Huichapan ignimbrite yielded 3.5 ± 0.16 (sample Am-81, Table 1). Excellent exposures of this tuff are found beside the Highway 55 that runs south to north between Aculco and the junction with the Mexico-Querétaro Expressway near San Sebastián de Barrancas (Figure 2). Good exposures are also found along the west-east highway between Amealco and Aculco. Spectacular exposures occur at Río Prieto canyon (Figure 15, a) (measured section 14, Appendix A) and at San Sebastián de las Barrancas (measured section 13, Appendix A).

The Huichapan Tuff includes a major ignimbrite which makes the bulk of the tuff, surge deposits, minor unwelded pumiceous pyroclastic flows, and mud- and ash- flows. A field description of Huichapan Tuff can be found in the Río Prieto and Piedras Grandes measured sections (sections 14 and 15, Appendix A). The Huichapan ignimbrite near Amealco caldera is similar in mineralogy and aspect to the felsic ignimbrite that surrounds the Huichapan caldera and that correspond to the ignimbrite of San Francisco Tuff described by Herrera and Milán (1981). It is a pink, vitric ignimbrite, with a crystal content ranging between 2 and 10% by volume; lithics make <5 vol. % near the contact with Amealco Tuff. It is a vitric tuff with a few content of crystals, including quartz, low-K sanidine. Pumice lumps are white or red-brown when oxidized, probably by vapor-phase alteration. Vesicles are commonly piped (tube pumices). The matrix is made of ash to lapilli-sized (<1-3 mm) and thick (up to 1 mm), colorless glass shards (Figure 15, b). The ignimbrite is partly to densely welded and has prominent columnar jointing, which is commonly vertical in the lower portions of the ignimbrite, but inclined either toward the east or the west in the upper portions (see cover photo of Cas and Wright, 1987), as if the upper portion moved after the ignimbrite was placed (rheomorphism?).

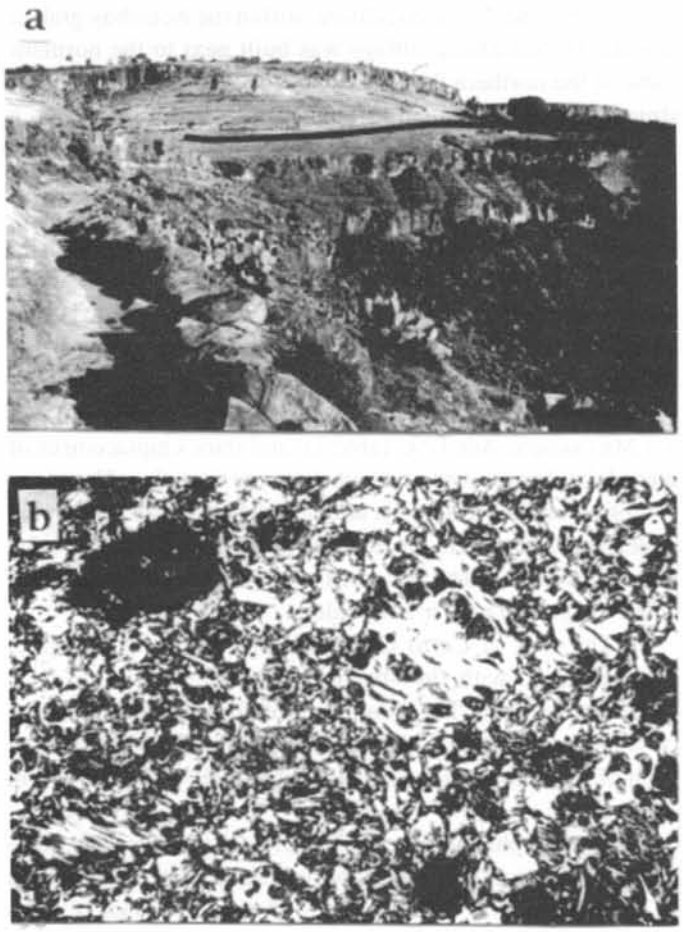

Figure 15. (a) The Huichapan Tuff (HT) at the southern wall of the Río Prieto canyon (sequence above black line); the sequence beneath the Huichapan Tuff is the Amealco Tuff (AT: sequence below black line). (b) Photomicrograph of the Huichapan Tuff ignimbrite. Note the uncollapsed shards and pumice fragments, and the crystal-poor nature of the rock (parallel light, longest dimension is 13 mm).

Milán and coworkers (1993) provide major element chemistry of the felsic San Francisco Tuff and the quite distinct, trachydacitic Donguinyó Tuff, this last one with a K-Ar age around 4.3 Ma (Nicholls, 1972; this age has not been corrected with the new decay constants of Steiger and Jäger, 1977). If the 3.5 Ma Huichapan Tuff is indeed correlatable with the San Francisco Tuff (as the present author believes), then Donguinyó Tuff was an earlier ignimbrite event of the Huichapan caldera, or perhaps of other unidentified source.

Magnetostratigraphy, geochemical, and geochronological studies are in progress to further constrain the source of the Huichapan Tuff (Aguirre-Díaz, in preparation; Aguirre-Díaz and Urrutia-Fucugauchi, in preparation).

El Rincón Rhyolite

Sierra El Rincón is a rhyolitic lava dome complex that

was placed after Amealco Tuff. The name of this unit is proposed as El Rincón Rhyolite. A sample from this complex yielded 2.9 Ma (sample Am-122, Table 1). Verma and others (1991) stated that Amealco Tuff was stopped by the Sierra El Rincón, 10 km to the northwest of the caldera, but here it is found that Sierra El Rincón was placed after the Amealco ignimbrites. This is evident with field relationships. At the southeastern flank of this complex, Amealco Tuff underlies lava from Sierra El Rincón. At the northern flank, Amealco Tuff is found again underlying the lava from Sierra El Rincón (measured section 5, Appendix A), and in a quarry farther to the north, near San Pedro, a felsic, thin (<1 m thick) ignimbrite, probably derived from a dome collapse of Sierra El Rincón, overlies Amealco Tuff (measured section 6, Appendix A). Amealco Tuff continues farther away to the north from Sierra El Rincón. In summary, Sierra El Rincón was not there when Amealco Tuff was erupted.

Fresh rock is hard to find in this lava dome complex, especially at high altitudes, because of the dense pine forest. However, at the lower flanks, outcrops of fresh rocks are more common. The rock is a perlitized obsidian. It is practically aphyric. The only phases observed were altered, mafic, euhedral crystals that only make 4% of the volume (Figure 16). The mafic phases are totally altered, but still preserving a euhedral shape. The original phase may have been either pyroxene or olivine, more probably olivine, as the shapes of the crystals correspond to those cut parallel to the c-axis of olivine. No other phases were observed. Glass is pink under the microscope. Gem-quality opal is mined at some sites in this lava dome complex. The obsidian is a peraluminous, high-silica rhyolite (SiO_2= 75.3 in wt. %, normalized volatile-free; sample Am-122, Table 2).

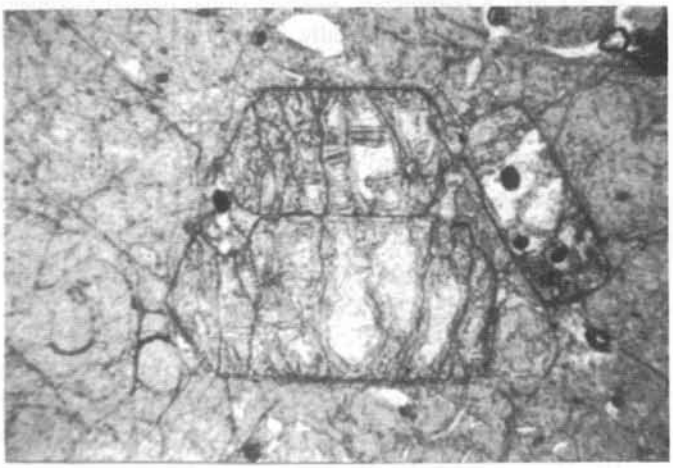

Figure 16. Photomicrograph showing the only crystal phase observed in El Rincón Rhyolite. It is an altered product possibly after olivine, as the altered mineral still preserves an olivine outline shape (parallel light, longest dimension of photomicrograph is 5 mm).

Garabato Andesite

Garabato dome was briefly described by Sánchez-Rubio (1984). He called it Garabato Andesite (*op. cit.*, p. 115) and the name is retained in this study. The rock is indeed an andesite (SiO_2=62.6; in wt. %, normalized volatile-free; sample Am-18, Table 2). Garabato dome was emplaced on the fault-trace of the Epitacio fault after Amealco caldera was displaced by this fault (Figure 3). However, as Sánchez-Rubio (1984) stated, Garabato dome was also displaced by this faulting, but the fault offset was only 25 m; thus, it was probably emplaced when the Epitacio fault was still active.

A K-Ar age of 2.5 Ma was obtained for this rock (sample Am-18, Table 1). It was emplaced about 1.2 m.y. after the central lava domes, which mark the end of the Amealco caldera cycle, or about 1.8 m.y. after the rim lava domes.

Garabato dome covers 4 km^2 and represents a dense rock equivalent volume of 0.1 km^3. It forms a small lava plateau with smooth-dipping flanks, up to 90 m high above the adjacent valley. The rock is porphyritic, with phenocrysts of plagioclase (5 vol. %), hornblende (8 vol. %), and biotite (1 vol. %). Microphenocrysts (<0.3 mm) of plagioclase make 25% of the volume. The groundmass is mostly plagioclase laths in a dark glass pigmented with tiny opaques. The largest plagioclase shows disequilibrium textures, such as fritted cores (sieve texture), mantled by clear plagioclase, or clear cores with fritted zones around them. Hornblende is subhedral to anhedral. It is strongly pleochroic from pale yellow to dark brown, almost red. It has oxidized rims, and contains abundant inclusions of euhedral Fe-Ti oxides. Biotite is rare, but when present it occurs as large crystals, up to 3 mm, and has rounded corners.

El Comal Andesite

The name El Comal Andesite is assigned to the products of El Comal volcano. The El Comal cone was named and briefly described by Sánchez-Rubio (1984) within his "inner caldera volcanics" group. It is an eroded scoria cone, up to 200 m high with respect to the adjacent valley at the south. It was placed right on the trace of the Epitacio fault (Figure 3), but the cone has not been displaced by this fault, so it is younger. It is the last volcanic event in the Amealco caldera area. The cone is formed by layered scoria fall deposits and bombs typical of strombolian type eruptions. A quarry at the southern flank of El Comal exposes the pyroclastic deposits. A short lava flow, up to 1 km long, was also erupted from this volcano, which eroded the northeastern crater and flank of the volcano, and flowed toward the caldera (Figure 3). This indicates that there was a paleoslope toward the caldera when the lava was erupted, in contrast to the lava from Palomas and Hormigas volcanoes, which flowed outward from the caldera. The assumed original outward southern slope of the Amealco caldera was "inverted" probably due to the faulting that displaced the southern portion of the caldera. A 2.2 Ma K-Ar age was obtained from the scoria fall deposits (sample Am-19, Table 1). Thus faulting along the Epitacio fault has to be older than 2.2 Ma. The lava flow overlies layered gravel and reworked

pumice deposits and ponded against the southern faulted flank of Zancudo central lava dome. It does not overlie Amealco ignimbrite as stated by Verma and coworkers (1991). The cone and associated lava flow cover an area of 1.9 km^2, and have a dense rock equivalent volume of 0.15 km^3. The composition of the El Comal products change with time from basaltic andesite to andesite (SiO_2=56.3-60.3 in wt. %, normalized volatile-free; Table 2).

The scoria fall deposits consist of an alternation of coarse-grained and fine-grained lapilli, with volcanic bombs, up to 1.5 m, scattered within the deposit. No breaks such as eroded surfaces or sedimentary deposits separate them, so the cone formed during several pulses that were close in time during the volcano activity, and probably grew within a few years as other cinder cones (*e.g.*, Parícutin; Foshag and González, 1956). The scoria is composed of black, vesiculated fragments. They are mostly phenocryst-poor rocks, with plagioclase (4 vol. %), orthopyroxene (2 vol. %), clinopyroxene (1 vol. %) and Fe-Ti oxide phenocrysts. The bombs, commonly as small black blocks (<15 cm), can have up to 15 vol. % of phenocrysts of plagioclase, orthopyroxene and Fe-Ti oxides. The groundmass in both bombs and scoria fragments is rich in plagioclase microlites in a dark glass. The plagioclase phenocrysts are up to 3 mm, subhedral to anhedral, some with fritted zones and rounded corners, and some are apparently skeletal with large brown to yellow glass inclusions similar to those observed in the Amealco ignimbrites, rim and central lava domes.

The lava flow is gray and platy-jointed. This rock is porphyritic and with a total phenocryst content of 27 vol. %. Plagioclase is the most abundant (18 vol. %), followed by clinopyroxene (4 vol. %), orthopyroxene (3 vol. %), and Fe-Ti oxides (2 vol. %). Glomerocrysts of these phases are common. Plagioclase is up to 6 mm, commonly has large glass inclusions with irregular shapes (Figure 17), and some have oscillatory zoning. Pyroxenes are generally part of the glomerocrysts, but single crystals also occur. Pyroxenes generally contain Fe-Ti oxide inclusions, but Fe-Ti oxides also occur as free, euhedral crystals, up to 0.5 mm. The groundmass is a fine-grained assemblage of plagioclase microlites and opaques in a dark glass. Except for the presence of oscillatory zoned plagioclase, the lava flow is mineralogically and texturally very similar to the intermediate products of Amealco caldera, such as the ignimbrites, Amealco Andesite, and Santa Rosa Andesite.

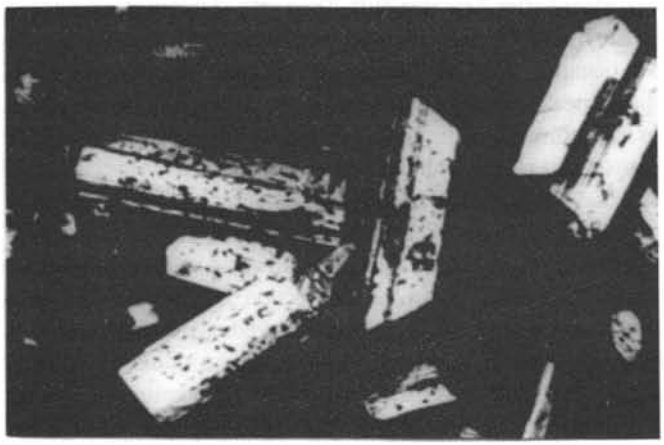

Figure 17. Photomicrograph (polarized light) of El Comal Andesite showing glomerocryst of plagioclase + pyroxenes + Fe-Ti oxides in a fine-grained matrix rich in glass. Note the large glass inclusions in the plagioclase's core, mantled by an inclusion-free zone (longest dimension of photomicrograph is 2.5 mm).

CONCLUSIONS

The Amealco caldera is a well preserved Pliocene volcanic center, 11 km in diameter, located in the central part of the Mexican Volcanic Belt (MVB). Stratigraphy and K-Ar dates indicate five major volcanic units in the history of the caldera: (1) Amealco Tuff, a 4.7 Ma pyroclastic sequence representing 77 km^3 of trachyandesitic-trachydacitic magma; (2) Brick pumice, a pyroclastic sequence with a more local distribution than Amealco Tuff and which was erupted from ring fracture vents and represents 2.35 km^3; (3) Amealco Andesite and Campana Dacite, 4.3 Ma lava domes that form the caldera rim and represent 3.8 km^3 of trachyandesitic magma and 0.8 km^3 trachydacitic magma, respectively; (4) La Cruz Rhyolite, five rhyolitic lava domes that were emplaced in the center of the caldera at 3.9 Ma and with a magma volume of 2.4 km^3; and (5) Santa Rosa Andesite, five trachyandesitic lava domes that were emplaced also at the center of the caldera at 3.7 Ma and with a magma volume of 4.3 km^3. Activity peripheral to the caldera includes two volcanoes, trachydacitic Palomas at 4.0 Ma and basalt-andesitic Hormigas at 3.7 Ma, rhyolitic lava domes named Coronita Rhyolite at 3.7 Ma; a hornblende andesite dome named Garabato Andesite at 2.5 Ma, and finally, El Comal scoria cone at 2.2 Ma, with a composition range from basaltic andesite to andesite. Besides the peripheral volcanism next to the caldera, Amealco Tuff is overlain by 2.9 Ma El Rincón Rhyolite, a lava dome complex 12 km to the north of the caldera, and by a 3.5 Ma widespread felsic Huichapan Tuff 20 km to the east of the caldera that has been misinterpreted as Amealco Tuff. Amealco Tuff overlies 5.7 Ma basalt and 4.7 Ma felsic ignimbrites.

Amealco Tuff, the major product erupted by the caldera, is a complex pyroclastic sequence with three gray to dark gray welded ignimbrites, Amealco I, Amealco II, and Amealco III. These ignimbrites are co-extensive for at least 25 km from the center of the caldera. Interlayered with them are pyroclastic and epiclastic deposits as voluminous as the ignimbrites. Breaks in activity are evident in the sequence in the form of paleosoil, reworked material at the top of deposits, or eroded irregular paleosurfaces. The total sequence is as thick as 100 m 25 km from the caldera, but averages 34 m. The type section, 50 m thick, is located at Epitacio Huerta, Michoacán. Amealco Tuff covers nearly 2,900 km^2 if all the

remnant outcrops are connected as a continuous unit. This distribution is based on that of the ignimbrites; the tephra fallouts covered an unmapped but wider distribution. Amealco Tuff distribution includes the Las Américas Formation, which corresponds to the southern distal facies of Amealco Tuff. It is unknown the eastern front of the ignimbrites, as it is covered by the Huichapan Tuff. The ignimbrites reached as far as 45 km from the caldera and have average thicknesses between 3 and 5 m, thus are low aspect ratio deposits. The dense rock equivalent volume of Amealco Tuff is 77 km^3, which excludes the unexposed intracaldera tuff, the tuff covered by the Huichapan Tuff to the east of Amealco caldera, the distal tephra fallout deposits, and the co-ignimbrite ash-fall deposits, which were eroded away. Therefore, this volume must be considered a minimum.

Because of its wide distribution, distinct nature, and K-Ar age control, the Amealco Tuff serves as a good stratigraphic marker. Many undated volcanoes in the mapped area, including large composite volcanoes, lava domes, scoria cones and ignimbrites, can be positioned stratigraphically with respect to Amealco Tuff. The same criteria can be applied to the 3.5 Ma Huichapan Tuff to the east of Amealco caldera, which is also a widespread deposit.

The predominant mineral assemblage of the Amealco caldera products is plagioclase + hypersthene + augite + titanomagnetite + ilmenite ± olivine ± apatite ± zircon. Besides these phases, the rhyolite domes rarely contain a little hornblende and biotite, also. All the products of Amealco caldera lack modal quartz and K-feldspar.

The total magma volume emitted from Amealco caldera is 92 km^3, which includes Palomas Dacite, but excludes Hormigas, Garabato and El Comal products. The 95% of the magma volume emitted from Amealco caldera is intermediate in composition, from basaltic andesite to trachydacite, and only 5.5% of the volume is rhyolite. Therefore, Amealco caldera is predominantly an intermediate composition center.

Amealco caldera was displaced by a regional south-facing normal fault, named Epitacio fault. This fault forms the northern shoulder of a graben that could be regarded as the western continuation of the narrower Acambay graben. The last unit in the Amealco caldera displaced by Epitacio fault is 2.5 Ma Garabato Andesite. The 2.2 Ma El Comal cone is on the trend of this fault and was not displaced by it. The 25 m offset in Garabato Andesite is much less than the 250 m offset needed to completely displace the southern caldera rim. Therefore, caldera displacement must have occurred between 3.8 and 2.5 Ma, the ages of the central domes and Garabato Andesite, respectively, probably closer to the younger limit as Garabato is displaced, also, and no later than 2.2 Ma, the age of the unfaulted Comal Andesite.

ACKNOWLEDGMENTS

The author is grateful to Daniel S. Barker for his guidance during this study, to Fred W. McDowell for allowing the use of his K-Ar laboratory and his collaboration for the gathering of the K-Ar ages, and to both of them and to Bruce N. Turbeville for reading and commenting on earlier versions of this work. Comments of reviewers Gail Mahood and Claus Siebe further improved the paper. Fernando Ortega-Gutiérrez and Dante J. Morán-Zenteno, former and actual directors of the Instituto de Geología of the Universidad Nacional Autónoma de México (UNAM), respectively, provided administrative support to carry out this project. This study was supported in part by the Dirección General de Asuntos del Personal Académico of UNAM, project No. IN106594, by endowments to Dr. Daniel S. Barker, and by the Geology Foundation of the Deparment of Geological Sciences of the University of Texas at Austin.

BIBLIOGRAPHICAL REFERENCES

Aguirre-Díaz, G.J., 1983, Estudio geológico-petrológico de la hoja Presa Solís, Jerécuaro, Guanajuato (un evento ácido en el Eje Volcánico): Mexico, D.F., Universidad Nacional Autónoma de México, Facultad de Ingeniería, B.Sc. thesis, 152 p. (unpublished).

———1993a, The Amealco caldera, Querétaro, México—geology, geochronology, geochemistry, and comparison with other silicic centers of the Mexican Volcanic Belt: Austin, University of Texas at Austin, Ph.D. dissertation, 401 p. (unpublished).

———1993b,La toba de Amealco y su correlación con la Formación Las Américas a través del *Graben* de Acambay: Unión Geofísica Mexicana, Geos, v. 13, no. 5, p. 24.

———1993c, A granulite xenolith in a tuff of the central Mexican Volcanic Belt: Eos, Transactions of the American Geophysical Union, v. 74, p. 575 (Abstract).

Allan, J.F.; Nelson, S.A.; Luhr, J.F.; Carmichael, I.S.E.; Wopat, M.; and Wallace, P.J., 1991, Pliocene-Recent rifting in SW Mexico and associated volcanism, *in* Dauphin, J.P., and Simoneit, B.R.T., eds., The Gulf and Peninsular Province of the Californias: American Association of Petroleum Geologists Memoir 47, p. 425.

Anguita, F.; Verma, S.P.; García-Cacho, L.; Milán, Marcos; and Samaniego-M., D., 1991, Mazahua—una nueva caldera en el Cinturón Volcánico Mexicano: Geofísica Internacional (Mexico), v. 30, p. 135-148.

Barker, D.S., 1983, Igneous rocks: New Jersey, Prentice Hall, 417 p.

Blake, S., 1990, Viscoplastic models of lava domes, *in* Fink, J.H., ed., Lava Flows and Domes: New York, Springer-Verlag, International Association of Volcanology and Chemistry of the Earth's Interior (IAVCEI) Proceedings in Volcanology 2, p. 88-126.

Campa, M.F.; Campos, M.; Flores, R., and Oviedo, R., 1974, La secuencia mesozoica volcánica sedimentaria metamorfizada de Ixtapan de la Sal, Mex.–Teloloapan, Gro.: Boletín de la Sociedad Geológica de México, v. 35, p. 7–28.

Carrasco-Núñez, Gerardo, 1988, Geología y petrología de los campos volcánicos de Los Azufres (Mich.), Amealco y El Zamorano (Qro.): Mexico, D.F., Universidad Nacional Autónoma de México, Facultad de Ingeniería, M.Sc. thesis, 148 p.

———1989, Petrología del campo volcánico Los Azufres: Boletín de Mineralogía, v. 4, p. 3-18.

Cas, R.A.F., and Wright, J.V., 1987, Volcanic successions, modern and ancient—a geological approach to processes, products and successions: London, Allen, Unwin and Hyman, 528 p.

Cathelineau, M.; Oliver, R.; and Nieva, D., 1987, Geochemistry of volcanic series of the Los Azufres geothermal field (Mexico): Geofísica Internacional (Mexico), v. 26, p. 195-272.

CETENAL, 1972a, Apaseo El Alto (F14-C75), Guanajuato: Mexico, D.F., Secretaría de Programación y Presupuesto (now INEGI), carta topográfica, escala 1:50,000.

———1972b, Presa Solís (F14-C85), Guanajuato: Mexico, D.F., Secretaría de Programación y Presupuesto (now INEGI), carta topográfica, escala 1:50,000.

———1973a, La Estancia (F14-C76), Querétaro: Mexico, D.F., Secretaría de Programación y Presupuesto (now INEGI), carta topográfica, escala 1:50,000.

———1973b, Amealco (F14-C8), Querétaro: Mexico, D.F., Secretaría de Programación y Presupuesto (now INEGI), carta topográfica, escala 1:50,000.

———1974a, San Juan del Río (F14-C77), Querétaro: Mexico, D.F., Secretaría de Programación y Presupuesto (now INEGI), carta topográfica, escala 1:50,000.

———1974b, Polotitlán (F14-C8), Hidalgo: Mexico, D.F., Secretaría de Programación y Presupuesto (now INEGI), carta topográfica, escala 1:50,000.

———1976, El Oro de Hidalgo (E14-A16), Estado de México: Mexico, D.F., Secretaría de Programación y Presupuesto (now INEGI), carta topográfica, escala 1:50,000.

Dobson, P.F., and Mahood, G.A., 1985, Volcanic stratigraphy of the Los Azufres geothermal area, Mexico: Journal of Volcanology and Geothermal Research, v. 25, p. 273-287.

Ferrari, L.; Garduño, V.H.; Pasquaré, G.; and Tibaldi, A., 1991, Geology of Los Azufres caldera, Mexico, and its relationships with regional tectonics, Journal of Volcanology and Geothermal Research, v. 47, p. 129-148.

———1993, The Los Azufres caldera, Mexico—the result of multiple nested collapse. Reply to a comment by Claude Robin and E. Padral: Journal of Volcanology and Geothermal Research, v. 56, p. 345-349.

Fink, J.H., ed., 1987, The emplacement of silicic domes and lava flows: Geological Society of America Special Paper 212 (preface).

Flores, Teodoro, 1920, Estudio geológico-minero de los distritos de El Oro-Tlapujahua: Instituto Geológico de México, Boletín 37, 87 p.

Foshag, W.F., and González-Reyna, Jenaro, 1956, Birth and development of Parícutin volcano: U.S. Geological Survey Bulletin 965-D, p. 355-489.

Fries, Carl, Jr.; Ross, C.S.; and Obregón-Pérez, Alberto, 1965 (1977), Mezcla de vidrios en los derrames cineríticos Las Américas de la región de El Oro-Tlalpujahua, Estados de México y Michoacán, parte centromeridional de México: Universidad Nacional Autónoma de México, Instituto de Geología, Boletín 70, 85 p.

Halsor, S.P., 1989, Large glass inclusions in plagioclase phenocrysts and their bearing on the origin of mixed lavas at Tolimán Volcano, Guatemala: Bulletin of Volcanology, v. 51, p. 271-280.

Herrera-F., J.J., and Milán-Valdez, Marcos, 1981, Estudio geológico de las zonas geotérmicas de Yexthó, Pathé y Taxidó, estados de Hidalgo y Querétaro: Comisión Federal de Electricidad, Internal Report 13-81 (unpublished).

Johnson, W.M., and Maxwell, J.A., 1981 (1989), Rock and mineral analysis, second ed.: Malabar, Florida, Robert E. Krieger Pub. Co., 489 p.

Langmuir, C.H., 1989, Geochemical consequences of in situ crystallization: Nature, v. 340, p. 199-205.

Le Bas, M.J.; Le Maître, R.W.; Streckeisen, A.; and Zanettin, B., 1986, A chemical classification of volcanic rocks based on the total alkali-silica diagram: Journal of Petrology, v. 27, p. 745-750.

Luhr, J.F., and Carmichael, I.S.E., 1985, Jorullo volcano, Michoacán, Mexico (1759-1774)—the earliest stages of fractionation in calc-alkaline magmas: Contributions to Mineralogy and Petrology, v. 90, p. 142-161.

Luhr, J.F.; Nelson, S.A.; Allan, J.F.; and Carmichael, I.S.E., 1985, Active rifting in soutwestern Mexico; manifestations of an incipient eastward spreading-ridge jump: Geology, v. 13, p. 54-57.

Mahood, G.A., 1980, Geological evolution of a Pleistocene rhyolitic center—Sierra La Primavera, Jalisco, Mexico: Journal of Volcanology and Geothermal Research, v. 8, p. 199-230.

McDowell, F.W., 1983, K-Ar dating—incomplete extraction of radiogenic argon from alkali feldspar: Chemical Geology, Isotope Geoscience, v. 1, p. 119-126.

Milán-Valdez, Marcos; Yáñez, C., Navarro-L.. I., Verma, S.P., Carrasco-Núñez, Gerardo, 1993, Geología y geoquímica de elementos mayores de la caldera de Huichapan, Hidalgo, México: Geofísica Internacional (Mexico), v. 32, p. 261-276.

Negendank, J.F.W.; Emmermann, R.; Krawczyk, R.; Mooser, F.; Tobschall, H.; and Werle, D., 1985, Geological and geochemical investigations on the eastern Trans-Mexican Volcanic Belt: Geofísica Internacional (Mexico), v. 24, p. 477-575.

Nelson, S.T., and Montana, A., 1992, Sieve-textured plagioclase in volcanic rocks produced by rapid decompression: American Mineralogist, v. 77, p. 1242-1249.

Nichols, R.C., 1970, The geology and geochemistry of the Pathé geothermal zone, Hidalgo, Mexico: Norman, University of Oklahoma, Ph.D. dissertation, 177 p.

Nixon, G.T.; Demant, A.; Armstrong, R.L.; and Harakal, J.E., 1987, K-Ar and geologic data bearing on the age and evolution of the Trans-Mexican Volcanic Belt, in Vernz S.P., ed., Special volume on Mexican Volcanic Belt: Geofísica Internacional (Mexico), v. 26, part 3A, p. 109-158.

Pradal, Evelyne, and Robin, Claude, 1994, Long-lived magmatic phases at Los Azufres volcanic center, Mexico: Journal of Volcanology and Geothermal Research, v. 63, p. 201-215.

Pallister, J.S.; Hoblitt, R.P.; Meeker, G.P.; Knight, R.J.; Siems, D.F., in press, Magma mixing at Pinatubo volcano—petrographical and chemical evidence from the 1991 deposits: submitted to USGS Profesional Paper.

Robin, Claude, and Nicolas, Emmanuel, 1978, Particularités géochimiques des suites andésitiques de la zone orientale de l'axe transmexicain, dans leur contexte tectonique: Bulletin de la Société Géologique de France, v. 20, 7^{e} série, p. 193-202.

Salas, G.P., 1988, Geología económica de México: Mexico, D.F., Fondo de Cultura Económica, 544 p.

Sánchez-Rubio, Gerardo, 1978, The Amealco caldera: Geological Society of America Abstracts with Programs, v. 10, p. 145 (abstract).

——— 1984, Cenozoic vulcanism of the Toluca-Amealco region, central Mexico: London, University of London, Imperial College of Science and Technology, M.Sc. thesis, 275 p. (unpublished).

——— 1986, Transmexican Volcanic Belt—Field seminar, *in* Nelson, S.A., and Sánchez-Rubio, Gerardo, eds., TransMexican Volcanic Belt field guide: Association Géologique du Canada, Division Volcanologique, and Universidad Nacional Autónoma de México, p. 79-108.

Silva-Mora, Luis, 1979, Contribution à la connaissance de l'Axe Volcanique Transmexicain—Étude géologique et pétrologique des laves du Michoacán oriental: Marseille, France, Université de Droit, d'Économie et des Sciences D'aix-Marseille III, Ph.D. dissertation, 230 p. (unpublished).

———1991, Caldera de Huichapan o del Astillero: Universidad Nacional Autónoma de México, Instituto de Geología; Universidad Autónoma de Hidalgo, Instituto de Investigaciones en Ciencias de la Tierra; Sociedad Mexicana de Mineralogía; Secretaría de Educación Pública, Subsecretaría de Educación Superior e Investigación Científica, 18 p.

———1995, Hoja Morelia 14Q-g(2), con Resumen de la geología de la hoja Morelia, estados de Michoacán y Guanajuato: Carta Geológica de México, serie 1:100,000, mapa con texto explicativo en el reverso.

Sparks, R.S.J.; Self, S.; and Walker, G.P.L., 1973, Products of ignimbrite eruptions: Geology, v. 1, p.115-118.

Steiger, R.H., and Jäger, E., 1977, Subcommission on geochronology—Convention on the use of decay constants in geo- and cosmochronology: Earth and Planetary Science Letters, v. 36, p. 359-362.

Suter, Max; Aguirre, G.J.; Siebe, Claus; Quintero-Legorreta, Odranoel; and Komorowski, J.C., 1991, Volcanism and active faulting in the central part of the Trans-Mexican Volcanic Belt, *in* Walawender, M.J., and Hanan, B.B., eds., I, Geological excursions in Southern California and Mexico: Boulder, Colo., Geological Society of America, p. 224-243.

Suter, Max; Quintero-Legorreta, Odranoel; and Johnson, C.A., 1992, Active faults and state of stress in the central part of the Trans-Mexican Volcanic Belt, Mexico; 1, The Venta de Bravo Fault: Journal of Geophysical Research, v. 97, p. 11,983-11,993.

Suter, Max; Quintero-Legorreta, Odranoel; López-Martínez, M.; Aguirre-Díaz, G.J.; Farrar, E., 1995, The Acambay graben: Active intra-arc extension in the Trans-Mexican Volcanic Belt, Mexico: Tectonics, v. 14, p. 1245-1265.

Thornton, C.P., and Tuttle, O.F., 1960, Chemistry of igneous rocks; 1, Differentiaton index: American Journal of Science, v. 258, p. 664-684.

Tilley, C.E., 1960, Differentiation of Hawaiian basalts—some variants in lava suites of dated Kilauean eruptions: Journal of Petrology, v. 1, p. 47-55.

Tsuchiyama, A., 1985, Dissolution kinetics of plagioclase in the melt of the system diopside-albite-anorthite, and origin of dusty plagioclase in andesites: Contributions to Mineralogy and Petrology, v. 89, p. 1-16.

Verma, S.P.; Carrasco-Núñez, Gerardo; and Milán, Marcos, 1991, Geology and geochemistry of Amealco caldera, Qro., Mexico, *in* Verma, S.P., ed., Calderas—genesis, structure and unrest: Journal of Volcanology and Geothermal Research, v. 47, p. 105-127.

Verma, S.P.; Verma, M.P., Carrasco-Núñez, Gerardo, and Milán, Marcos, 1989, Geology and geochemistry of Amealco caldera, Querétaro, Mexico: Annales Geophysicae, Special Issue for the 14th General Assembly, Barcelona, Spain, p. 58 (abstract).

Wilcox, R.E., 1954, Petrology of Parícutin volcano, Mexico: U.S. Geological Survey Bulletin 965 C, p. 281-354.

Yáñez-García, Camilo, 1984, Exploración geológica de la caldera de Huichapan, Estado de Hidalgo: Sociedad Geológica Mexicana, Convención Geológica Nacional, 7, Resúmenes, p. 171-173 (abstracts).

APPENDIX A
MEASURED SECTIONS

The coordinates of the base of each measured section are provided in each of them (Sections 1-26). An index map of their localities (Figure A-1) is included in this appendix. Elevation, in meters, is indicated to the left of the sections. Also to the left, and with the prefix "Am", are indicated the numbers of the samples that were gathered from the measured sections. The terminology used is that recommended by Cas and Wright (1987) and references therein. Explanation of symbols is provided in Figure A-2.

Figure A-1. Location map of the measured sections.

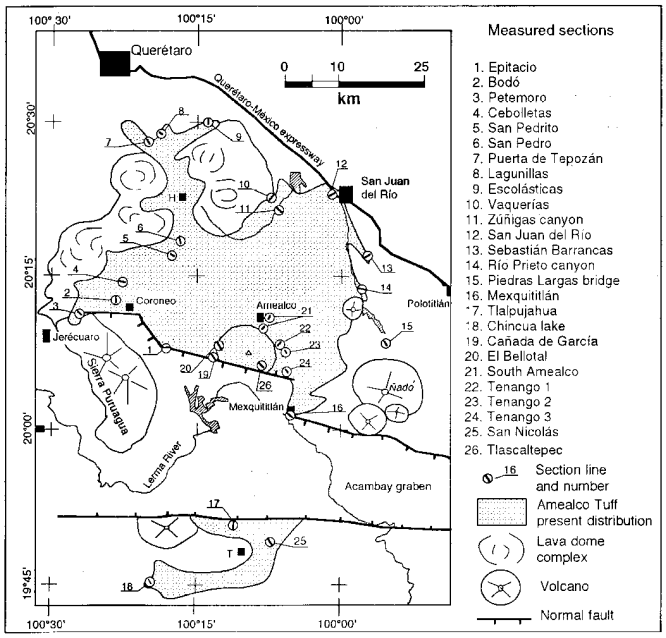

Figure A-2. Explanation of symbols used in the measured sections.

APPENDIX A
MEASURED SECTIONS

The location coordinates for the base of each measured section are provided in each section. An index map of them is included in this appendix. Elevation, in meters, is indicated to the left of the section. Also to the left, and with the prefix "Am", are indicated the numbers of the samples that were gathered from the measured sections. The terminology used is that recommended by Cas and Wright (1987) and references therein.

Symbols used

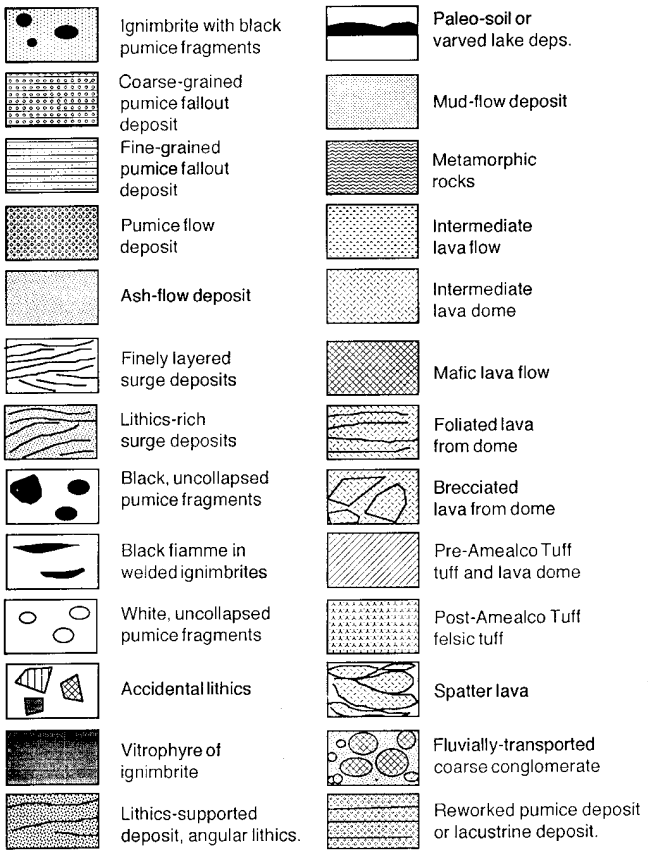

PLATE 1

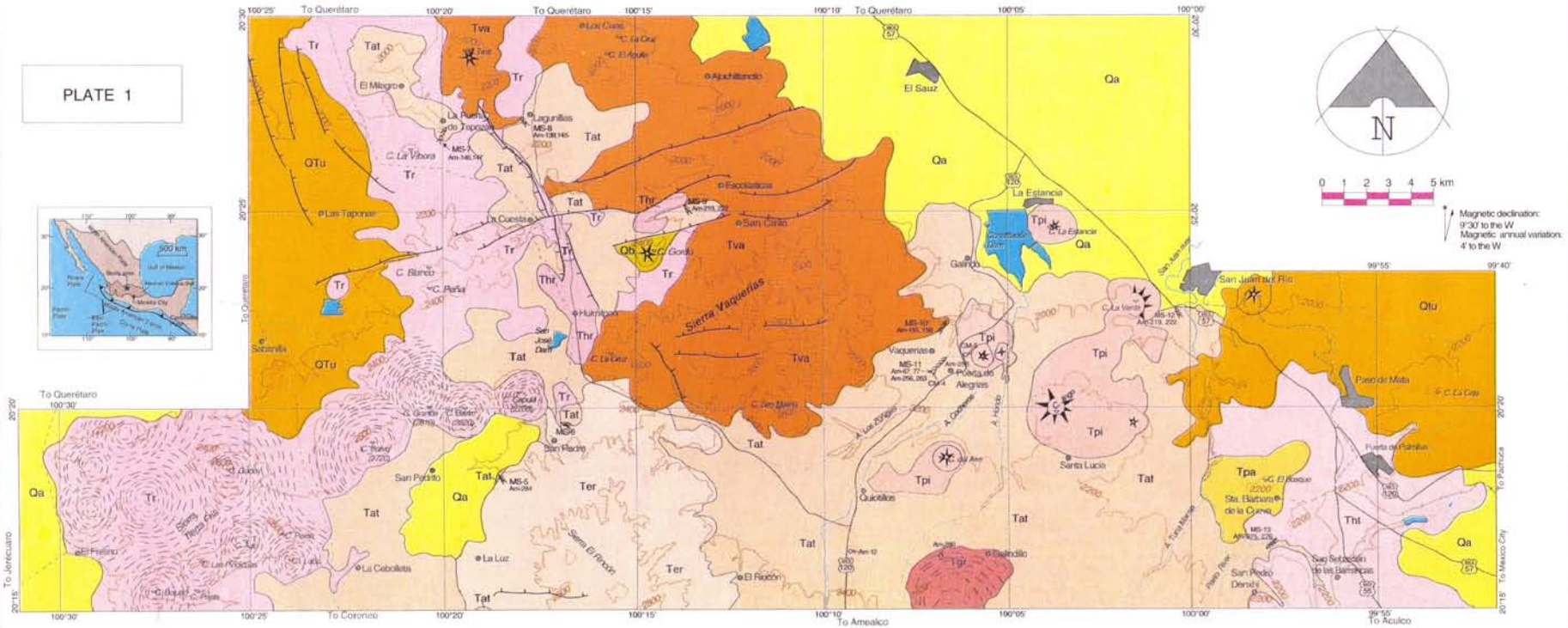

Geologic mapping by Gerardo J. Aguirre-Díaz from 1988 to 1991
Computer color separation was made by José de Jesús Vega-Carrillo.

GEOLOGIC MAP OF THE AMEALCO CALDERA REGION

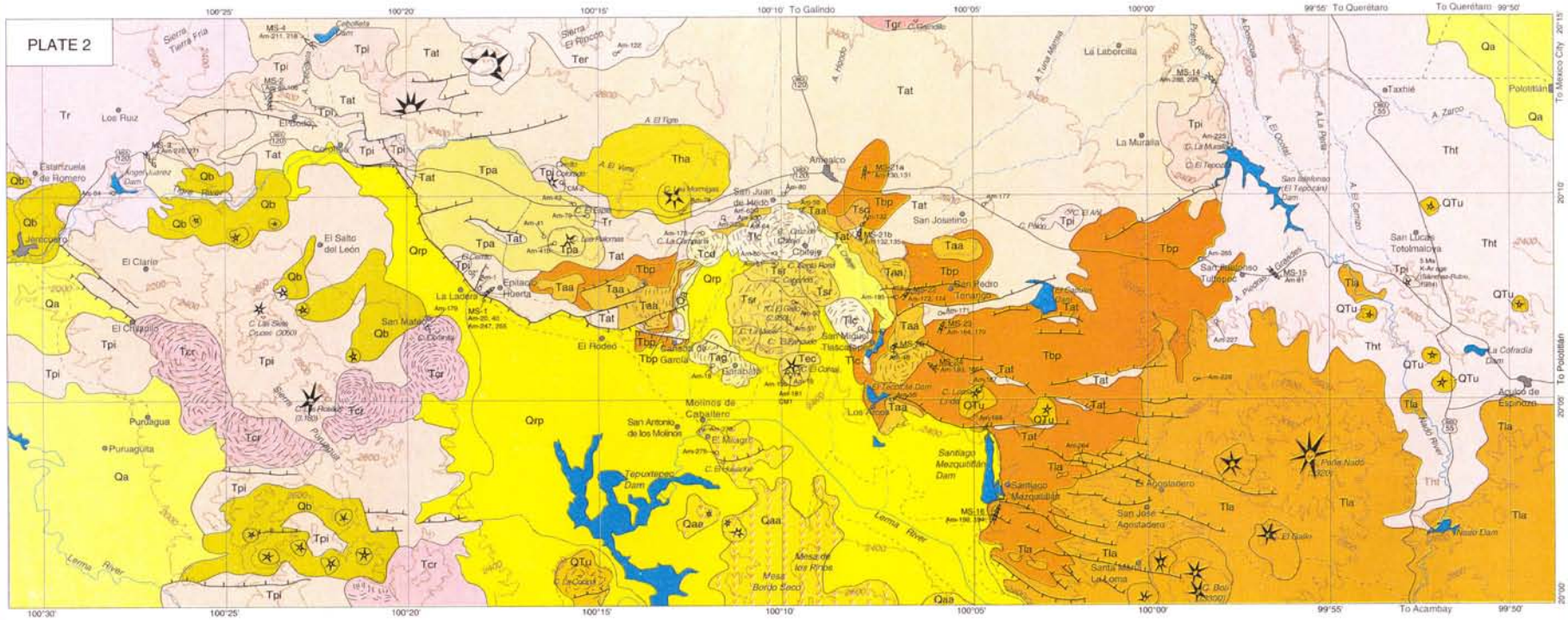

Geologic mapping by Gerardo J. Aguirre Díaz from 1988 to 1991

Computer color separation was made by José de Jesús Vega-Carrillo

GEOLOGIC MAP OF THE AMEALCO CALDERA REGION (CONTINUED)

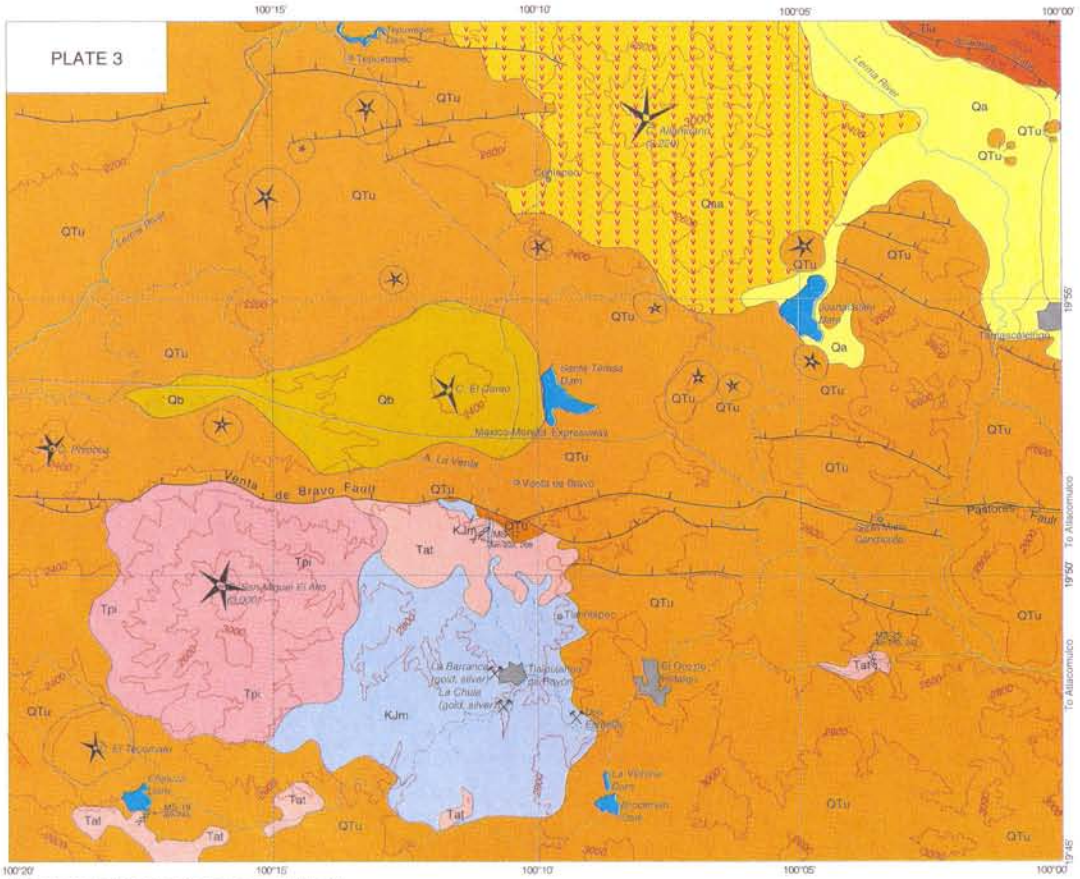

Geologic mapping by Gerardo J. Aguirre Diaz from 1988 to 1991

Computer color separation was made by José de Jesús Vega-Carrillo.

Radiometric age (Ma) (K-Ar method)

EXPLANATION

Quaternary

- Qa — Alluvium and talus
- Qrp — Reworked pumice and lake deposits
- Qb — Scoria-cinder cones and mafic lava flows
- Qaa — Altamirano andesite: intermediate lava flows and tephra
- QTu — Undifferentiated Tertiary and Quaternary volcanic rocks

Pliocene

- 2.2 ± 0.1 Tec — El Comal scoria cone: andesitic flows and scoria-fall
- 2.5 ± 0.1 Tág — Garabato andesite: hornblende andesite
- 2.9 ± 0.7 Ter — El Rincón rhyolite: lava dome complex of Sierra El Rincón
- 3.4 ± 0.1 Thi — Huichapan tuff: felsic ignimbrite-surge-fallout sequence
- 3.7 ± 0.2 Thir — Hormigas andesite: trachyandesitic lava flows
- 3.8 ± 0.2 Tse — Santa Rosa andesite: central lava domes of the Amealco caldera
- 3.9 ± 0.2 Tlc — La Cruz rhyolite: central lava domes of the Amealco caldera
- 4.1 ± 0.4 Tpa — Palomas andesite: trachyandesitic-trachydacitic lavas and tephra
- 4.3 ± 0.1 Tcd — Campana lava dome: trachydacite
- 4.3 ± 0.2 Taa — Amealco andesite: trachyandesitic rim lava domes of the Amealco caldera
- 4.7 ± 0.3 Tat, Tatb — Amealco tuff: trachyandesitic-trachydacitic pyroclastic-ignimbrite-surge-fallout sequence.
- 4.8 ± 0.3 Tr — Pliocene rhyolite: felsic ignimbrite, pumice fallouts and lava domes
- Tlo — La Loma andesite: intermediate lavas of volcanoes Ñadó, Botí and El Gallo
- 5.6 ± 0.2 Tsv — Sierra Vaquerías: intermediate volcano-lava dome complex

J-K

- KJm — Mesozoic (Jurassic-Cretaceous) metasediments of the Tlalpujahua-El Oro region

- Thu — Huimilpan tuff felsic ignimbrite
- Tco — Coronita rhyolite: lava domes
- Tsc — Spatter cone
- Tbc — Brick pumice: pre, co, and post Taa pumice deposits
- Tga — Galindillo rhyolite lava dome
- Tpi — Undifferentiated Pliocene intermediate lavas and breccias

SYMBOLS

- Paved highway
- Unpaved road
- Railroad tracks
- Village or town
- City or major town
- River
- Water reservoir
- Stream
- Contour line (m.a.s.l.)
- Peak
- Contact, dotted where concealed
- Normal fault
- Strike and dip
- Sample site
- Measured section and number
- Volcano
- Lava dome
- Mine

GEOLOGIC MAP OF THE AMEALCO CALDERA REGION (CONTINUED)

Tilley, C.E., 1960, Differentiation of Hawaiian basalts—some variants in lava suites of dated Kilauean eruptions: Journal of Petrology, v. 1, p. 47-55.

Tsuchiyama, A., 1985, Dissolution kinetics of plagioclase in the melt of the system diopside-albite-anorthite, and origin of dusty plagioclase in andesites: Contributions to Mineralogy and Petrology, v. 89, p. 1-16.

Verma, S.P.; Carrasco-Núñez, Gerardo; and Milán, Marcos, 1991, Geology and geochemistry of Amealco caldera, Qro., Mexico. *in* Verma, S.P., ed., Calderas—genesis, structure and unrest: Journal of Volcanology and Geothermal Research, v. 47, p. 105-127.

Verma, S.P.; Verma, M.P., Carrasco-Núñez, Gerardo, and Milán, Marcos, 1989, Geology and geochemistry of Amealco caldera, Querétaro, Mexico: Annales Geophysicae, Special Issue for the 14th General Assembly, Barcelona, Spain, p. 58 (abstract).

Wilcox, R.E., 1954, Petrology of Parícutin volcano, Mexico: U.S. Geological Survey Bulletin 965 C, p. 281-354.

Yáñez-García, Camilo, 1984, Exploración geológica de la caldera de Huichapan, Estado de Hidalgo: Sociedad Geológica Mexicana, Convención Geológica Nacional, 7, Resúmenes, p. 171-173 (abstracts).

APPENDIX A
MEASURED SECTIONS

The coordinates of the base of each measured section are provided in each of them (Sections 1-26). An index map of their localities (Figure A-1) is included in this appendix. Elevation, in meters, is indicated to the left of the sections. Also to the left, and with the prefix "Am", are indicated the numbers of the samples that were gathered from the measured sections. The terminology used is that recommended by Cas and Wright (1987) and references therein. Explanation of symbols is provided in Figure A-2.

Figure A-1. Location map of the measured sections.

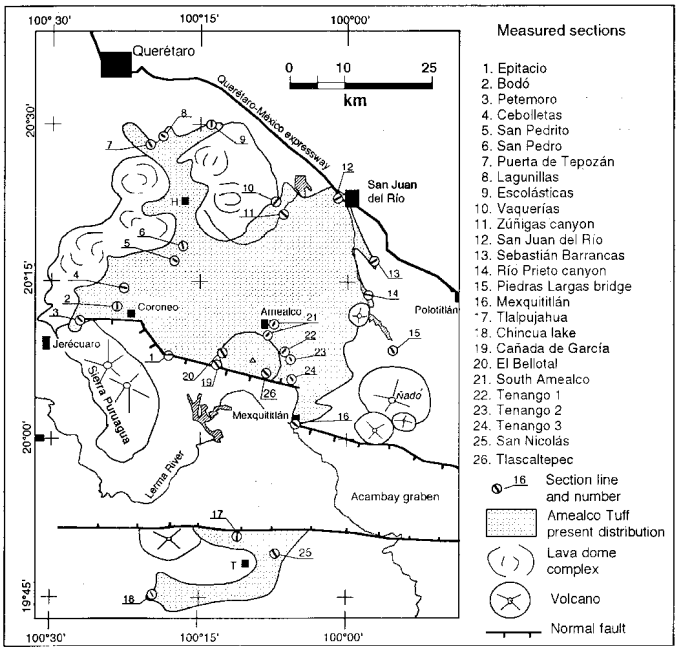

Figure A-2. Explanation of symbols used in the measured sections.

APPENDIX A
MEASURED SECTIONS

The location coordinates for the base of each measured section are provided in each section. An index map of them is included in this appendix. Elevation, in meters, is indicated to the left of the section. Also to the left, and with the prefix "Am", are indicated the numbers of the samples that were gathered from the measured sections. The terminology used is that recommended by Cas and Wright (1987) and references therein.

Symbols used

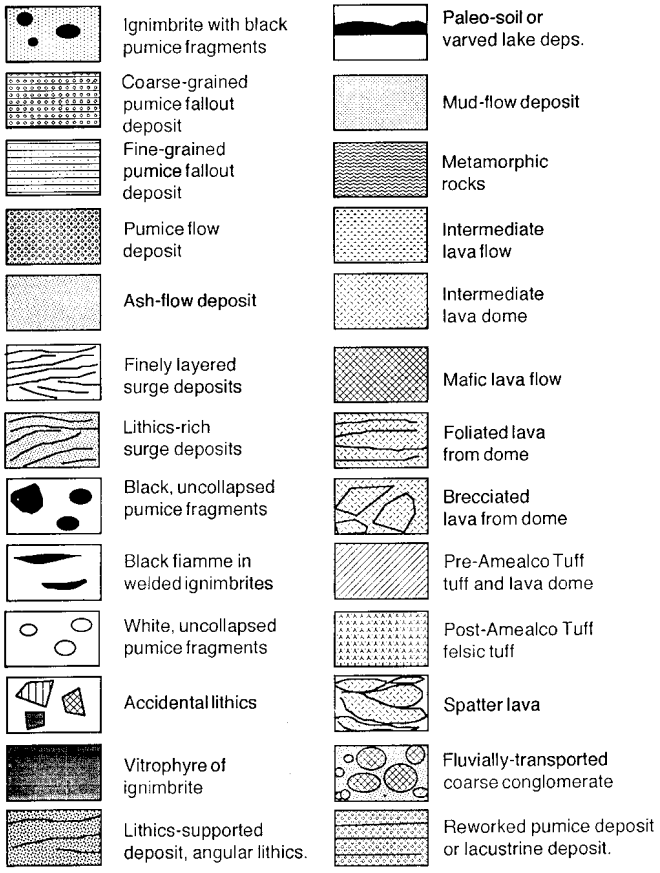

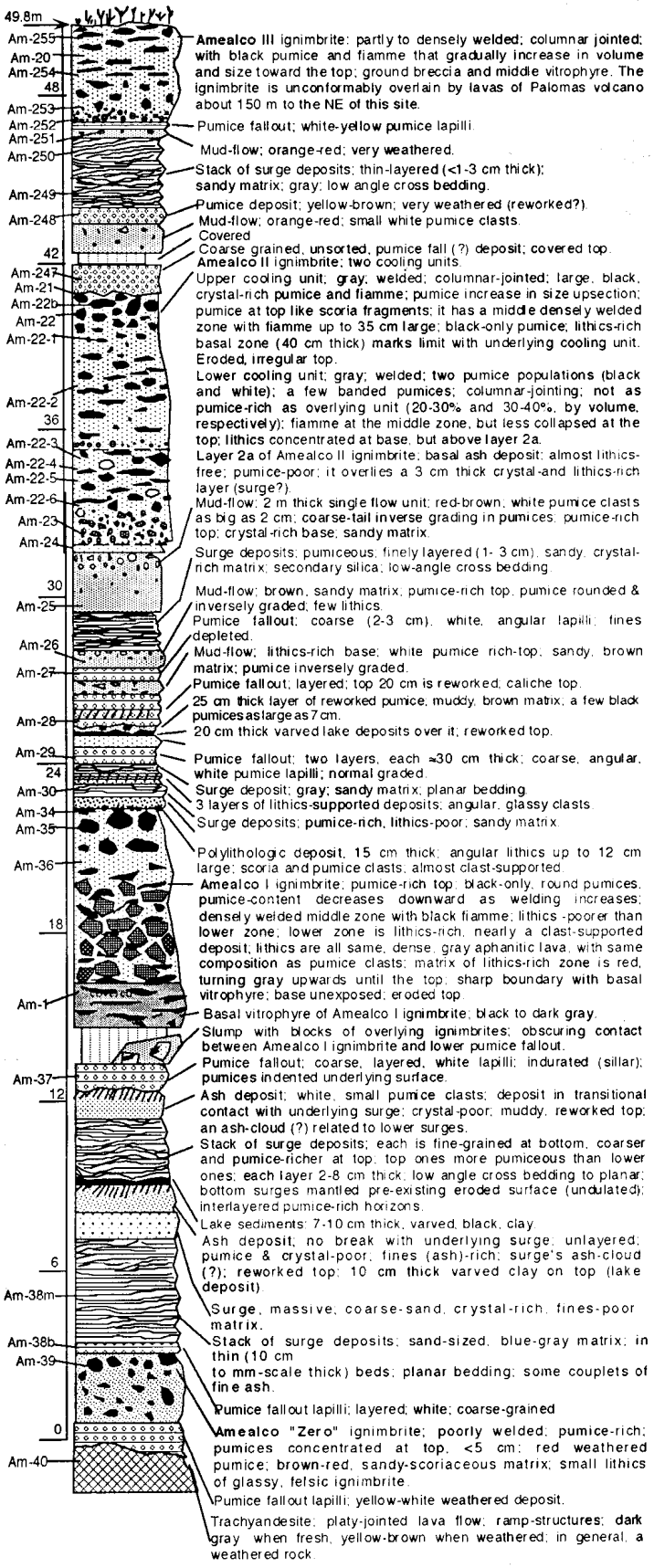

Section 1.- EPITACIO: 15 km to the west, {base at 20° 8' 1" lat N, 100° 18' 8" long W}.

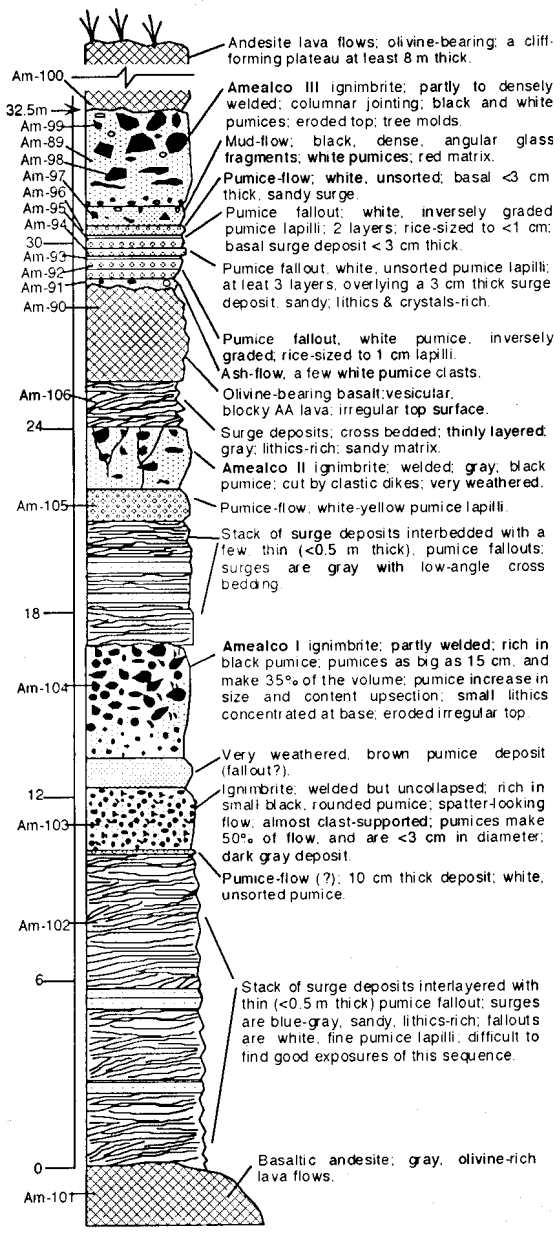

Section 2.- BODÓ: 30 km to the west, {base at 20° 12' 44" lat N, 100° 23' 40"}.

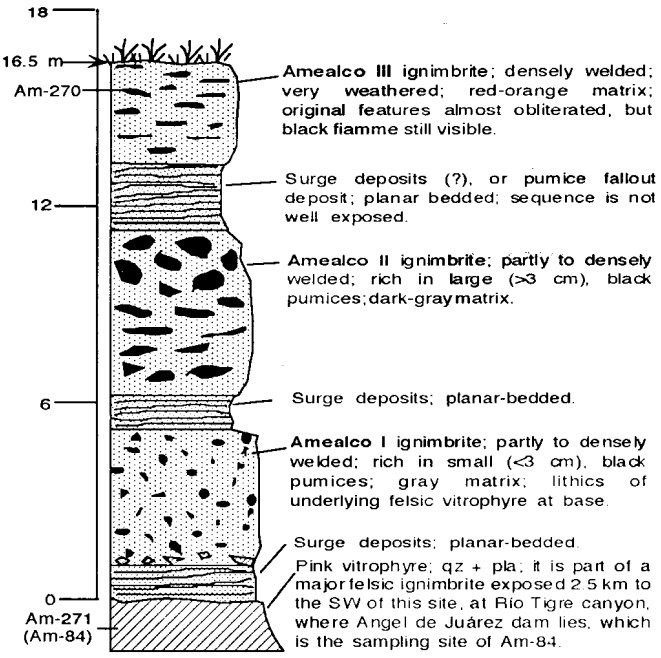

Section 3.- PETEMORO: 32 km to the WNW
{base at 20° 11' 28" lat N, 100° 27' 3" long W}.

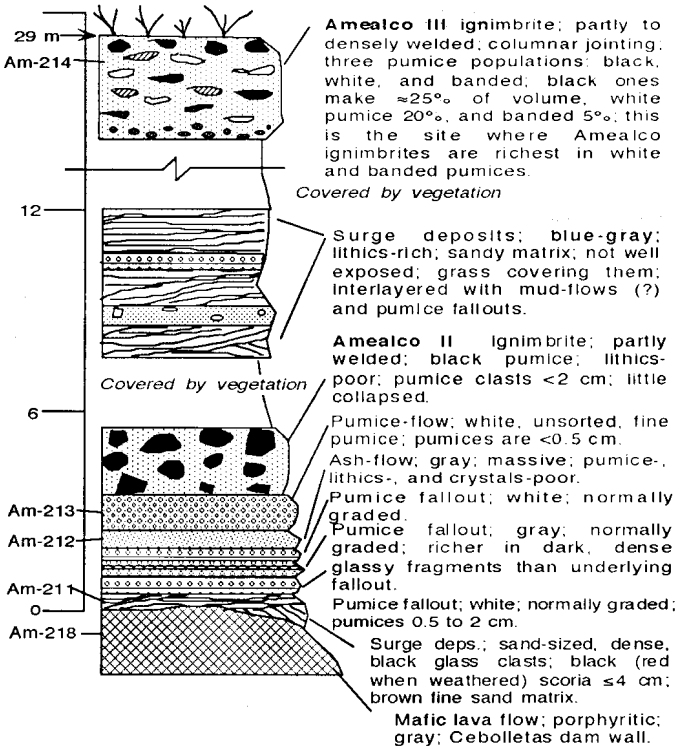

Section 4.- CEBOLLETAS: 35 km to the northwest
{base at 20° 14' 26" lat N, 100° 22' 37" long W}.

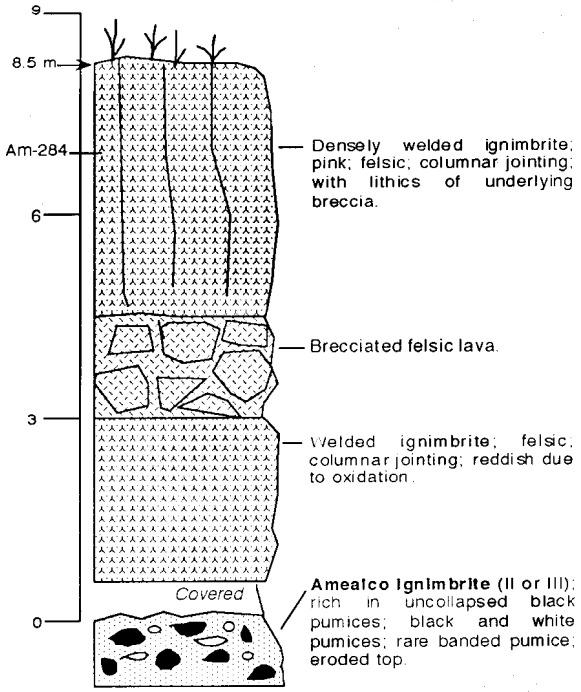

Section 5.- SAN PEDRITO: 23 km to the NE
{base at 20° 18' 15" lat N, 100° 18' 30" long W}.

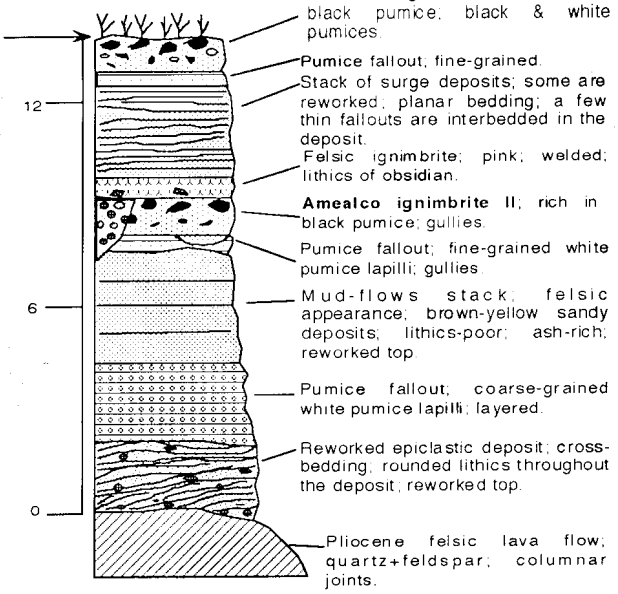

Section 6.- SAN PEDRO: 26 km to the NW
{base at 20° 19' 48" lat N, 100° 16' 45" long W}.

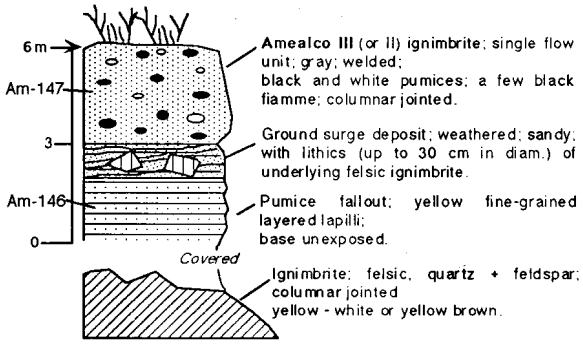

Section 7.- PUERTA DEL TEPOZÁN: 40 km to the N
{base at 20° 27' 0" lat N, 100° 19' 55" long W}.

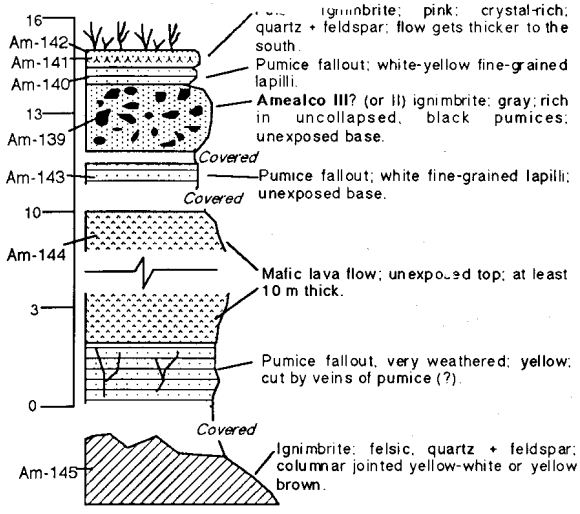

Section 8.- LAGUNILLAS: 40 km to the N
{base at 20° 27' 28" lat N, 100° 17' 36" long W}.

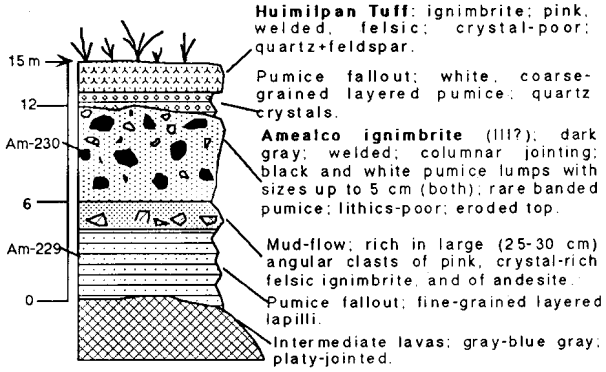

Section 9.- ESCOLÁSTICAS: 40 km to the NNE
{base at 20° 25' 06" lat N, 100° 13' 33" long W}.

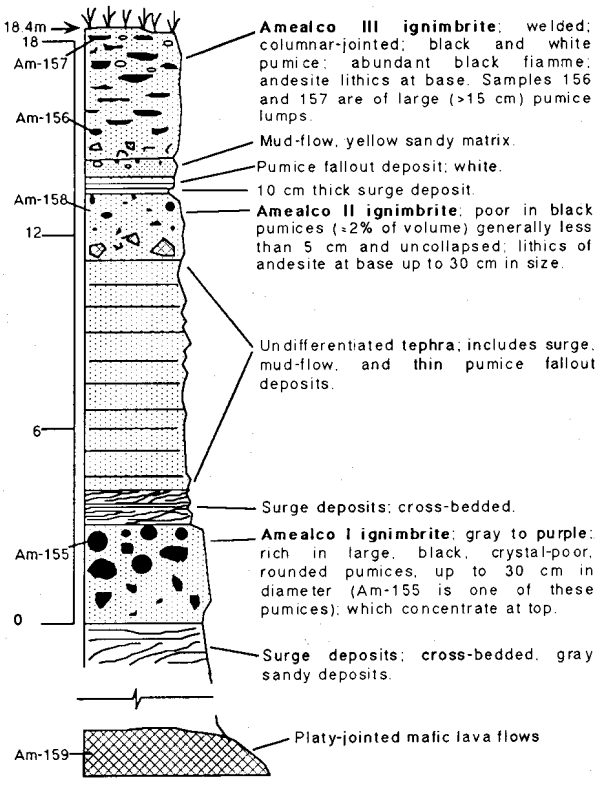

Section 10.- VAQUERÍAS: 30 km to the NNE
{base at 20° 22' 6" lat N, 100° 6' 43" long W}.

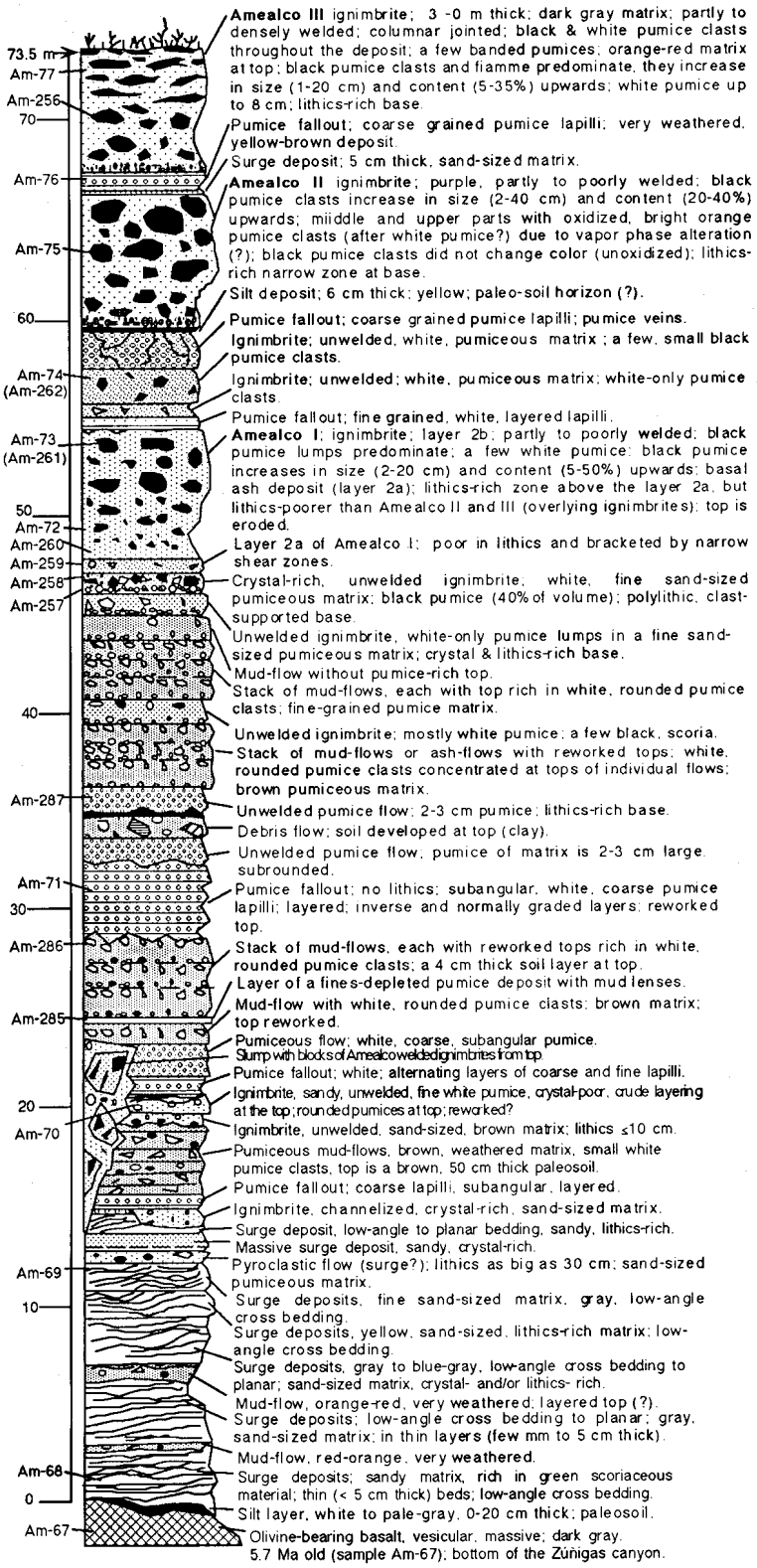

Section 11.- ZÚÑIGAS CANYON: 28 km to the NNE
{base at 20° 21' 8" lat N, 100° 6' 50" long W}.

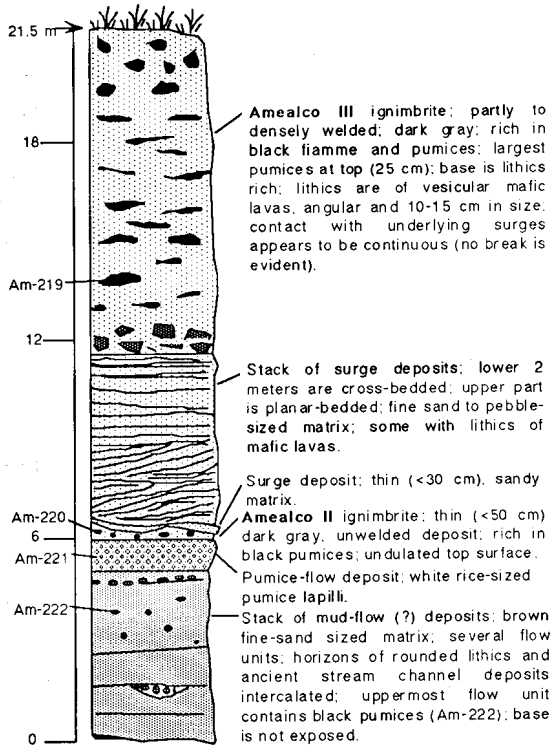

Section 12.- SAN JUAN DEL RÍO: 32 km to the NNE
{base at 20° 22' 21" lat N, 100° 0' 20" long W}.

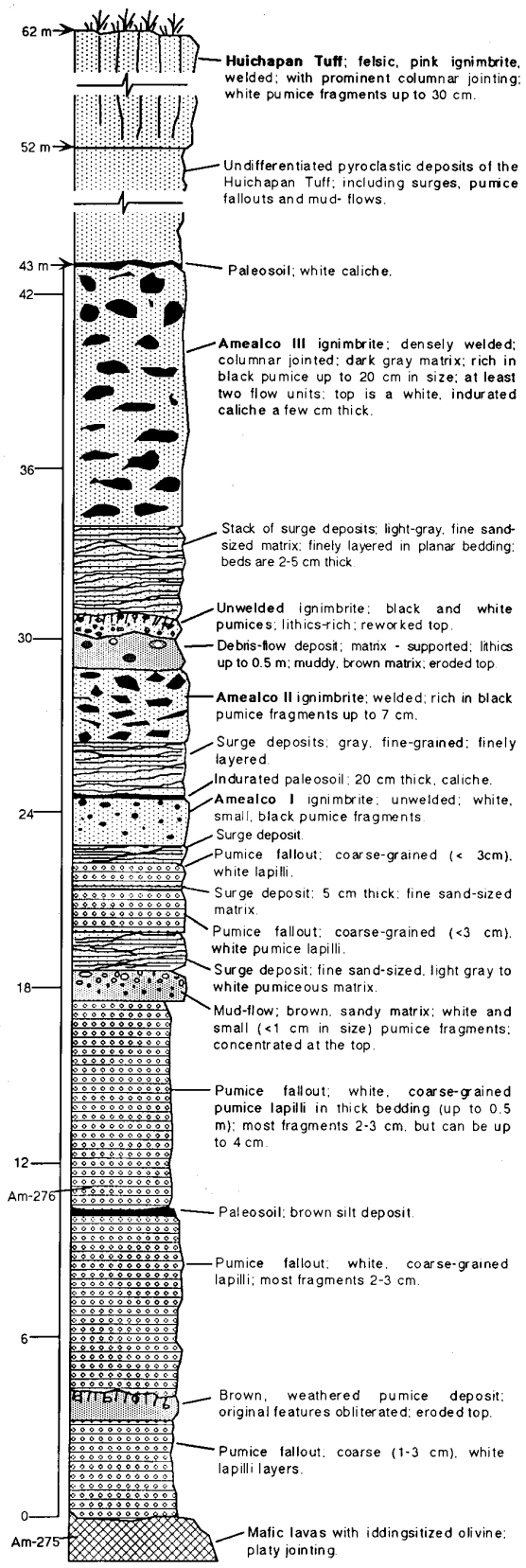

Section 13.- SAN SEBASTIÁN BARRANCAS (28 km to the NE) {base at 20° 16' 31" lat N, 99° 57' 54" long W}.

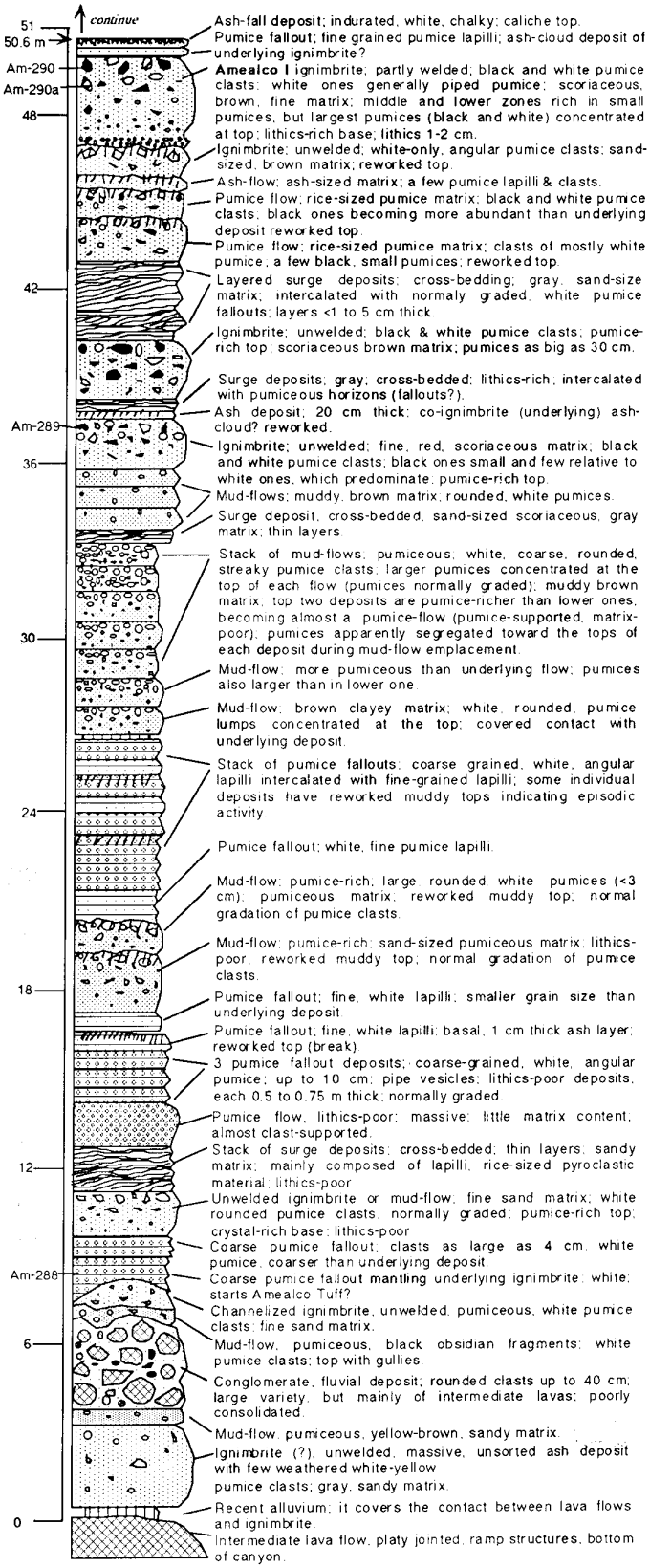

Section 14.-RÍO PRIETO CANYON; 25 km to the NE, {base at 20° 13' 44" lat N, 99° 58' 20" long W}.

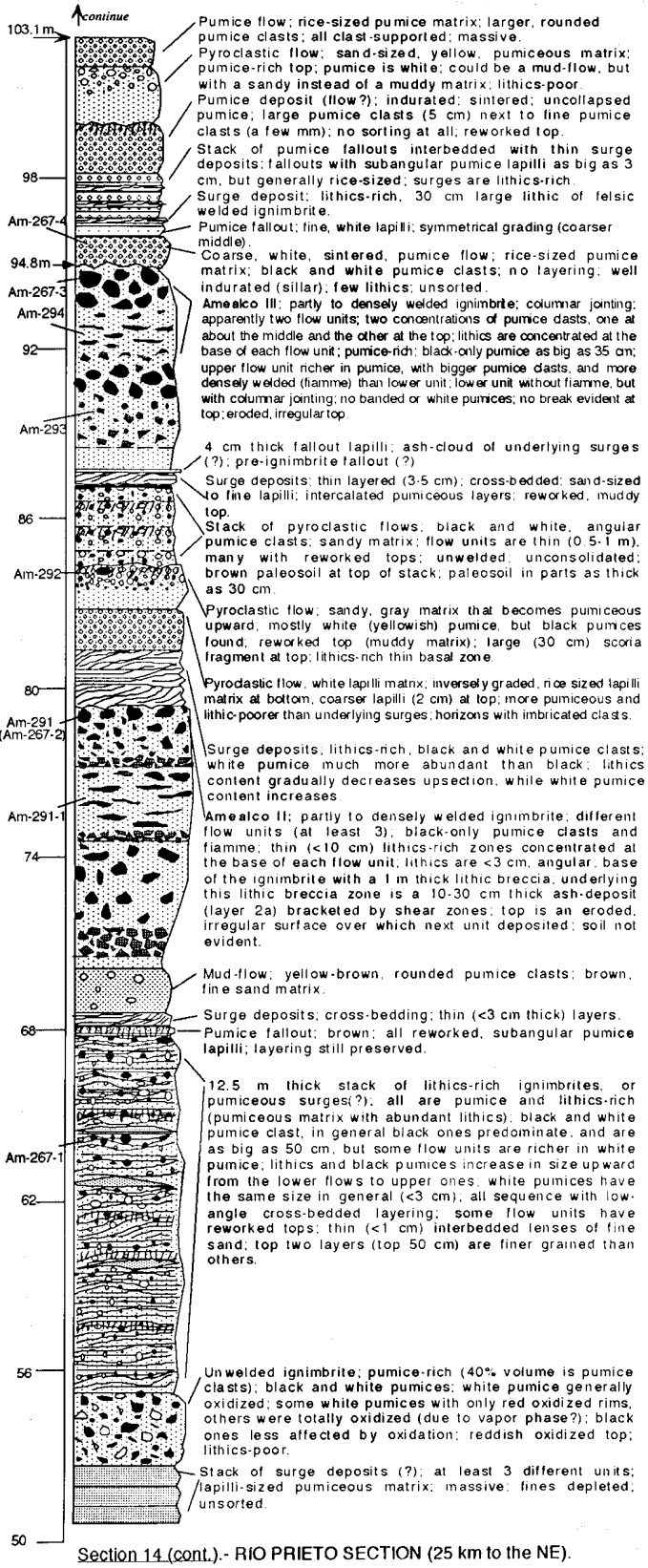

Section 14 (cont.).- RIO PRIETO SECTION (25 km to the NE).

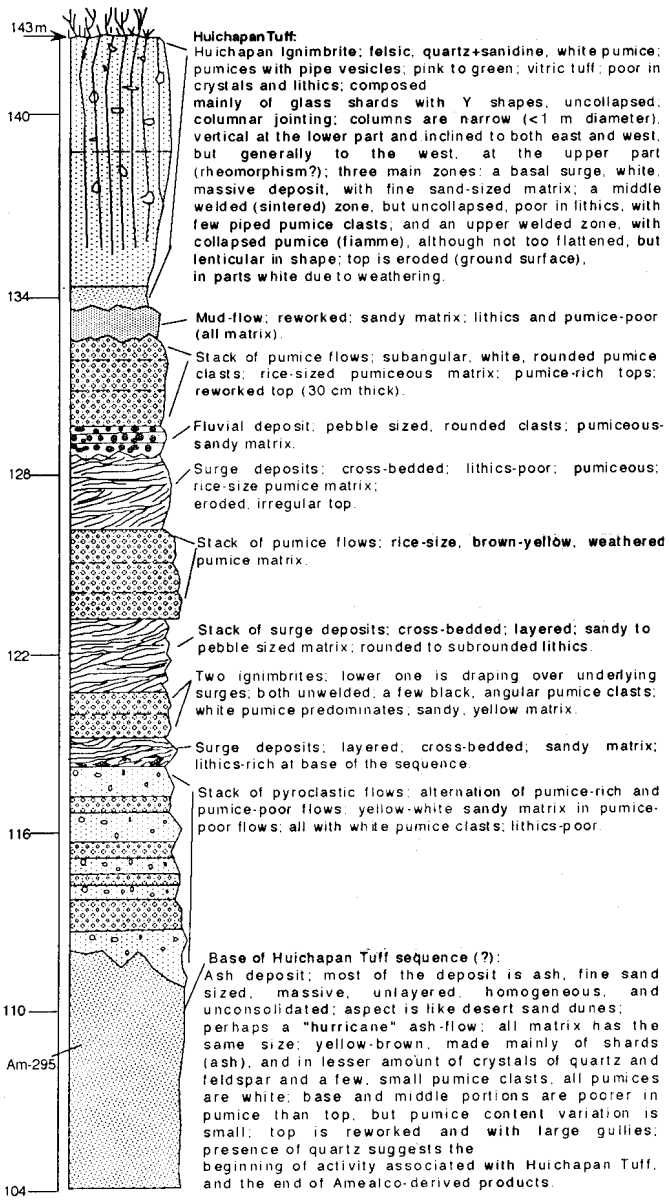

Section 14 (cont.).- RIO PRIETO CANYON (25 km to the NE).

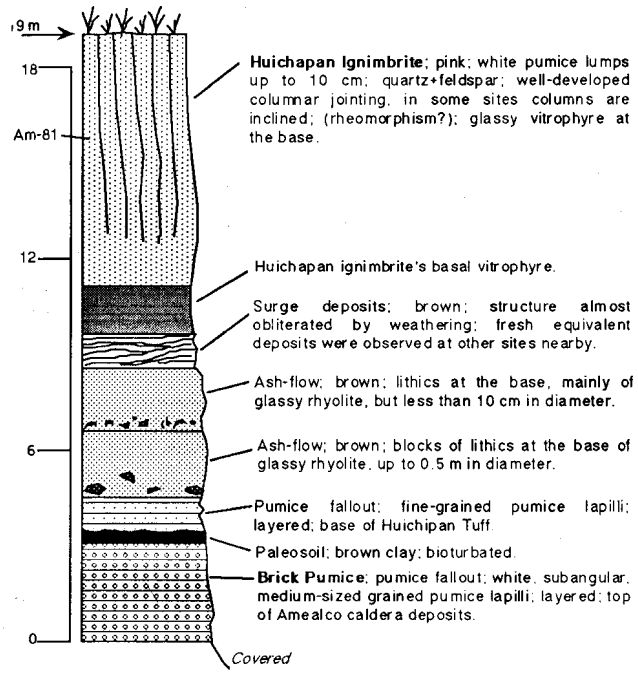

Section15.- PIEDRAS GRANDES BRIDGE: 25 km to the E {base at 20° 8' 38" Lat N, 99° 56' 36" Long W}.

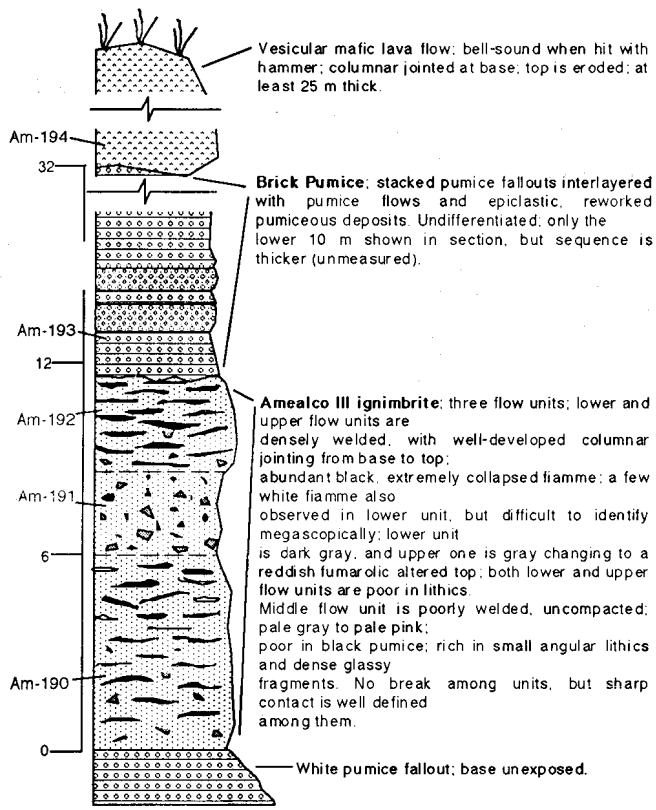

Section16.- MEXQUITITLÁN SECTION: 13 km to the SE {base at 20° 2' 4" lat N, 100° 4' 20" long W}.

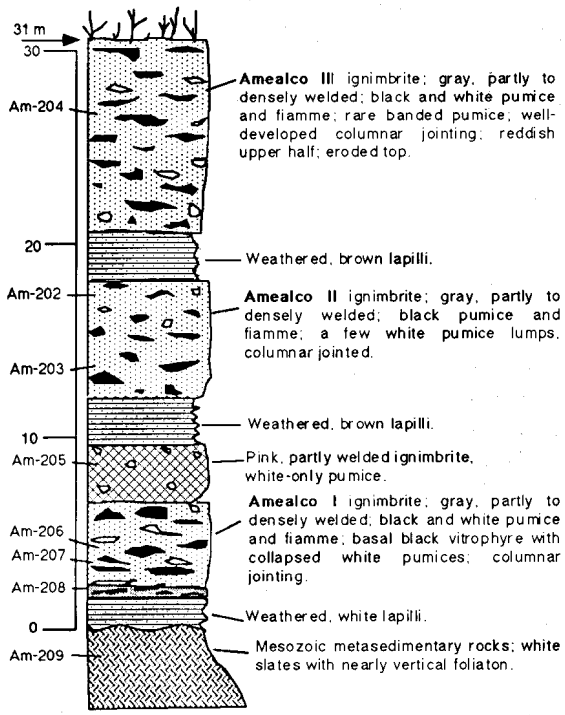

Section17.- TLALPUJAHUA: 31 km to the south; {base at 19° 50' 45" lat N, 100° 11' 15" long W}.

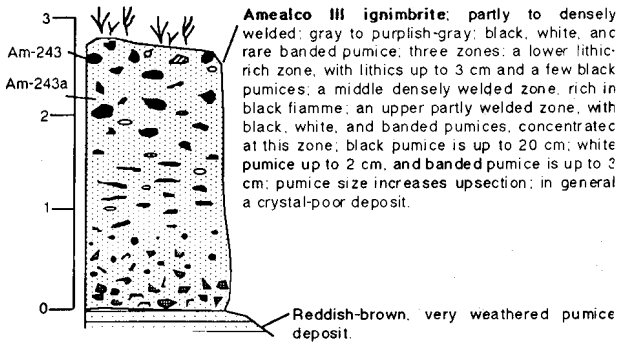

Section-18.- CHINCUA SECTION: 38 km to the SW {base at 19° 45' 34" lat N, 100° 17' 34" long W}.

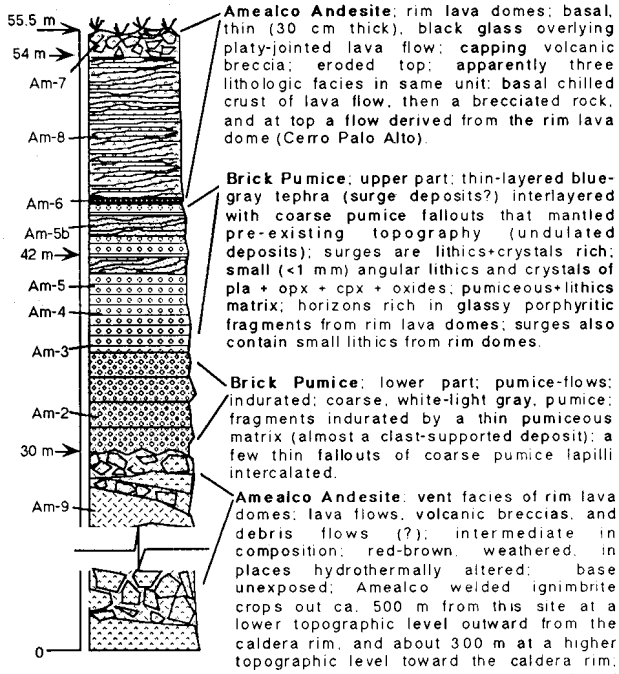

Section19.-CAÑADA DE GARCíA: on SW caldera rim {base at 20° 7" 13" lat N, 100° 13' 23" long W}.

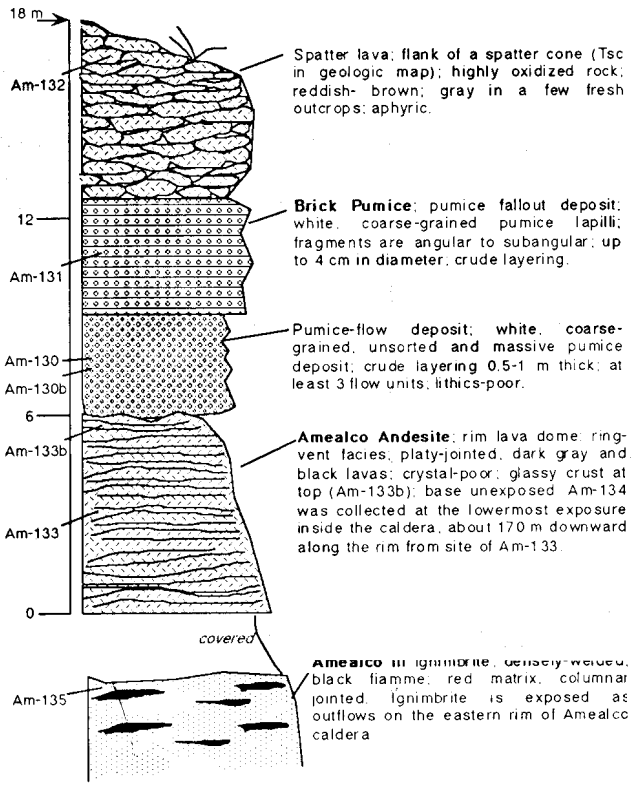

Sections 21a and 21b.- SOUTH AMEALCO: composite section that extends 3-5 km between the caldera rim to the immediate northeastern flank of the caldera, just south of Amealco town {Base of 21a at 20° 11' 7" lat N, 100° 7' 43" long W; base of 21b at 20° 9' 46" lat N, 100° 7' 45" long W}.

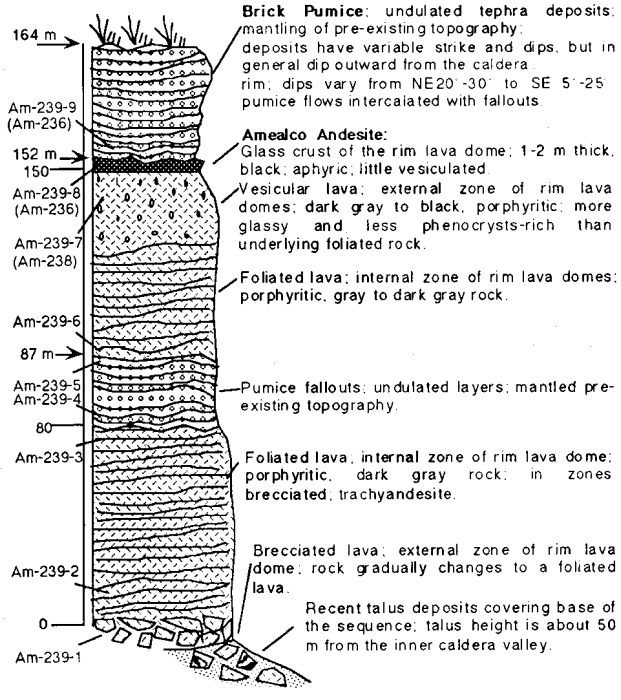

Section20.- EL BELLOTAL: not to scale, western caldera rim; 2.5 Km to the west {base is 20° 07' 50" lat N, 100° 12' 45" long W}.

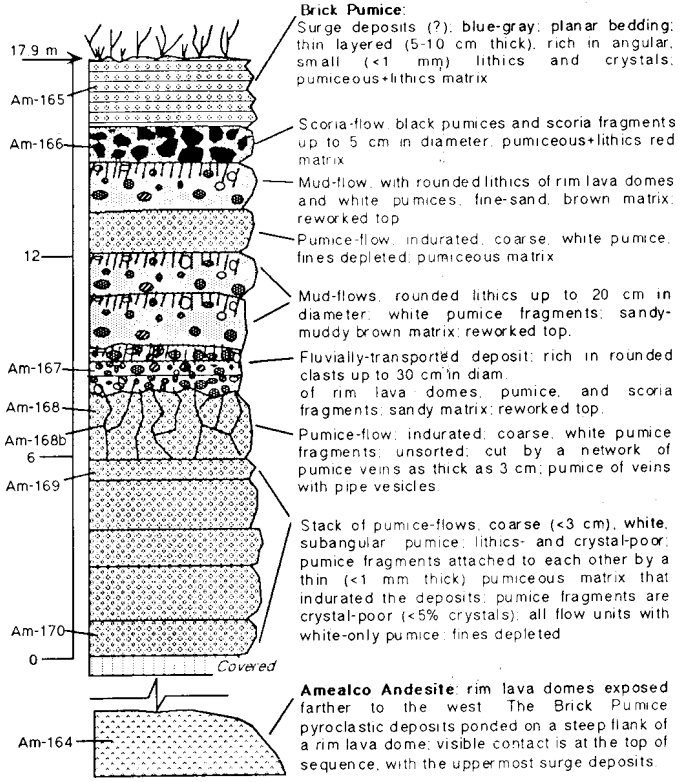

Section22.-TENANGO- 1: 7 km to the east {base at 20° 7' 58" lat N, 100° 6' 40" long W}.

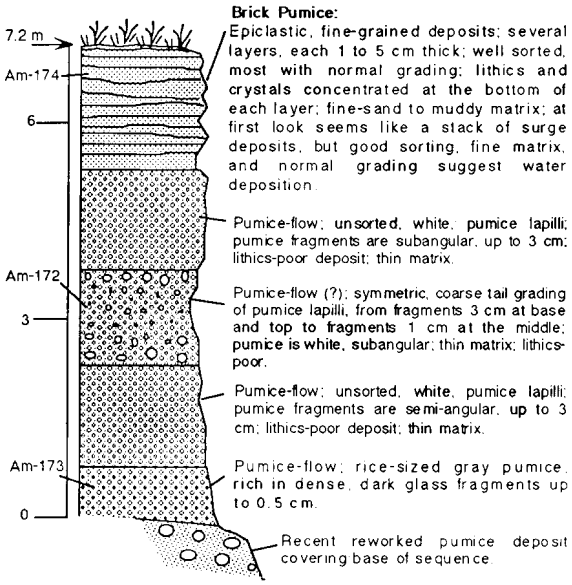

Section 23.- TENANGO-2 : 8 km to the east (base at 20° 7' 4" lat N, 100° 5' 40" long W).

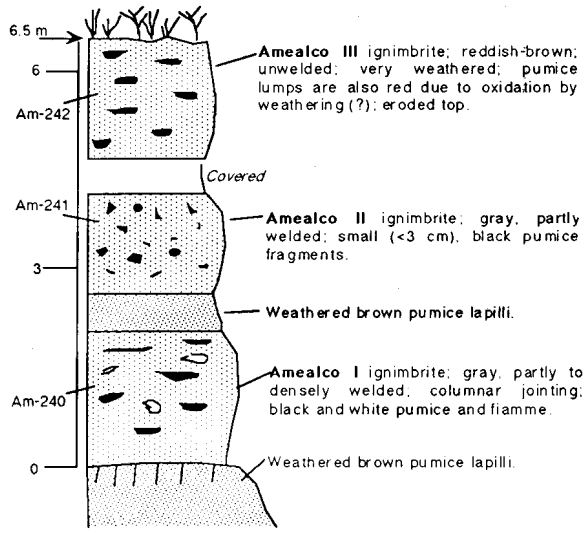

Section 25.- SAN NICOLÁS TLALTELONGO: 34 km to the SSE (base at 19° 48' 25" lat N, 100° 3' 46" long W)

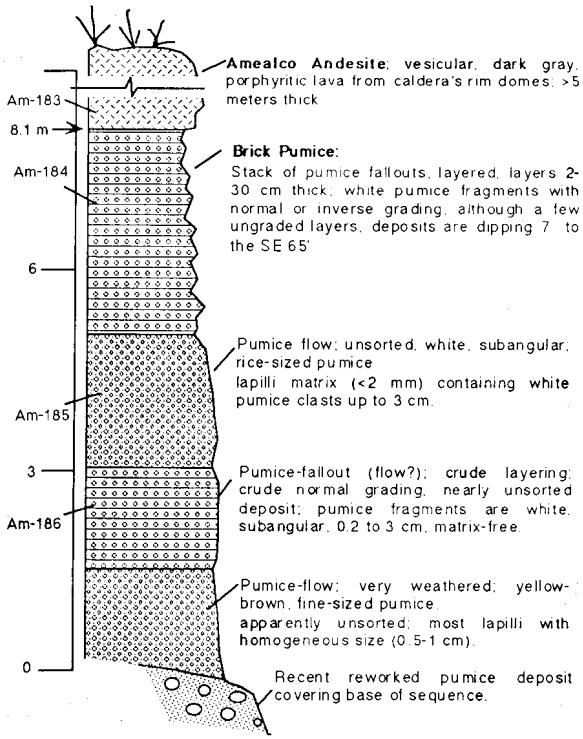

Section 24.- TENANGO-3 SECTION: 8 km to the SE (base at 20° 6' 5" lat N, 100° 5' 50" long W).

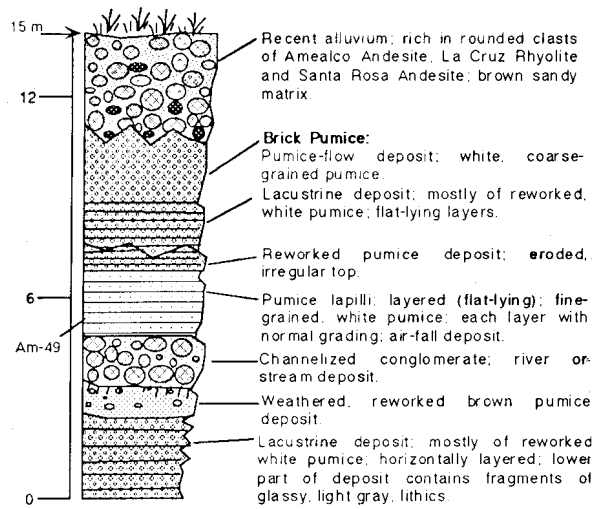

Section 26.- SAN MIGUEL TLASCALTEPEC: inside caldera (base at 20° 6' 18" lat N, 100° 7' 30" long W).

APPENDIX B
PETROGRAPHIC DESCRIPTION OF THE AMEALCO CALDERA UNITS

Amealco Tuff

Ignimbrites. Plagioclase is the most abundant mineral. It is generally subhedral, tabular, and with polysynthetic twinning. Plagioclase crystals range from <0.3 mm to 6 mm. The most common size is ~3 mm. Most crystals are unzoned and unfritted. Crystals generally have broken margins and are internally fractured. Large brown and pale yellow glass inclusions commonly occur within plagioclase phenocrysts (Figure 10, b, c). Occasionally, inclusions of Fe-Ti oxides occur in plagioclase too. Orthopyroxene is the second most abundant mineral phase. It is colorless and lacks pleochroism. Crystals are subhedral, generally prismatic with rounded corners. Orthopyroxene is commonly rich in Fe-Ti oxide inclusions. Sizes of orthopyroxene range from <1 mm to 5 mm. Clinopyroxene is less abundant than orthopyroxene, but it is an ubiquitous mineral. Twinned crystals are common. Sizes range from <0.3 mm to 2 mm, but generally in the order of 1 mm. Olivine is sporadically found in the ignimbrites. It occurs as prismatic, small, fractured crystals with oxidized borders and fractures (iddingsitized?). In some near-vent sites, olivine is as abundant as the orthopyroxene (2-3 vol. %). Olivine has been found attached to a brown glass with the same composition as that of brown pumices, thus suggesting that olivine crystallized from the Amealco magma and it is not xenocrystic.

Amealco ignimbrites commonly contain glomerocrysts, up to 10 mm in diameter. They are either of plagioclase + orthopyroxene + Fe-Ti oxides, or plagioclase + orthopyroxene + clinopyroxene + Fe-Ti oxides, or only of both pyroxenes + Fe-Ti oxides. Many glomerocrysts contain an interstitial brown glass. Clots of interlocking feldspar, with interstitial glass, are also found in the ignimbrites, but in lesser abundance than the glomerocrysts with ferromagnesian phases. The glass in the coarse glomerocrysts may be interpreted as trapped liquid in cumulates. In the finer interlocking feldspar clots, glass could be interstitial liquid from the solidification zone in the magma chamber (Langmuir, 1989).

Tephra deposits. Tephra interlayered with the major ignimbrites, particularly the surge deposits, contains, in general, the same mineralogy as the ignimbrites: plagioclase, orthopyroxene, clinopyroxene, Fe-Ti oxides, accessory apatite, and occasionally olivine. It also includes mingled glass populations (brown and colorless glass). Plagioclase, as in the ignimbrites, contains large brown glass inclusions, but in many cases, glass inclusions are even larger and more abundant than those observed in the ignimbrite plagioclases. The pyroxenes commonly have Fe-Ti oxide inclusions, also. Glomerocrysts of plagioclase + clinopyroxene + olivine and of plagioclase + orthopyroxene + Fe-Ti oxides are common in these deposits. Some surge deposits are rather crystal-poor, mainly composed of dense, angular, glassy fragments, with a few crystals of plagioclase and pyroxenes and a few vesiculated glass clasts (juvenile). Many of the dense fragments contain olivine, clinopyroxene and plagioclase, and could be interpreted as accidental. Air-fall tuffs are generally depleted in fines, and mainly composed of angular pumice fragments. Pumice in fallout deposits is generally crystal-poor, with phenocrysts of plagioclase, orthopyroxene, and, in lesser amounts, clinopyroxene and Fe-Ti oxides.

Brick Pumice

Pumice flow deposits. These deposits are mainly composed of subangular, white, highly vesiculated, coarse pumice lapilli, with a very thin (<1 mm thick), pale-yellow glassy matrix between fragments. Distinct pumice populations are found in some of the post-rim dome flows in the form of black and white to yellow pumices. In general, fragments are larger than 1 cm, mostly in the 1-3 cm range. There is no sorting of the pumice lapilli. There are 1 mm fragments next to >3 cm fragments. Pumice is nearly aphyric and highly vesiculated, but a few percentage (<6 vol. %) is dense angular fragments of either brown or colorless glass. Colorless dense glass fragments contain microlites and crystallites of plagioclase and pyroxene (?), and brown dense glass fragments are generally microlitic, but some contain phenocrysts of plagioclase and orthopyroxene. Brown and colorless dense glass may be juvenile, but fragments with a dusty-looking devitrified or altered matrix may be accidental. Crystal contents as bulk deposit are generally less than 5 vol. %. Loose crystals of plagioclase are generally around 1 mm, anhedral to subhedral, with internal fractures and untwinned. Plagioclase commonly exhibits undulatory extinction and contains large brown glass inclusions. This texture indicates a fast growth of the plagioclase, but skeletal crystals were not observed. Orthopyroxene and clinopyroxene occur as single crystals or as crystal clots attached to brown dense glass. Clots are up to 1.5 mm. Orthopyroxene is more abundant than clinopyroxene (2 and 1 vol. %, respectively), and commonly occurs as tabular, subhedral crystals. Clinopyroxene is either prismatic or tabular. Both ortho- and clinopyroxene rarely exceed 1 mm. Fe-Ti oxides occur either as single crystals, or as part of dense glass fragments.

Pumice fallout deposits. They have very similar petrographic characteristics to the pumice-flow deposits, such as mainly being composed of subangular white to yellow pumice lapilli. The main difference is that the fallouts lack the thin glassy matrix observed in the pumice-flows and also lack the concentration of lithics at the base of each unit. Mingled dark and white pumices were not observed in the fallout deposits.

Surge deposits. They are rich in small, dense, angular, glassy lithics, generally less than 2 mm in size. Crystals occur loosely or within the lithics, including plagioclase, orthopyroxene, clinopy-

roxene, and Fe-Ti oxides. Total crystal content ranges from 10 to 25 vol. %. Matrix is made up of pumice plus tiny crystals and lithics (<0.3 mm). Clots, up to 2 mm, of plagioclase, orthopyroxene, and Fe-Ti oxides, plus a microlite-rich, unvesiculated brown glass are ubiquitous in these deposits. They may be lithic fragments from blasted rim domes, particularly for the post-dome deposits (*e.g.*, co-rim dome deposits), since they show very similar textures to the rim lava domes. In the case of the pre-rim dome deposits, they could be glomerocrysts with glass attached to the crystals, erupted as juvenile pyroclastic fragments. Angular lithic fragments in these pre-rim dome deposits are made up of fresh, brown dense glass, rich in black hairy-shaped crystallites (trichites), which may be juvenile. In general, single crystals of plagioclase in pre-, co- and post-rim dome deposits are broken, anhedral to subhedral, unfractured, unzoned, unfritted, and without undulatory extinction; in other words, very clear-looking crystals, generally tabular and <0.3 to 1 mm. Single orthopyroxene and clinopyroxene are rather small crystals, up to 1 mm, anhedral to subhedral. Orthopyroxene is generally tabular, and clinopyroxene tabular and prismatic.

Amealco Andesite (rim lava domes)

The textures of the Amealco Andesite show a wide variation, from porphyritic and relatively phenocryst-rich (30 vol. %) to aphanitic or microlite-rich, glassy rocks, poor in phenocrysts (<1 vol. % of phenocrysts). As explained above, this variation is due to the different lithofacies that a single dome can exhibit. In spite of the variation of textures and physical aspect, the Amealco Andesite varies little in chemical composition (Aguirre-Díaz, 1993a). For instance, glassy, phenocryst-poor samples are trachyandesite as are the phenocryst-rich samples. Amealco Andesite includes plagioclase, orthopyroxene, clinopyroxene, Fe-Ti oxides, apatite, and rare olivine. Glomerocrysts of these phases are common and up to 6 mm. Glass in the glomerocrysts is either intergranular or, more commonly, also attached externally to the phenocrysts.

Three plagioclase populations, plus the groundmass microlite variety, are evident. The first group consists of large (up to 3 mm) plagioclase phenocrysts, mostly tabular, but also equant, with large glass inclusions. Glass inclusions are up to 0.25 mm in the largest crystals, have irregular amoeba shapes, and are generally colorless, although several are pigmented because of abundant opaque crystallites. Several crystals have cores rich in large glass inclusions mantled by a zone free of glass inclusions. The mantled crystals may indicate that initially the plagioclase grew fast, trapping the liquid, but final growth stages were slow enough to avoid the trapping of liquid, or that the plagioclase was resorbed and later re-equilibrated with the liquid. The second plagioclase population is rather small, on the order of 1 mm. Crystals are subhedral to euhedral, generally tabular, free of inclusions, unzoned but with undulatory extinction. The third group is the plagioclase that occurs in crystal clots. This plagioclase is generally euhedral to subhedral and tabular. It is clear, inclusion-free, and unzoned. Plagioclase in clots occurs as interlocking, fine crystals or as glomerocrysts. In the former, plagioclase is thin, lath-shaped, euhedral to subhedral, and less than 0.3 mm, with brown glass filling the wide space between crystals; in the latter, plagioclase is larger than 0.3 mm and up to 3 mm, is anhedral, and occurs together with two pyroxenes, apatite and Fe-Ti oxides. Glomerocrystic larger plagioclase commonly contains inclusions of tiny euhedral apatite, orthopyroxene, clinopyroxene, Fe-Ti oxides, and glass, suggesting a long residence time in the magma chamber, because other phases were enclosed by the plagioclase as it grew. These characteristics also suggest that glomerocrystic plagioclase was formed earlier than the other plagioclases that lack crystal inclusions and probably earlier than the group rich in glass-inclusions. Clots of interlocking fine plagioclase may represent fragments from the solidification zone (Langmuir, 1989) of the magma chamber.

Pyroxenes and Fe-Ti oxides occur either as free crystals or in glomerocrysts. Free orthopyroxene is tabular or prismatic, euhedral or subhedral, and less than 1 mm in size. It commonly contains inclusions of Fe-Ti oxides, and euhedral or subhedral apatite as large as 0.25 mm. Pyroxenes are unzoned and free of reaction rims. Glomerocrystic orthopyroxene is rather large, up to 2 mm, also containing inclusions of apatite and Fe-Ti oxides. Clinopyroxene in the glomerocrysts is generally tabular, up to 2 mm, and rich in Fe-Ti oxides. Free clinopyroxene is either tabular or prismatic, subhedral, and smaller than glomerocrystic clinopyroxene. Single twinned prismatic clinopyroxene is common.

Campana Dacite

Although plagioclase grew quite large (up to 5 mm), it is anhedral to subhedral, with rounded margins and poorly-developed polysynthetic twinning, absent in most of the crystals. It is unzoned and exhibits undulatory extinction, with abundant, colorless glass inclusions. Crystals in clots contain both glass and clinopyroxene + Fe-Ti oxides inclusions. Some crystals show skeletal plagioclase in the cores, mantled by an inclusion-free plagioclase, but with a jagged, resorbed margin. Biotite is mottled and shows a reaction corona of Fe-Ti oxides and clinopyroxene.

Palomas Dacite

Early-erupted products. Lava flows located to the north of Palomas volcano are porphyritic, with a crystal content of 30 vol. %. Their groundmass is made of microlitic plagioclase and a dark glass pigmented with tiny opaques. Hornblende is abundant (10 vol. %), with sizes up to 3.2 mm. Hornblende is pleochroic, from yellow to dark brown, and commonly has an oxidized rim. Phenocrystic plagioclase is as abundant as the hornblende (10 vol. %), and shows disequilibrium textures, such as resorption embay-

ments and rounded corners, and is generally fritted. Some crystals exhibit complex cores that contain inclusions of orthopyroxene, clinopyroxene and Fe-Ti oxides; the core in turn is mantled by oscillatory zoned plagioclase with sharp margins and corners. Plagioclase also occurs in glomerocrysts. Glomerocrystic plagioclase is generally less resorbed than the free crystals. It shows undulatory extinction and is unzoned. Most of the glomerocrysts are only of plagioclase, but there are some that include hornblende and pyroxenes. Orthopyroxene is small, with sizes up to 0.5 mm, and comprises only 2 % of the volume. It occurs either in glomerocrysts or as free crystals that can be prismatic or tabular. Some samples exhibit hornblende partly replacing orthopyroxene. Clinopyroxene is slightly more abundant than orthopyroxene (3 vol. %) and larger (up to 1 mm), and occurs as single crystals or in glomerocrysts.

Middle products. Highly vesiculated scoria flows; vesicles make up about 45% of the volume and are generally elongated, parallel to the flow direction. The mineralogy is mainly of plagioclase and pyroxenes. Hornblende is absent, and Fe-Ti oxides are rare, except as the tiny crystals that form part of the groundmass. The groundmass is a microlites-rich glass; microlites are of plagioclase and the glass is pigmented with opaques.

Late products. Aa lava flows from the middle of the sequence, that overlie the tephra deposits but underlie the aa lava, contain about 23 vol. % phenocrysts, including plagioclase (15 vol. %), opaques after hornblende (3 vol. %), orthopyroxene (2 vol. %), clinopyroxene (2 vol. %) and Fe-Ti oxides (1 vol. %). Plagioclase exhibits a wide variation in size, from large phenocrysts up to 3.2 mm to microphenocrysts 0.3-1 mm, to microlites <0.3 mm. Glomerocrysts are rare. Three plagioclase populations are evident. One is rich in colorless glass inclusions, and with zones of skeletal plagioclase, mantled by inclusion-free plagioclase, indicating a fast growth, followed by a late re-equilibration with the liquid. A second group is about the same size range as the former, but does not contain glass inclusions, and does not exhibit skeletal plagioclase zones, but rather is clear, unzoned, and shows polysynthetic twinning. The third group is made by the microphenocrysts, which are subhedral plagioclase laths with well-developed polysynthetic twinning. Hornblende is assumed to have been part of the mineral assemblage, but no crystals were found; only opaques with acicular or lath shapes that may have been originally hornblende, now totally oxidized. Ortho- and clinopyroxenes are small (<0.5 mm) crystals, either tabular or prismatic, some of them with Fe-Ti oxide inclusions.

The black aa lava of Palomas volcano is texturally very similar to Amealco Andesite (rim lava domes), except for the occurrence of hornblende in the former. This lava is porphyritic, with phenocrysts of plagioclase, orthopyroxene, clinopyroxene, totally replaced hornblende by Fe oxides, and Fe-Ti oxides, plus apatite and zircon as accessories. The groundmass is mainly a dark glass pigmented with Fe-Ti oxides and aligned microlites of plagioclase; glass makes the bulk of the rock; 60% of the volume is glass and 25% microlitic plagioclase. Phenocrysts make up about 15% of the volume; plagioclase is the most abundant (10 vol. %), followed by orthopyroxene (2 vol. %), clinopyroxene (2 vol. %), and Fe-Ti oxides (1 vol. %, including the acicular opaques after hornblende). All phenocrysts of plagioclase are practically >2 mm, thus only two sizes occur in these rocks: large phenocrysts and groundmass microlites. Phenocrysts are generally single crystals; glomerocrysts are uncommon. Plagioclase is subhedral to anhedral, unfritted, most with sharp edges and corners, but a few rounded and zoned crystals are also present. As in the Amealco Tuff ignimbrites and the Amealco Andesite rim lava, many plagioclase phenocrysts contain large, brown glass inclusions with irregular shapes. Phenocrysts are generally untwinned and fractured. Plagioclase microlites are euhedral laths with polysynthetic twinning, with sizes <0.3 mm. Oxidized hornblende, as acicular small crystals of opaque oxides, is practically absent, making less than 0.5 vol. %. Clinopyroxene (2 vol. %) and orthopyroxene (2 vol. %) commonly occur as microphenocrysts (<0.3 mm), although some clinopyroxenes are up to 0.5 mm. Prismatic crystals, particularly of orthopyroxenes, are more common than tabular crystals.

The textural variation observed through the volcanic evolution of Palomas is not rare in volcanoes about the size of Palomas; for instance, Parícutin and Jorullo volcanoes exhibit textural and compositional differences from early to last erupted products (Wilcox, 1954; Luhr and Carmichael, 1985).

Santa Rosa Andesite and La Cruz Rhyolite (central lava domes)

Santa Rosa Andesite. It is generally porphyritic with microlitic groundmass. It contains plagioclase, orthopyroxene, clinopyroxene, Fe-Ti oxides, and apatite. Textures are similar to those in the Amealco Andesite (rim domes), but with a more crystal-rich groundmass. Santa Rosa Andesite contains 30-35 vol. % phenocrysts, most of which are concentrated in glomerocrysts. Glomerocrysts are up to 7 mm, and are composed mostly of plagioclase, but many also include two pyroxenes and Fe-Ti oxides. The minerals in these clots are rather coarse, particularly plagioclase (20-25 vol. %), which is relatively large, with single crystals up to 3 mm. It is subhedral and commonly tabular and, in contrast to older Amealco caldera products, exhibits oscillatory zoning. Large glass inclusions with regular shapes, sometimes parallel to the concentric zoning, occur irregularly in Santa Rosa plagioclase (Figure 14). Less commonly, glass inclusions are concentrated in the cores of the plagioclase, occasionally with an inclusion-free, concentrically zoned plagioclase mantle. Orthopyroxene (5 vol. %) commonly forms part of the glomerocrysts, but it also occurs as single crystals. It is tabular, up to 2 mm in the glomerocrysts, and generally <1 mm as single crystals. It generally contains inclusions of Fe-Ti oxides. Clinopyroxene (3 vol. %) is also more commonly found in the glomerocrysts than as single crystals. It is up to 1 mm for both the glomerocrystic and

the single crystals, and mostly with tabular shapes. Inclusions of Fe-Ti oxides are common. There is also twinned, prismatic, equant clinopyroxene, but it is much less common than in the Amealco Andesite. Fe-Ti oxides (2-4 vol. %) can be up to 0.3 mm. They are usually equant, but elongated anhedral oxides are also present. As the pyroxenes, the Fe-Ti oxides are more abundant in crystal clots than as single crystals. Apatite is euhedral, and <0.3 mm. It also is present as inclusions in the Fe-Ti oxides, pyroxenes, and plagioclase. Occasionally, oval clots, up to 6.5 mm, of interlocking crystals are also observed. These clots are mostly composed of small plagioclase laths, <0.3 mm. They also contain laths of two pyroxenes and equant Fe-Ti oxides, all <0.3 mm. The space between the interlocking crystals is filled with optically continuous, anhedral plagioclase, which probably formed later than the plagioclase lath network. Since the mineralogy is the same as that of the host rock, these clots may be juvenile. The glass inclusions of the plagioclase indicate that resorption occurred in different stages during the plagioclase growth, as the inclusions are parallel to the concentric zoning and have a regular shape (square or rectangular). In contrast to the clots observed in Amealco Andesite, there is no intergranular glass in the Santa Rosa Andesite clots, suggesting that these magma bodies were cooled more slowly than the rim lava domes. Both dome types contain plagioclase with large glass inclusions, but maybe with different origins: glass inclusions in the plagioclase of the rim lava domes are probably liquid trapped due to a relatively fast growth of the plagioclase, whereas those in the plagioclase of Santa Rosa Andesite are due to resorption.

La Cruz Rhyolite. It has distinct features with respect to the Amealco caldera units so far described. Mineralogy is practically the same, but textural differences are evident. The rhyolite has a perlitic vitreous texture. It is porphyritic, with a crystal content varying between 10 and 15 vol. %. The matrix is a perlitized, colorless to pale pink glass. It contains plagioclase (8-10 vol. %), orthopyroxene (2-3 vol. %), Fe-Ti oxides (1-2 vol. %), and sparse biotite (<1 vol. %). Some domes, such as El Barco, also exhibit clinopyroxene (1-2 vol. %) and rare olivine phenocrysts that form part of crystal clots (see below). Zircon and apatite are accessories. Although the rock has a rhyolite composition, modal quartz and alkali feldspar are absent. Three plagioclase populations are evident. One has a rather peculiar texture, consisting of skeletal plagioclase cores that are surrounded by an unzoned and clear plagioclase mantle. It generally occurs as single crystals. A second population is commonly observed in the crystal clots, but also occurs as single crystals. It consists of a zoned plagioclase with concentric fritted zones and even totally fritted cores. The third population is a clear plagioclase completely free of glass inclusions that commonly occurs as large crystals (≤3 mm) in glomerocrysts. All plagioclase has rounded corners. Orthopyroxene generally occurs in glomerocrysts, but it also occurs as single, small crystals. It is subhedral to anhedral, tabular, up to 1 mm in the glomerocrysts, and less than 0.3 mm as single crystals. Clinopyroxene is relatively abundant in the El Barco lava domes, particularly in the outcrops occurring next to the San Miguel dam (Figure 3). Large (up to 3 cm in diameter) enclaves, green in hand specimen, are common features in these rocks. The enclaves are crystal clots (Figure 15, a, b), with an interlocking texture, of plagioclase + pyroxene + Fe-Ti oxides and rare olivine; the space between crystals is occupied by a yellow-brown glass. These enclaves may be fragments from the solidification zone of the magma chamber (Langmuir, 1989).

APPENDIX C: K-Ar GEOCHRONOLOGY

Twenty five samples were selected for K-Ar dating (Table 1). The K-Ar analyses were performed in the Department of Geological Sciences of the University of Texas at Austin. K analyses were performed with flame photometry using Na buffering and Li internal standard. Ar analyses were performed using the isotope dilution technique with a gas-source mass spectrometer operated under computer control. The 25 K-Ar ages performed span the whole range of the Amealco caldera activity, and include both pre- and post-caldera volcanism. Many of the units are dated with two or more samples from different localities. For some samples (samples Am-1, Am-179, Am-63, Am-81, Table 1) paired ages of different phases were performed to cross-check the results. Glass was used for many of the K-Ar analyses, as it is the phase richest in K of the selected samples. None of the Amealco caldera products contains sanidine or sufficient biotite; two (Palomas and Garabato andesites) contain hornblende but it was too oxidized for a reliable analysis. For Amealco Tuff there was no other choice than to use the glass and plagioclase. Other units that also lack K-rich phases are the rim domes (Amealco Andesite), the central andesitic domes (Santa Rosa Andesite), the Hormigas Andesite, and the El Comal Andesite. Garabato and Palomas andesites were dated using whole-rock or groundmass separates. Groundmass separates are richer in K than whole-rock samples; thus, when practical, groundmass separates were analyzed instead of the whole-rock material. Rhyolite samples, such as those of La Cruz Rhyolite and Huichapan Tuff, have alkali feldspar, but with a K content much lower (about 3 wt. %) than common sanidine (usually about 10%). Glass was analyzed for these samples also.

The laboratory used for these K-Ar determinations has been commonly used for mid-Tertiary or older samples; thus the relatively young age expected for the Amealco samples, along with their lack of K-rich minerals, were the reasons for choosing material richer in K, such as glass and groundmass, in order to obtain higher radiogenic argon concentrations. Several tests were performed to find the optimum amount of sample needed for analysis. At the beginning, it was thought that larger amounts (600-700 milligrams) would provide better results, but this approach produced unexpected problems. In the case of glass the melt was so viscous that argon apparently

was unable to escape completely from the sample. Thus, longer melting times and higher temperature settings were needed than those usually required to get a complete extraction. Significance of this problem was magnified with the sequential extraction of 10 to 14 samples using the same crucible, as is routinely done in this laboratory. In addition, with larger samples of glass the amount of "dirty" gases (H_2O and CO_2 among others) overwhelmed the clean up capacity of the vacuum line and resulting in erratic behavior of the mass spectrometer. The feldspars were cleaner during argon extraction, but argon was also difficult to extract completely from large samples, in spite of using an equivalent amount of a zero-age basalt as a flux (McDowell, 1983), and temperatures above 1,600°C for 40 minutes. Also, the increased weight did not improve the proportion of radiogenic argon in the experiments, as the atmospheric argon came from the samples and not from the vacuum line. Best results were obtained by mixing an equivalent weight of zero-age basalt as a flux to glass and feldspars, with sample amounts in the order of 200-400 milligrams. 500-600 milligrams were found to be the best amounts for groundmass and whole-rock samples.

Accuracy and precision

Accuracy is regularly checked with standards with well known ages and by a large number of repeat analyses of mineral separates and whole-rock samples in the span of several years in this laboratory. However, as the Amealco samples are younger than the standards that have been commonly used, a cross-checking of the results was needed to test their reliability. The cross-checking included: (1) paired analysis using different phases (*e.g.*, glass and plagioclase) from a sample, (2) multisampling of a single unit, and (3) dating pre-Amealco caldera rocks as well as post-Amealco rocks that bracket in time the Amealco caldera products. The results of individual samples (paired analyses) and of individual units (multisampling) agree and are consistent with the stratigraphy of the units. K precision is well determined by pooling of replicate data. Relative errors are 0.9% for alkali feldspar (K >2 %), 1.2% for plagioclase (K < 2%), 1% for whole rock and hornblende. Furthermore, K analysis was performed in duplicate or triplicate. If the error obtained by the duplicates was significantly larger than that of the pooled values, then the error, at one sigma standard deviation, of the duplicate or triplicate was used instead. Ar analytical error is computed from a pool of replicates with radiogenic argon contents larger than 40%. Errors obtained in this way are 1.7% for whole-rock samples, 2% for plagioclase and K-feldspar, and 1.8% for hornblende. If the sample has less than 40% radiogenic argon content, additional error sources must be included in the error computation (see Equation 1, below). As most samples of Amealco contain radiogenic argon contents less than 40% of the total argon (Table 1), the additional terms were used routinely. As in K analytical precision, if the error obtained by the duplicates and triplicates was larger than those obtained from the pooled errors or those computed using the extra-terms, then the duplicate-triplicate error, at one sigma standard deviation, was instead used.

The equation used to calculate the error of the age for samples with radiogenic argon (%) is an equation that has been used for many years in the K-Ar laboratory of the University of Texas (U.T.).

The Equation 1 is:

$$\text{K-Ar error} = \{\sigma K^2 + \sigma Ar^2 + (\sigma^{40}Ar/\sigma^{36}Ar)^2[((100\text{-}r)/r)^2 + \sigma MD^2][((100\text{-}r)/r)^2\}^{0.5}$$

where σ is error at one sigma standard deviation, r is the radiogenic argon content, in percent, and MD is the mass discrimination factor.

Precision of the data was acceptable, in general with errors of less than 8% of the age, and more than half of the data even less than 5% of the age. However, a few samples have errors up to 15% of the age, and one (Am-122) has an excessive error of 22% apparently caused by an excessive atmospheric argon content.

Assigned Ages

When comparing different samples of individual units, for example Amealco Tuff or Amealco Andesite, the ages show some inherent scatter. Thus, the weighted mean of the results was computed in order to assign a representative age to the units. These results are the ones used as the most representative of the dated units, and are shown in Table 1.

APPENDIX D
HOW VOLUMES WERE ESTIMATED IN THIS WORK

In the previous work on this area, the estimation of the volume of Amealco caldera products has been a major problem, particularly for Amealco Tuff (Amealco Ignimbrite). The volume of the "Amealco Ignimbrite" was first estimated at about 500 km^3 (Sánchez-Rubio,1984), and it was later estimated to be up to 180 km^3 (Sánchez-Rubio,1986), then it was estimated to be at least 35 km^3 (Sánchez-Rubio,1986). Carrasco-Núñez (1988) proposed 72 km^3, but later he and others estimated it as 65 km^3 (Verma *et al.*, 1991). These discrepancies resulted because the volumes were estimated without knowing the distribution of Amealco Tuff.

Table D-1 summarizes the estimated volumes of the Amealco caldera units. However, a few notes are necessary to explain the method for computing the volumes.

The areas of the units were calculated using an Apple Macintosh™ computer and the program Canvas™ (Deneba Systems, Inc.). This graphics program has a tool that computes the area of surfaces with any shape. In order to be able to use

Table D-1. Summary data for the estimation of Amealco caldera volume.

Unit	Thickness (m)	Area (km^2)	Density (g/cm^3)	Rock volume (km^3)	DRE volume (km^3)	% from total
Ame Zero	2.00	719.50	1.30	1.44	0.75	
Tephra-1	7.50	2878.00	1.40	21.59	12.09	
Ame-1	3.50	2878.00	2.15	10.07	8.66	
Tephra 2	9.70	2878.00	1.90	27.92	21.22	
Ame-2	4.00	2878.00	2.40	11.51	11.05	
Tephra 3	5.50	2878.00	1.60	15.83	10.13	
Ame-3	5.00	2878.00	2.40	14.39	13.81	
Total Amealco Tuff				102.74	77.71	84.58
Palomas lavas	10.00	37.43	2.50	0.37	0.37	
Palomas cone	200.00	2.21	2.50	0.44	0.44	
Total Palomas				0.82	0.82	0.89
Hormigas lava	20.00	24.31	2.60	0.49	0.54	
Hormigas cone	130.00	1.93	2.60	0.25	0.26	
Total Hormigas		26.24		0.74	0.80	
Sta. Rosa dome	280.00	2.49	2.50	0.80	0.80	
Zancudo dome	320.00	2.76	2.50	1.10	1.10	
Gallo dome	500.00	10.50	2.50	1.80	1.80	
Capando dome	300.00	4.83	2.50	0.43	0.43	
La Mesa dome	240.00	0.88	2.50	0.21	0.21	
Total Santa Rosa dome				4.34	4.34	4.73
Chiteje dome	350.00	9.53	2.40	1.79	1.72	
San Juan dome	300.00	in Chiteje dome	2.40	0.21	0.20	
El Barco domes	190.00	2.07	2.40	0.47	0.45	
Total La Cruz Rhyolite				2.47	2.37	2.58
Rim NE	200.00	5.66	2.50	1.13	1.13	
Rim Tenango	200.00	5.52	2.50	1.10	1.10	
Rim Arco	50.00	1.66	2.50	0.08	0.08	
Rim North	150.00	0.97	2.50	0.15	0.15	
Rim Bellotal	250.00	7.73	2.50	1.03	1.03	
Total Amealco Andesite				3.50	3.50	3.81
Brick SW	30.00	17.27	1.50	0.52	0.31	
Brick NE	15.00	5.52	1.50	0.08	0.05	
Brick E	30.00	110.70	1.50	3.32	1.99	
Total Brick Pumice				3.92	2.35	2.56
Campana dome	300.00	2.62	2.50	0.79	0.79	0.86
Garabato dome	50.00	4.01	2.50	0.10	0.10	
Comal	100.00	1.93	2.00	0.19	0.15	
Total erupted from Amealco Caldera (excludes Hormigas, Garabato and Comal)				118.58	91.88	100.00
Trachyandesite + trachydacite make	94.86% from the total volume					
Rhyolite makes	5.14% from the total volume					

Total area = 2,878.00 km^2
Density rock equivalence at 2.5 g/cm^3

this program, the map of the studied area was input to the computer by means of a scanner; the scanned map was then retraced (digitized) using Canvas™. The digitized contour of each mapped unit makes a multi-sided polygon. The program is able to calculate the area of that polygon, giving the result in square inches. The real area in square kilometers is obtained by an easy computation using a conversion factor. The area values gotten in this way are provided in the summary table (Table D-1).

Amealco Tuff. Three areas of this unit were computed, depending upon which limits are assumed. As described in the main text, Amealco Tuff is not exposed within the Acambay graben, just to the south of the caldera. The present area, that includes the outcrops north of this graben and those south of it, resulted in 1,741 km^2 and 208 km^2, for the northern and southern exposures, respectively; this excludes the intracaldera area, which is 81 km^2, so a total of 2,030 km^2 is the presently exposed area. The inferred tuff within the Acambay graben covers 848 km^2, using the inferred limits as shown in Figure 3. Thus a total of 2,878 km^2 is obtained including the inferred distribution. This area estimate is a minimum, since the tuff clearly extended farther to the east, where it remains buried by younger deposits. An eastern inferred tuff using arbitrary limits covers an additional area of 1,775 km^2. This last value was not included in the volume calculations, so 2,878 km^2 was the area used in the estimate (Table D-1).

Amealco Tuff was divided in different subunits depending upon their physical characteristics. The major ignimbrites are generally welded and denser than the interlayered tephra. The division is shown in Table D-1. Several bulk density values were measured from samples of the measured section at Epitacio (Figure 6), following the procedure described in Cas and Wright (1987, p. 226-227); the most representative density values are also shown in Table D-1, which were used to compute the dense rock equivalent volume.

The average thickness was estimated for each of the subunits; this average thickness was used to compute the volume of that particular subunit. The thicknesses were gotten from the measured sections. If a distal section does not include one of the subunits, a value of zero was used in the average.

To cross-check the values gotten in this way, a second approach was used, in which the distribution of Amealco Tuff is assumed as a circular one. Since the tuff reached, at least, 30 km from the caldera, in all directions (the eastward assumed), then the distribution is the area of a 30 km radius circle: 2,827.4 km^2, which is very close to the real area distribution mentioned above (2,878 km^2). For each subunit a regular-shaped distribution of a quarter of the 30 km radius circle, the half, or the total circle was assumed, depending upon the direction from the caldera in which the subunit was more abundant and thicker. Thus, Amealco Zero only occurs to the west of the caldera, and with a localized distribution, so that a quarter of the circle was used. Tephra 1 used the north half of the circle; Pumice 1 (included in Tephra 1 in Table D-1) the west quarter; Tephra 2, Tephra 3, and Amealco 1, 2 and 3 ignimbrites used the whole circle. A total of 97 km^3 of rock volume, and of 77 km^3 dense rock equivalent volume was obtained in this way, which agrees very well with the values obtained in the former approach (shown in Table D-1).

The volumes of the volcanoes, domes, and lava flow were computed by breaking the dome, lava flows, or volcanoes in tetrahedra and cubes; adding the volumes of these smaller regular-shaped parts provides the total rock volume of the respective body. If a volcano had more or less a regular geometric shape, the volume of that shape was used instead (*e.g.*, cones). The total value for each unit is provided in Table D-1. The areas of the lava domes and volcanoes with associated lava flows shown in Table D-1 were obtained with the Canvas™ computer program. The thicknesses of the cones and lava domes shown in the table are the height of the respective volcanic body with respect to its lowermost elevation on one of its flanks. These areas and thicknesses are included in Table D-1 just to provide extra information about the volcanic forms, but these values were not used in the computation of the volumes. As explained above, the volumes were computed by adding the tetrahedra and cubes that compose each of these bodies. The density for each of these units was assumed and not measured as in Amealco Tuff. The dense rock equivalence was computed assigning a 2.5 g/cm^3 value for the dense rock, that falls within the range of the density of an andesitic glass (Barker, 1983, p. 146).

Manuscript received: October 20, 1994.
Corrected manuscript received: June 2, 1995.
Manuscript accepted: June 23, 1995.